Characterization of Fractured Basement Reservoir, Melut basin, Southeast Sudan

BY

Mohamed Abdelgader Ahmed Yassin

A Thesis Presented to the

DEANSHIP OF GRADUATE STUDIES

KING FAHD UNIVERSITY OF PETROLEUM & MINERALS

DHAHRAN, SAUDI ARABIA

In Partial Fulfillment of the
Requirements for the Degree of

MASTER OF SCIENCE

In

GEOLOGY

JUNE 2012

KING FAHD UNIVERSITY OF PETROLEUM & MINERALS
DHAHRAN 31261, SAUDI ARABIA

DEANSHIP OF GRADUATE STUDIES

This thesis, written by **MOHAMED ABDELGADER AHMED YASSIN** under the direction of his thesis advisor and approved by his thesis committee, has been presented to and accepted by the Dean of Graduate Studies, in partial fulfillment of the requirements for the degree of **MASTER OF SCIENCE IN GEOLOGY.**

Thesis Committee

Dr. Mustafa M. Hariri (Chairman)

Dr. Mohammad H. Makkawi (Member)

Dr. Osman M. Abdullatif (Member)

Dr. Abdulaziz Al Shibani
(Department Chairman)

Dr. Salam A. Zummo
(Dean of Graduate Studies)

19/6/12

Date:

ACKNOWLEDGEMENT

I would like to express my sincere gratitude to KFUPM for support this research, and Sudapet Company and Ministry of Petroleum for the permission to use the data and publish this thesis. Without any doubt, the first person to thank is Dr. Mustafa M. Hariri, my supervisor, who has been a great help, revision and correction.Thanks also are due to the committee members, Dr.Mohammad H. Makkawi& Dr. Osman M. Abdullatif for their guidance, help and reviewing this work. I am greatly indebted to the chairman of the Earth Sciences Department, Dr. Abdulaziz Al-Shaibani for his support and assistance during my studies at KFUPM. Special thanks to Sudapet Company management. Of these; I am especially grateful to Mr. Salah Hassan Wahbi, President and CEO of Sudapet Co.; Mr. Ali Faroug, Vice Presedent of Sudapet Company; my managers Mr. Ibrahim Kamil and Mr. HamadelnilAbdalla; Mr. HaidarAidarous, Sudapettraining and development; Mr. Abdelhafiz from finance. I would also like to express my sincere appreciation to my colleagues at Sudapet and PDOC, NourallaElamin, Atif Abbas, YassirAbdelhamid and Ali Mohamed. Thanks to Dr. Gabor Korvin from KFUPM for discussion. Likewise, I would like to thank Earth Sciences Department faculty and staff. I extend thanks to my colleagues in the department for their support. Thanks to my colleagues HassanEltom andAmmar Adam for continuous discussions. Sincere thanks to my friends HatimDafallah, Mohamed Ibrahim and Mohamed Elgaili. I would like to gratitude my colleagues form KFUPM, Ali Al- Gahtani and Ashraf Abbas. Thanks for the Sudanese community at KFUPM for their support. Finally, this work would not be possible without the support, patience, help, and prayers of my father, mother, wife, son, brothers, grandmother and all family to whom I am particularly grateful.

Table of Contents

ACKNOWLEDGEMENT iii
LIST OF FIGURES vii
LIST OF TABLES x
THESIS ABSTRACT xi
ملخص الرسالة xii

CHAPTER ONE

INTRODUCTION

1.1 Overview 1
1.2 Location and Physiographic Features 2
1.3 Problem Statement 5
1.4 Motivation 5
1.5 Objective 6
1.6 Methodology 6
1.6.1 Fracture Characterization 6
1.6.1.1 Fractures and Lineaments Defined from Gravity Data 8
1.6.1.2 Faults Defined from Seismic Data 8
1.6.1.3 Fractures and Lineaments Defined from Satellite images Data 9
1.6.1.4 Fractures Defined from Well Data 9
1.6.1.5 Model of Fracture Origin 10
1.6.1.6 In-situ Stress Analysis 10
1.6.1.7 Hydrocarbon Migration 10
1.6.2 Fracture Modeling 10
1.6.2.1 Geo-cellular Model Description 11
1.6.2.2 Analyzing Fracture Properties 11
1.6.2.3 Fracture Sets Identification 11
1.6.2.4 Fracture Intensities Generation, Upscalling and Simulation 11
1.6.2.5 Discrete Fractures Network (DFN) Model Construction 11

CHAPTER TWO

GEOLOGIC AND TECTONIC SETTING

2.1 Geology of NE Africa 12

2.2 Regional Geology of Sudan 14

2.3 Geology of the Study Area 15

2.3.1 Basement Complex of Nuba Mountains 18

2.3.2 Basement Complex of Ingessana Hills 24

2.3.3 Basement Description from Subsurface Data 24

2.3.4 Sedimentary Units of Melut Basin 25

2.4 Tectonic Setting 28

2.4.1 Rift and Sag Phases in Melut Basin 31

2.4.2 Structural Style in Melut Basin 36

2.5 Melut Basin Stratigraphy 40

2.5.1 The Early Cretaceous Strata 40

2.5.2 The Late Cretaceous Strata 42

2.5.3 The Tertiary Strata 42

2.5.4 The Quaternary Strata 43

CHAPTER THREE

FRACTURE CHARACTERIZATION

3.1 Fracture Concept 45

3.2 Types of Fractures 45

3.3 Fracture Creation Processes 46

3.3.1 Fractures Related to the Magma Cooling and Emplacement 46

3.3.2 Fault-Related Fracture Systems 48

3.3.3 Fold-Related Fracture Systems 50

3.4 Fractures and Lineaments Defined from Gravity Data 52

3.4.1 Lineaments Orientation Analysis 52

3.5 Faults Defined from Seismic Data 52

3.5.1 Faults Orientation Analysis 55

3.6 Fracture and Lineaments Defined from Satellite Images 60

3.6.1 Lineaments Orientation Analysis 60
3.6.2 Basement Outcrops Length Analysis 65
3.7 Fracture Defined from Well Data 65
3.7.1 Fractures Identification 65
3.7.2 Fractures Orientation Analysis 72
3.8 Orientation Analysis Summary 77
3.9 In-situ Stress Analysis 82
3.10 Model of Fracture Origin 85
3.10.1 Fractures Related to Basement Formation 85
3.10.2 Proterozoic Tectonic Fractures 86
3.10.3 Faults Related Fractures 93
3.11 Hydrocarbon Migration 97

CHAPTER FOUR

FRACTURE MODELING

4.1 Geo-cellular Model Description 99
4.2 Analyzing Fracture Properties 100
4.3 Fracture Sets Identification 100
4.4 Fracture Intensities Generation, Upscalling and Simulation 104
4.5 Discrete Fractures Network (DFN) Model Construction 110
4.5.1 Stochastic Model 110
4.5.1.1 Fracture Distribution 115
4.5.1.2 Fracture Geometry 115
4.5.1.3 Fracture Orientation 116
4.5.2 Deterministic Model 117

CHAPTER FIVE

CONCLUSIONS AND RECOMMENDATIONS

4.6 Conclusions 122
4.7 Recommendations 124
References 126
Vita 131

LIST OF FIGURES

Figure 1-1: Location Map of Sudan showing the study area 3
Figure 1-2: Map showing the concession blocks, the study area (Block 3&7) 4
Figure 1-3: Flow chart showing the approaches and objectives 7
Figure 2-1: Geological map of the Sudan 16
Figure 2-2: Geological map of the study area and vicinity..... 17
Figure 2-3: Sketch map of the Nubian- Arabian Shield with the Red Sea closed..... 20
Figure 2-4: The Nubian Shield and the Saharan metacraton marked by N-S trending 21
Figure 2-5: Schematic diagram showing the tectonic evolution..... 23
Figure 2-6: Show the meta-sediment rock (Schist) in well Ruman NE-1 26
Figure 2-7: Show the meta-igneous rock (Gneissic biotiteGranodiorite) Ruman NE-1... 26
Figure 2-8: Show the meta-sediment rock (Schist) in well Ruman NNE-1 27
Figure 2-9: Location map of north-east African rift basins 30
Figure 2-10: Regional tectonic setting of Africa 32
Figure 2-11: Two stage development of African rifts during Early Cretaceous..... 35
Figure2-12: Basement Time Structure Map (TWT- Tow Way Time Map) 37
Figure 2-13: Line 7 and Line 8 regional dip lines (after Mann, 1989). 37
Figure 2-14: Simple thin- skin detachment, Melut basin..... 39
Figure 2-15: Line 7 Dip line to basin forming thick-skin fault..... 39
Figure 2-16: Stratigraphic column for the Melut Basin. 41
Figure 3-1: Showing the three modes of fracturese 47
Figure 3-2: Fracture systems related to cooling of large plutonic bodies 47
Figure 3-3: Rose diagrams of shear fractures related to faults system 49
Figure 3-4: Block diagram, Showing 60 degree dipping normal fault 49
Figure 3-5: A block diagram showing the fracture patterns observed on folds 51
Figure 3-6: Hypothetical model for the radial and concentric line fracture 51
Figure 3-7: Gravity map, showing Lineament superimposed over gravity image. 53
Figure 3-8: Show the area of Ruman 3D seismic survey and wells locations..... 54
Figure 3-9: Show faults interpretation in Ruman 3D..... 56
Figure 3-10: Show faults interpretation in Ruman 3D..... 56
Figure 3-11: Top basement, where the basement surface is posted on the seismic..... 57

Figure 3-12: Shows the structural map of basement in Ruman area 57
Figure3-13: Simplified structural map of the Melut Basin. 58
Figure 3-14: Geo-seismic cross-sections in Nuba Mountains and Ingessana Hills. 59
Figure 3-15: Geo-seismic cross-sections showing the major thick-skin 59
Figure 3-16: Satellite image around Melut basin superimposed over Sudan map. 61
Figure 3-17: Integrated lineament map superimposed over satellite image 62
Figure 3-18: Satellite image for Nuba Mountains and Ingessana Hills 63
Figure 3-19: Histogram and rose diagram 64
Figure 3-20: Lineaments with different direction interpreted from Satellite image 66
Figure 3-21: Lineaments with WNW-ESE direction interpreted from Satellite image 67
Figure 3-22: Lineaments with NW-SE direction interpreted from Satellite image 68
Figure 3-23: Lineaments with N-S direction interpreted from Satellite image 69
Figure 3-24: Lineaments with NE-SW direction interpreted from Satellite image 70
Figure 3-25: Showing histogram and cdf (cumulative distribution function) 71
Figure 3-26: Relation between dip angle, dip azimuth & strike 73
Figure 3-27: Stereonet and rose diagram 73
Figure 3-28: Dips are presented as tadpoles on a dip track 73
Figure 3-29: Statistical analysis of all basement fracture dip, azimuth and strike 74
Figure 3-30: Statistical analysis of all continuous conductive fractures in Ruman N-2... 74
Figure 3-31: Statistical analysis of the conductive fractures in the basement 76
Figure 3-32: Statistical analysis of all continuous conductive fractures 76
Figure 3-33: Statistical analysis of all continuous conductive fractures..... 78
Figure 3-34: Upper Hemisphere-Schmidt projection for fracture 78
Figure 3-35: Plate showing Lineaments interpreted from Gravity 79
Figure 3-36: Rose diagrams A, B, C and D 81
Figure 3-37: Borehole stress orientation..... 83
Figure 3-38: Drilling induced fractures dips in Ruman NNE-1 84
Figure 3-39: Upper Hemisphere-Schmidt projection and rose diagrams 84
Figure 3-40: Bouguer anomaly images, showing Ruman area 87
Figure 3-41: Three-dimensional cartoon of the Saharan Metacraton 91
Figure 3-42: Statistical plots of all foliation in Ruman NNE-1 92

Figure 3-43: Rose diagrams showing the classification of fractures pattern 94
Figure 3-44: Upper Hemisphere-Schmidt projection for all fractures 95
Figure 3-45: Structural map from seismic 96
Figure 3-46:Geo-Seismic Cross-section, showing Ruman Basement 98
Figure 3-47:Ruman structural map, showing Ruman trap 98
Figure 4-1: The base map of the modeled area 101
Figure 4-2: The structural maps of the top and base basement surfaces. 101
Figure 4-3: The structural map of top basement. 102
Figure 4-4: The generated 3-D grid of the model 102
Figure 4-5: Elements representing the attitude of the fractures. 103
Figure 4-6: The schmidt stereonet, visualizing all the fractures from all the wells 103
Figure 4-7: Total intensity logs (curves). 105
Figure 4-8: Upscaled total intensity for the five wells 105
Figure 4-9: Upscaled fracture intensities for each fracture set at all the wells 106
Figure 4-10: Upscaled fracture intensities for each fracture set at all the wells 107
Figure 4-11: Variogram simple spherical model 109
Figure 4-12: Variogram analysis of well data for the different fracture sets 111
Figure 4-13: Variogram analysis of well data for the different fracture sets 112
Figure 4-14: The interpolated total intensity in Ruman area 113
Figure 4-15: The interpolated intensities for the each fracture set in Ruman area 114
Figure 4-16: Three Dimensional Discrete Fracture Network (DFN) 119
Figure 4-17: Three Dimensional Discrete Fracture Network (DFN)all fracture sets 120
Figure 4-18: Schmidt stereonet extracted from the DFN model for QC 121

LIST OF TABLES

Table 1: Orientations analysis (fractures strike) using different source of data 81
Table 2: The constant parameters for the Fisher model for fracture orientation 118

THESIS ABSTRACT

NAME: Mohamed Abdelgader Ahmed Yassin
TITEL OF THESIS: Characterization of Fractured Basement Reservoir, MelutBasin, Southeast Sudan

MAJOR FIELD: Geology

DATE OF DEGREE: June 2012

Basement reservoirs can be of different types; fractured granitic, fractured quartzite, and/ or fractured Schist and Gneiss. In the fractured basement reservoirs, hydrocarbon is entrapped within the fractures network within the basement rocks. Porosity and permeability in basement reservoirs is controlled by the fractures and not by the rocks matrix as in the conventional reservoirs. Hydrocarbon-hosted in fractured basement reservoir was reported in many locations in Sudan since 2007 and the Melutbasin is one of those areas. Mapping and characterization of faults and fractures in those areas are important steps towards the quantification of hydrocarbon potentiality in the region. The main objective of this study is to characterize and model fractures system within the basement reservoir in Ruman area, Melut basin. The aim of this study is tobetter understand those fractures origin, distribution and connectivity. To achieve the goal of this study fractures, faults and lineaments were studied in different scales and from surface and subsurface data; well data, gravity, seismic data and satellite images. Obtained data wascharacterized base on orientation, length and intensity. Moreover; geostatistical extrapolation for areas in-between wells, stochastic and deterministic models were also conducted to determine the Discrete Fracture Network (DFN) model. Areas of fractures concentration and distribution were delineated using this technique. Compatible and parallel NW-SE, NNW-SSE to N-S, WNW- ESE to E-W and NE-SW trends were observed from the interpreted data of satellite images, gravity, wells and seismic data. It is evident from Rose-Diagrams generated for the faults detected from seismic dataand fracturesobserved from the FMI-log of five wells that they are having similar trends. The same trends can also be noticed in gravity data and lineaments determined from satellite images. Three stages model were proposed for the origin of the fractures associated with the basement; fractures developed during the emplacement and cooling of the igneous pluton, fractures related to the Proterozoic tectonic events and faults related fractures (developed during Melut basin rifting).The outcome of this study delineated the possible origins of the fractures system hosting hydrocarbon in the basement rocks. Additionally the study characterized and defined the possible trends of those fractures and how are they related to different origin. The study also addressed the possible role of the major faults in hydrocarbon migration.From the in-situ stress analysis, faults and fractures trends were tested for the most susceptible at present day.The study outcomes and methodology can be used for hydrocarbon exploration and development in this area and for other areas of similar geological structural settings.

MASTER OF SCIENCES DEGREE
KING FAHD UNIVERSITY OF PETROLEUM & MINERALS
DHAHRAN, SAUDI ARABIA
JUNE 2012

ملخص الرسالة

الاسم: محمد عبد القادر أحمد يسن

عنوان الرسالة: توصيف مكامن صخور الاساس المتكسرة، حوض ملوط، جنوب شرق السودان

التخصص الرئيسى: جيولوجيا

تاريخ نيل الدرجة: يونيو 2012

خزانات صخور الاساس يمكن أن تكون من أنواع مختلفة؛ صخور الجرانيت المتكسرة، صخور الكوارتزايت المتكسرة، و / أو صخور الشست والنايس المتكسرة. فى خزانات صخور الاساس المتكسرة , يحبس النفط والغاز فى شبكة الكسور في صخور الاساس. المسامية والنفاذية في خزانات صخور الاساس المتكسرة تعتمد على الكسور ولاتعتمد على المسامية والنفاذية بين الحبيبات كما في الخزانات التقليدية. النفط والغاز فى خزانات صخور الاساس المتكسرة وجدت في العديد من المواقع في السودان منذ عام 2007 وحوض ميلوت هو واحد من تلك المناطق.

تخريط وتحديد خصائص التصدعات والتشققات في تلك المناطق هي خطوات هامة نحو تحديد أماكن النفط والغاز في المنطقة. الهدف الرئيسي من هذه الدراسة هو توصيف ونمزجة نظم الكسور داخل خزان صخور الاساس المتكسر في منطقة رمان، حوض ملوط. الهدف من هذه الدراسة هو أن نفهم على نحو أفضل أصل هذه الكسور، توزيعها وعلاقة الاتصال فيما بينها. لتحقيق الهدف من هذه الدراسة؛ الكسور، الصدوع والتوجهات والملامح تمت دراستها باحجام مختلفة من المعلومات السطحية والتحت سطحية؛ معلومات من الابار، الجاذبية، البيانات السيزمية وصور الأقمار الصناعية. المعلومات المتحصل عليها تمت دراستها على أساس الاتجاهات, الطول والكثافة. علاوة على ذلك، الجيولوجيا الاحصائية أستعملت لدراسة الكسور فى المناطق ما بين الآبار، وأجريت أيضا نماذج عشوائية وحتمية لايجاد نموذج شبكات الكسور المتقطعة (DFN). وقد حددت مناطق تركيز الكسور وتوزيعها باستخدام هذه التقنية.

الاتجاهات المتوافقة والمتوازية فى اتجاه شمال غرب - جنوب شرق, شمال شمال غرب - جنوب جنوب شرق الى شمال - جنوب، غرب شمال غرب - شرق جنوب شرق الى شرق غرب و شمال شرق - جنوب غرب فسرت من الملامح (بواسطة صور الأقمار الصناعية)، معلومات الجاذبية، الآبار ومعلومات المسح الزلزالي. يتضح من مخططات الروز التى انتجت من أتجاهات الصدوع من البيانات السيزمية والكسور المنتجة من الابار الخمسة. الابار أظهرت أن لديها اتجاهات مماثلة في الاتجاهات ذاتها التى فسرت بواسطة البيانات الجاذبية والملامح من صور الأقمار الصناعية.أقترحت ثلاثة نماذج لأصل الكسور المرتبطة بصخور الاساس؛ كسور تكونت خلال عمليات التبريد خلال تموضع الصخور النارية، كسور تكونت خلال الأحداث التكتونية فى عصر البروترزويك وكسور تكونت نتيجة للصدوع (خلال عمليات الخسفى حوض ملوط).نتائج هذه الدراسة حددت الاصول المحتملة للنظم الكسور التى تستضيف النفط والغاز. بالإضافة إلى ذلك تميزت هذه الدراسة بتحديد الاتجاهات المحتملة لتلك الكسور وعلاقتها بالمنشأ المختلف للكسور. الدراسة تناولت أيضا الدور المحتمل للصدوع الكبيرة في هجرة النفط والغاز. يمكن استخدام نتائج الدراسة فى وضع منهجية تنقيب وتطوير النفط والغاز فى هذه المنطقة والمناطق الاخرى المشابهة من ناحية الجيولوجية التركيبية.

درجةالماجستير
جامعةالملكفهدللبترولوالمعادن
الظهران،المملكةالعربيةالسعودية
يونيو2012

CHAPTER ONE

INTRODUCTION

1.1 Overview

Basement hosting hydrocarbon was discovered accidentally worldwide during drilling for other targets in sedimentary basins. Usually this takes place when drilling is gone deep and reached the basement oil was found (Petford and McCaffrey, 2003). Currently, basement rocks are consideredin many countries as important reservoirs for hydrocarbon.

Basement rocks are any metamorphic or igneousrockswhich are unconformably overlain by a sedimentary sequence.“Basement reservoirs include fractured or weathered granites, fractured quartzites, and metamorphic rocks such as fractured Schistand Gneiss” (Landes et al., 1960). It is very important to mention that no matrix porosity is within fresh basement, so that fractures are the main defined porosity and permeability. Landes (1960) stated that “the only major difference between basement rock and the overlying sedimentary rock oil deposits is that in the former case the original oil-yielding formation (source rock) cannot underlie the reservoir”.

Fractured basement hydrocarbon reservoirs are found in many countries such as Venezuela, Brazil,USA (basement in California, Kansas and Texas), North Africa (Morocco, Libya, Algeria and Egypt), Middle East (Yemen), West Siberia Basin, China, Southeast Asia in Vietnam and Indonesia (Koning, 2000). The Bach-Ho fractured granite reservoir in Vietnam produces about 130,000 BOPD(Petford and McCaffrey, 2003).

Those basement related hydrocarbon discoveriesencouraged considering shallow basement in other areas as target for exploration. Among those, the fractured basement reservoirs in Sudan became new targets for exploration activities.

1.2 Location and Physiographic Features

Melut Basin is approximately bounded by the longitudes 32° 00′ and 34° 00′ E and latitudes 8° 00′ and 11° 30′ N. The basin extending is about 310 km in a NNW direction with an average width of 100 km (Figure 1-1).

Melut basin is located in the Upper Nile State in southeastern Sudan and divided into two concession blocks (Block 3&7) (Figure 1-2); currently the major part of this basin became located in the South Sudan after North and South Sudan were split into two countries (Rowell, 2010) (Figure 1-2).

The area of study is located at the northwest part of north Melut basin, where the hydrocarbon were discovered in the fractured basement reservoir, namely Ruman area and the surrounding basement outcrops (Figure 1-1).

Destination to the study area from Khartoum is about 800 km and it can be accessed through a variety of transportation means depending on weather conditions, seasons and means. The accessibility to Melut basin by vehicles, trucks and air craft's are available throughout the year.

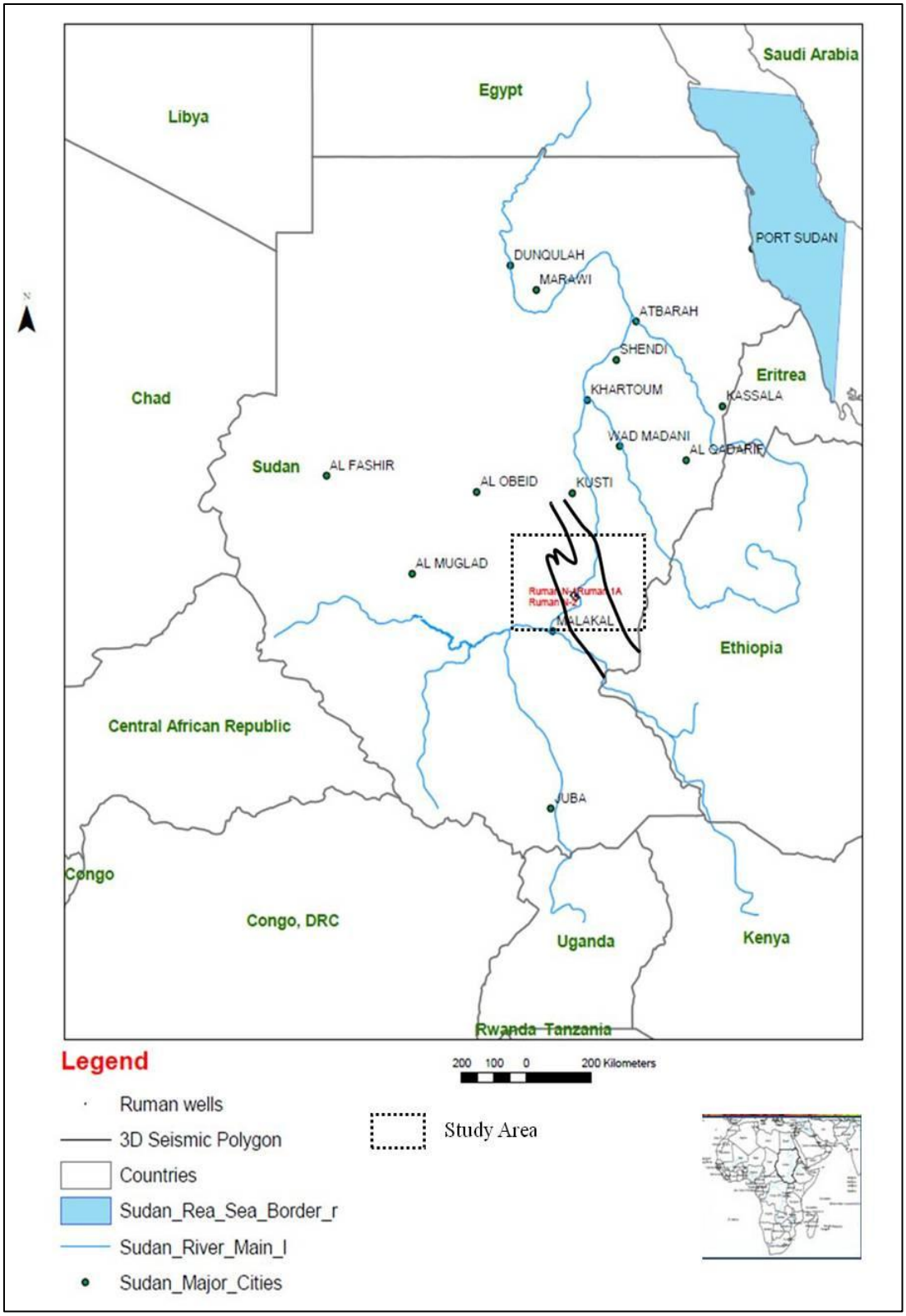

Figure 1-1: Location Map of Sudan showing the study area, 3D seismic polygon, Ruman wells with approximate outlines of the Melut basin and Sudan major cities

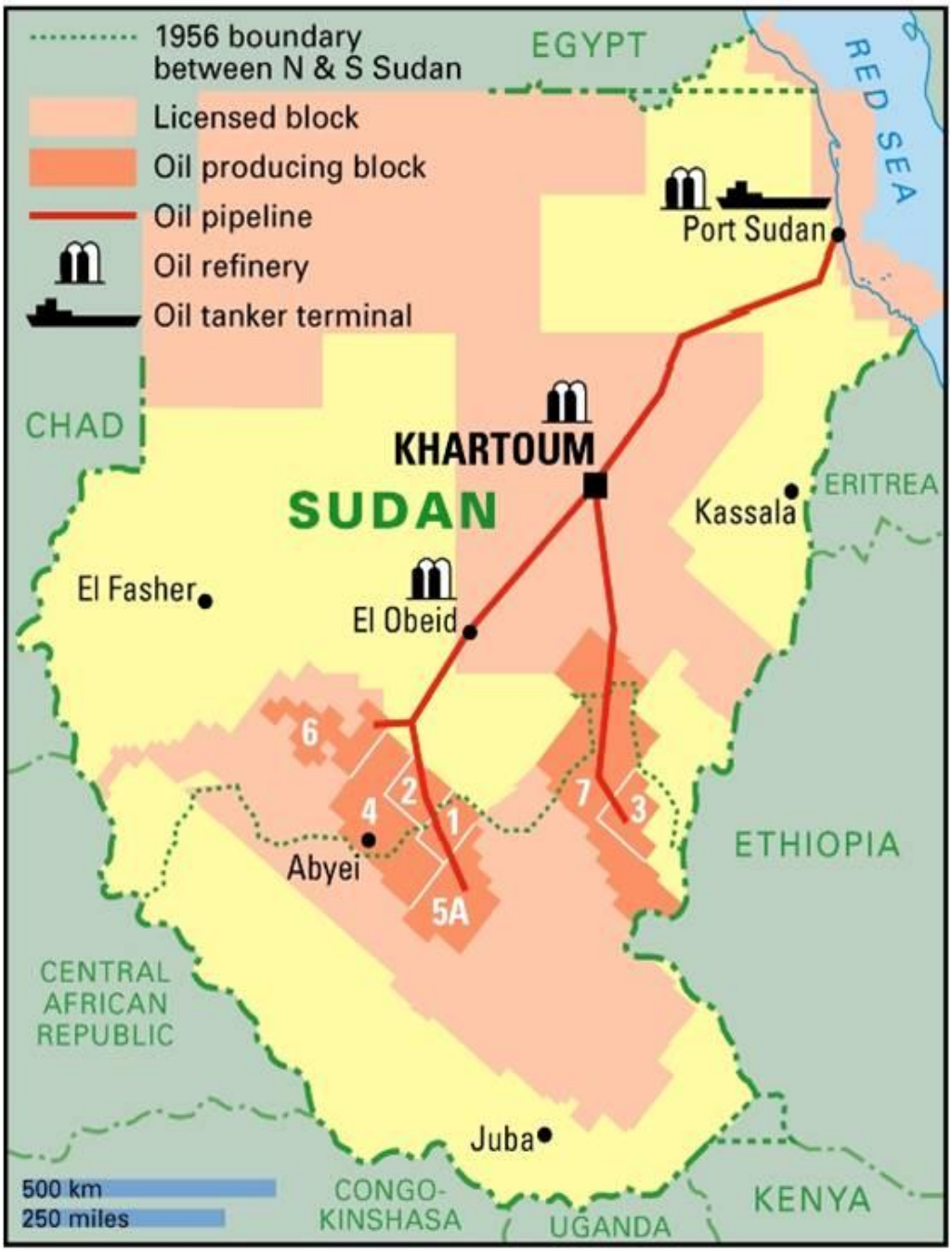

Figure 1-2: Map showing the concession blocks, the studyarea (Block 3&7) and the new boundary between North and South Sudan (after Rowell, 2011)

Generally Melut basin has a flat land, with approximately 390 m ground elevation above the mean Sea Level. Most of the region became swampy plains during the rainy season. The drainage system is generally towards the northwest, of which the White Nile River represents the main drainage elements.

1.3 Problem Statement

The challenging problem in fractured basement reservoirs comes from the fact that, oil-in-placed may be held within an extensive fracture network on a variety of different scales rather than within the matrix porosity of the formation. Understanding of the fracture distribution and connectivity within basement reservoirare the main toolsto improve exploration and production.This information will not be useful unless those fractures are characterized and a reliable fractured basement reservoir model is built.

1.4 Motivation

Fractured reservoirs hold large petroleum reserves in the world, yet they are still poorly understood. Additionally, several of those basement fields are producing for more than 30 years with a total production of more than 0.5 billion barrels of oil. The current revolutions in data acquisition, hardware computer processing capabilities and software's for data analysis and integration lead for more discoveries of such type of traps.The availability of the 3D seismic and well data that penetrated basement encouraged and further motivated theconduction of this study.

1.5 Objective

Since 2007 hydrocarbons in fractured basement reservoir were reported in many locations in Sudan and the area of study is one of those areas. The mapping of fault and fracture in the area of study is therefore an important step towards quantifying the hydrocarbon potentialityin the region. The objective of this study is to characterize and model fractures system within the basement reservoir in Ruman area through better understanding of their origin, distribution and connectivity.

1.6 Methodology

To achieve the objective of this study, four types of datasets were used. Data used in this study includesFormation Micro-Imager (FMI) of five wells. The other types of data are 3D seismic data, gravity data and satellite images for the outcrops.

Fractured reservoir characterization and modeling cannot be completed unless clear understanding of the types and causes of fractures are understood.Unraveling the complexities of the fracture systems requires a systematic approach integrating all available data forms. In this study the following scheme of fractures study was developed and used (Figure 1-3).

1.6.1 Fracture Characterization

Fracture characterization is the first step of a reservoir study, preparing data for modeling stage. The aim of Natural Fracture Reservoir (NFR) characterization is to determine fracture properties at well locations as well as correlation and interpolationthroughout the inter-well regions.

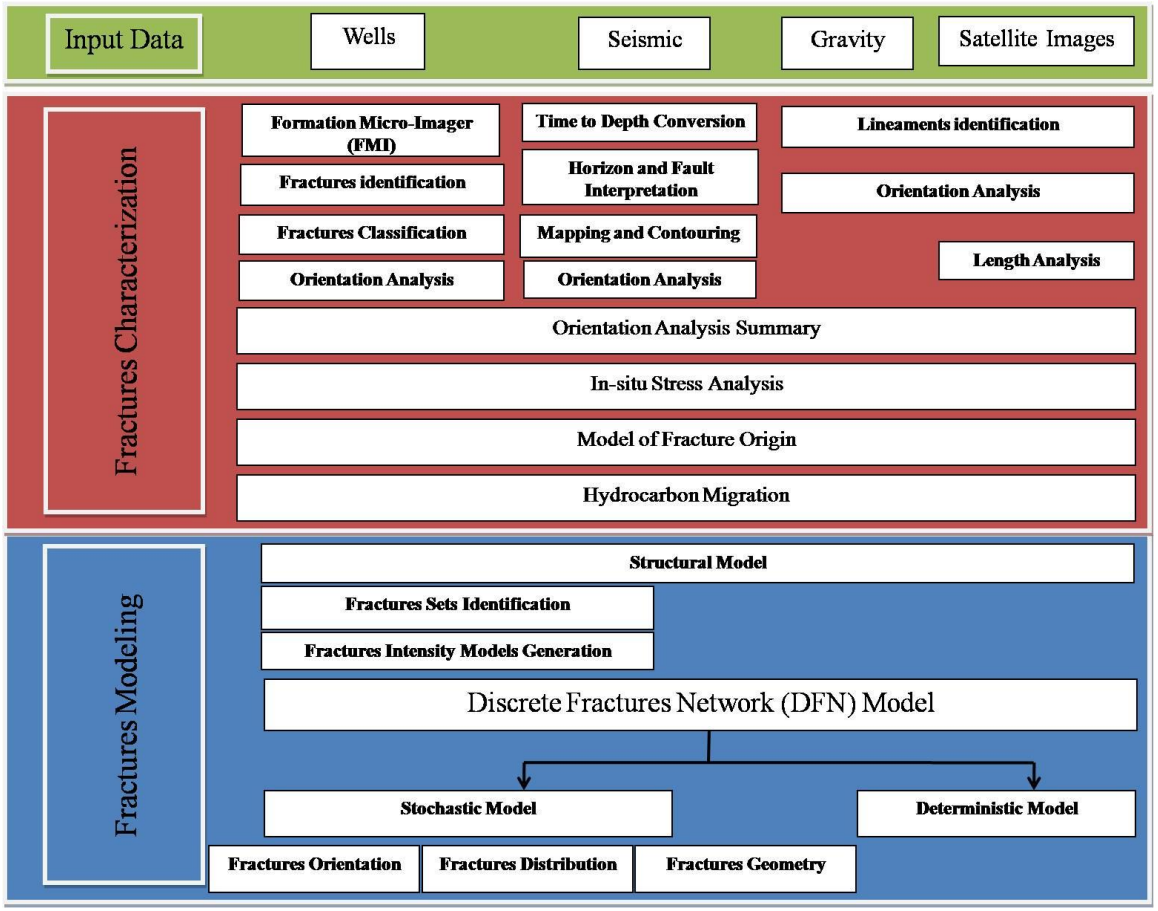

Figure 1-3: Flow chart showing the approaches and objectives

In doing so, it is essential that all available field data be effectively combined and utilized. Fracture Characteristics include fracture identification, orientation, distribution and geometry. To characterize fractures associated with basement reservoir the following procedure was followed:

1.6.1.1 Fracturesand Lineaments Defined from Gravity Data

Gravity data helps to understand the general configuration of the basin and used to interpret the regional faults and the general orientation of lineaments. Gravity data measures variations in the Earth's gravimetric field caused by variations in density of the underlying rocks. It provides information on numerous dense sources, including deep sources such as the structure and composition of dense basement and shallow sourcessuch as faults, dykes and sills, as well as cultural features. Standard Free-air and Bouguer anomaly images will contain information from all these sources. Gravity lineaments were interpreted from data set of land gravity using Bouguer anomaly with grid cell size 2km and also by using satellite gravity with low resolution 5 km. It helps to understand the general lineaments orientation and length in the study area.

1.6.1.2 Faults Defined from Seismic Data

Seismic data represent the main source of the interpreted faults in the study area. Fractures identification from seismic data conducted by several steps, started by converting the 3D seismic cube from time to depth domain using wells and seismic velocity data. The previous step followed by interpreted the basement top from well data and tie it with the seismic data, after that interpretation of basement top horizon was

conducted parallel with the fault picking. Finally mapping and contouring were conducted.

1.6.1.3 Fracturesand Lineaments Defined from Satellite images Data

Satellite images of the basement outcrops around the area of study; represent the outcrops analog of the subsurface basement.

Analysis of trends, lengths and nature of lineaments within the outcrop can help to understand the characteristics and behavior of the subsurface fractures associated with the basement reservoir. A digital GIS database has been generated for the surface lineaments using satellite images and trendsanalysis for those lineaments were conducted using rose diagrams. Lengths were also measured for all the interpreted surface lineaments and length analyses conducted using different techniques of stochastic modeling parameters.

1.6.1.4 FracturesDefined from Well Data

The foundation of the fracture modeling relies mostly on the Formation Micro-Imager (FMI) data interpretation that provides high-resolution picture of near borehole resistivity. This image of borehole geometries allows features like fractures and some intrusive contacts to be described and classified. Moreover, fracturesgeneral attitudes and trends are determined from well data.This information allows statistical analysis and builds diagrams related to fracture density and distribution and illustratesdata related to fractures fabric. Statistical analysis of fracture intensity (number of fractures per unit of volume, 1/m3) was also conducted using logs data to help in fracture modeling.

1.6.1.5 Model of Fracture Origin

To identify the origin model of those faults and fractures within the basement, lineaments (fractures) extracted from gravity, seismic, satellite image and well data were analyzed base on their orientation. GIS framework was used to analyze the outcrops lineaments, and categorize them based on their orientation.

1.6.1.6 In-situ Stress Analysis

An additional step which is often of value in basements is to determine whether present day in-situ stress is acting to dilate apertures and hence promote fracture permeability on particular fracture orientations. During this study, fractures were tested regarding the current stress direction.

1.6.1.7 Hydrocarbon Migration

Basement prospects are usually structural highs, with substantial vertical relief. Fractured basements are commonly believed to be charged through the flanks or through thetop of the basement structure. During this study, hydrocarbon migration were tested and analyzed.

1.6.2 Fracture Modeling

Fracturemodeling consists of many steps starting from analyzing thefracture properties and defining different fracture sets, generating theintensities of the different fracture sets based on comparisons withfield data and finally generating the discrete fracture network.

1.6.2.1 Geo-cellular Model Description

For better representations of fractured reservoir, model geometry was built based on the basement tops from wells and the seismic interpretation of the basement horizon.

1.6.2.2 Analyzing Fracture Properties

Data from the five wells were imported and analyzed inPETREL software (Schlumberger, 2009).Fractures orientation (dip angle and dipazimuth) were imported, together with their positions into the wells.

1.6.2.3 Fracture Sets Identification

The fracture data were analyzed in a stereonet, which plots the poleto the fracture plane characterized by its dip and azimuth.

1.6.2.4 Fracture Intensities Generation, Upscalling and Simulation

Using the fracture sets identified in the previous step, the next step was to find how fracture intensity varies vertically and horizontally in the area of study.

1.6.2.5 Discrete Fractures Network (DFN) Model Construction

A fracture network is a group of planes representing fractures. Fractures are two scales, seismic scale and sub-seismic scale fractures. Inthis study, the sub-seismic fractures of the same type and generated at the same time are grouped into a fracture sets and then modeled stochastically.The seismic scale (faults) were interpreted from seismic data, and then modeled deterministically as a separated fracture set.

CHAPTER TWO

GEOLOGIC AND TECTONIC SETTING

2.1 Geology of NE Africa

The Precambrian basement of Sudan and adjacent areas of NE Africa comprises twodistinct major geodynamic systems. These are the Archean-Early Proterozoic high-grade gneisses of sialic nature, which were reworked during the Pan African tectono-thermal episode (Schandelmeier et al., 1987a; Vail, 1982), and the Late Proterozoic juvenile low-grade mobile belts comprising volcano-sedimentary sequences and ultramafic remnants of island arc affinity (Vail, 1982).

The Archean-Early Proterozoic high-grade gneisses and migmatites with interfolded supracrustal meta-sediments comprise most of the basementexposures west of the River Nile in Sudan, is referred to as the Nile Craton, the Sudan Shield (Kroner, 1975; Vail and Hughes, 1987), and East Sahara Craton.

These high-grade rocks were recorded at various localities in the interiors of Sudan. Schandelmeier et al., (1983) reported such rocks in the CebelUweinat area near

the border between Sudan, Egypt and Libya. They are also studied in the WadiHawar and Nubian Desert (Abdel Rahman et al., 1993; Schandelmeier et al., 1987a). Similar rocks have been described in the Nuba Mountains (El Ageed and El Rabaa., 1981), and from the Ingessana-Kurmuk area (Abdel Rahman et al., 1993). On the other hand the low-grade juvenile rocks are mainly exposed east of the Nile and they constitute part of the northern extent of the Late Proterozoic Arabian-Nubian Shield (Schandelmeier et al., 1987b; Vail, 1982).

The development of the Late Proterozoic juvenile mobile belts (Arabian-Nubian Shield) in NE Africa began initially with rifting in proto-oceanic basins followed by formation of several island arcs, and by later growth of Andean-type magmatic arcs. The closure of the oceanic basin resulted in the accretion and coalescence of these arcs. Subsequently the whole system collided with the ancient east African coast. These processes led to crustal thickening and shortening, calc-alkaline magmatism, emplacement of ophiolitic belts, thrusting, shearing and strike-slip faulting.

The structural development of the Central and East Sahara Craton in NE Africa began in the Late Archean. This area has undergone various crustal deformation events in Early and Middle Proterozoic, completed under the Late Proterozoic Pan African Tectono Thermal Episode. These deformational events comprise the early three-stages deformation events during the Early to Middle Proterozoic (Schandelmeier et al., 1987a), characterized by an initial folding at about 2100 Ma, drift and rotation of Gondwana at around 2000 Ma and the subsequent formation of transcontinental shear zones. The collision of North African continental plate with the West African craton during the Late

Pan African Episode generated a compressive stress at the margin of the plate which resulted in the formation of transcontinental shear zones during that time.

2.2 Regional Geology of Sudan

The geology of Sudan comprises four major geological units (Vail, 1982; Vail et al., 1990), namely are:

1- The Basement Complex, comprising highly folded and metamorphosed ortho- and para-gneisses and schist's intruded by syn- and late- to post-tectonic, of subduction related calc-alkaline bimodal granitoid complexes it called batholithic granitoids.

2- An-orogenic high-level alkaline igneous complexes comprising gabbros, granites and syenites with associated volcanics, a lot of them are in the form of well-developed ring complexes.

3- Extensive Phanerozoic sedimentary strata, forming a largely undeformed cover to the basement rocks and to some of the intrusive complexes.

4- Cenozoic midplate basaltic volcanism which occurs as discrete volcanic centers alone or in associated fields, and plateaus of basaltic flows associated with the East African Rift Valley magmatism.

Sudan geology (Figure 2-1)(GRAS, 1988) is diverse with a combination of metamorphic, igneous and sedimentary rocks.Sudan basins are largely underlain and surrounded by Precambrian rocks, particularly in the southwest, centre and northeast, which were almost exclusively reactivated during the Neoproterozoic Pan-African tectono-thermal event (from 1200 Ma to 500 Ma). Large parts in the north of the country

are covered by continental clastic sequences of the predominantly Mesozoic Nubian cycle (previously Nubian Sandstone), and in the south by Tertiary to Quaternary unconsolidated superficial sediments. In north and northwestern part of Sudan, the oldest sedimentary basins were encountered and it isfrom the Cambro-Ordovician age (Whiteman, 1971).Data from Mesozoic basins such as surface geology, regional gravity and magneticindicate that these basins are deep and filled by thick column of continental sediments duringthe Mesozoic time. The gravity, seismic and drilling data acquired in interior Mesozoicbasins in the central and southern Sudan indicated that more than 13,000 meters of clasticsediments occur within the deepest central trough of these rift basins (Schull, 1988).

2.3 Geology of the Study Area

The Melut Basin is characterized by flat plains. This plain area is underlain and surrounded by regionally metamorphosed Precambrian and Paleozoic rocks and minor (syn-late- to post-tectonic) Mesozoic/Cenozoic intrusive and extrusive igneous rocks. These rocks are exposed inthenorthwest and the northeast of the study area in the Nuba Mountains and Ingessana Hills, respectively (Figure 2-1 and Figure 2-2) (GRAS, 2005).The surrounding basement terrains represent the source area for the sediments filling the Melut Basin (Schull, 1988). The basement rocks around Melut basin is predominantly of Precambrian metamorphic rock with limited occurrences of intrusive igneous rocks (Schull, 1988).

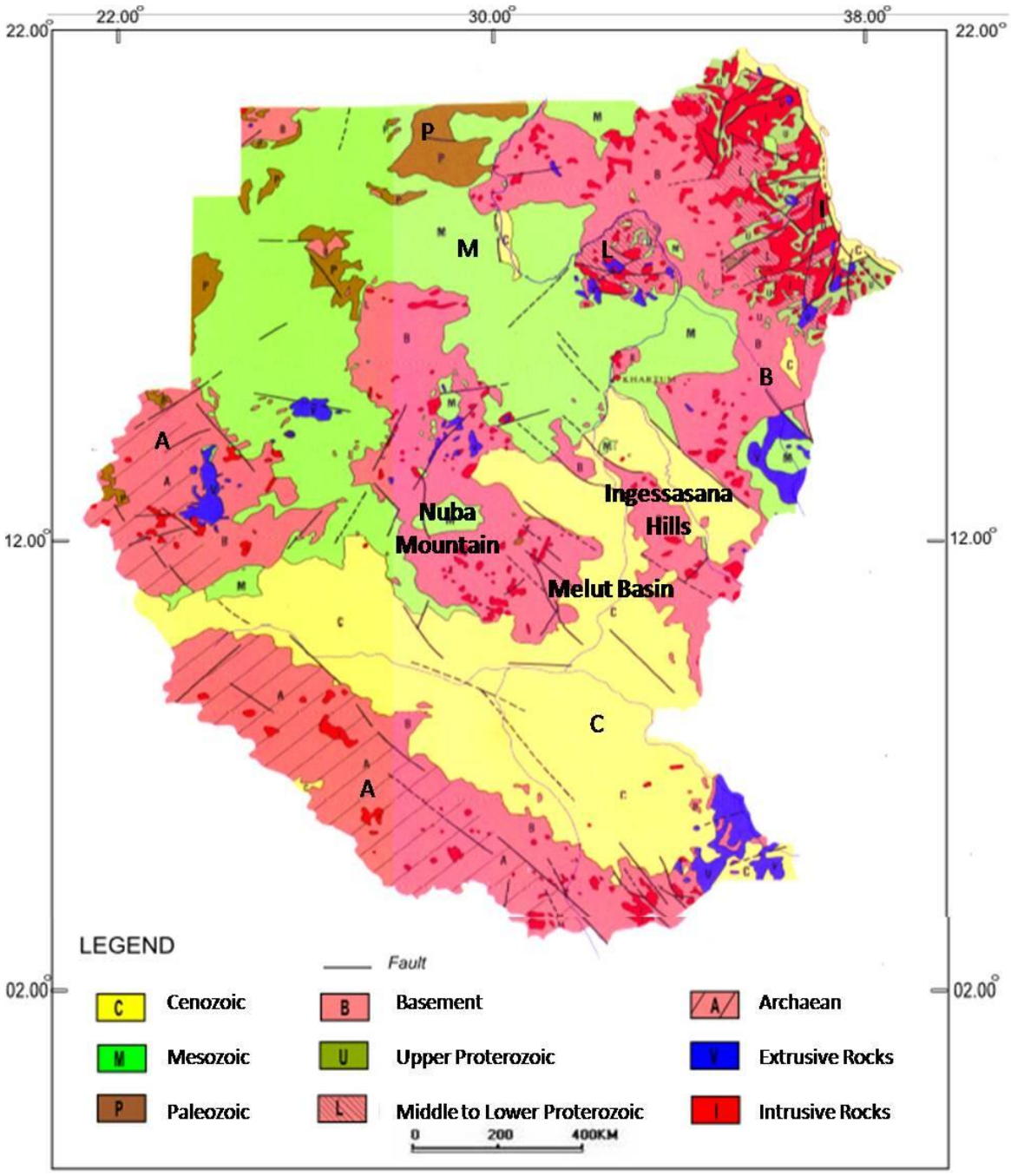

Figure 2-1: Geological map of the Sudan showing the diversity of Sudan geology with a combination of metamorphic, igneous and sedimentary rocks. It show also Melut basin, Nuba Mountains and Ingessana Hillslocations (after GRAS, 1988)

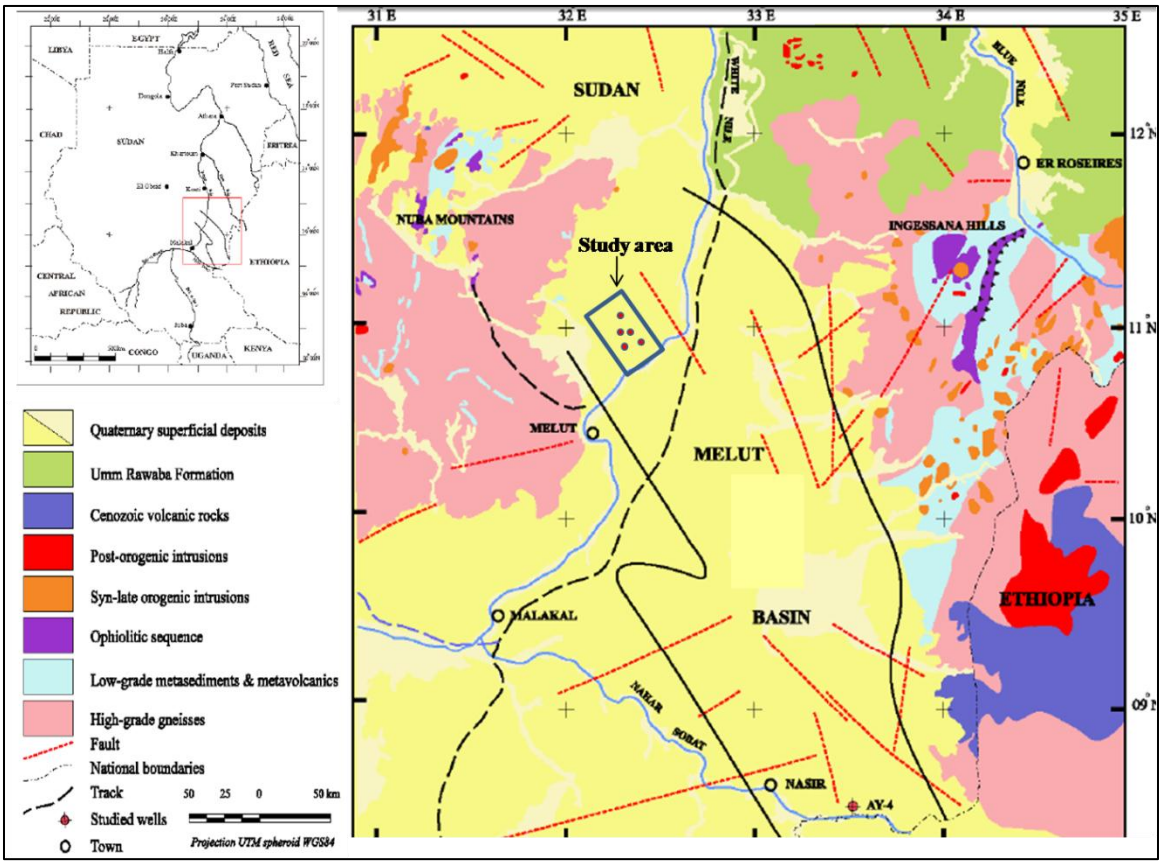

Figure 2-2: Geological map of the study area and vicinity, showing Melut basin, study area and Ruman wells (modified after GRAS, 2005)

The primary composition of the rocks is granitic or granodioritic gneiss that dated to 540 Ma ± 40 Ma(Schull, 1988). Basement rocks underlying the Melut basin belong to the "Juvenile belt" of the Arabian-Nubian shield. The basement rocks assemblage comprises various types of granitoids, schist, marbel and mafic ultra-mafic materials that altered in different degree to serpentine, talc and carbonate materials that altered in different degree to serpentinite, talc and carbonate materials. The K/Ar isotope age determination made for basic igneous rock retrieved from one well in the area revealed age of 551 Ma± 21 Ma (Schull, 1988). The Basement has been penetrated and cored in two wells and interpreted as granodioritic gneiss (Schull, 1988). The Basement Type in North Melut basin generally composed of metamorphic and igneous rock granodioritic gneiss and some dolerite dykes (Schull, 1988).

2.3.1 Basement Complex of Nuba Mountains

As we mention before, the basement complex of Sudan includes reworked Precambrian inliers reactivated during Pan African tectono-thermal activities, namely the Nuba Mountains (Figure 2-1 and Figure 2-2), the Darfur block, Bayuda and Nubian deserts. The NE Nuba Mountains is composed of high-grade gneisses and low-grade green-schist volcano-sedimentary sequence. The contact between this two rock types is marked by the Kabusophioliticmelange zone (Abdelsalam and Dawoud, 1991) (Figure 2-3). Based on many studies done by Abdelsalam and Dawoud (1991); Abdelsalam et al., (2002); El Ageed and El Rabaa., (1981); Vail(1972); Vail and Sadig(1987); Whiteman(1971), the stratigraphic and tectonic subdivisions of the Basement Complex of the NE Nuba Mountains can be described from older to younger as: High-grade gneisses,

Low-grade green-schist-faciesassemblage, Kabusophioliticmelange rock assemblage, Syn-late orogenic granites and Post-orogenic granites.

On the regional scale, the boundary between theNubian Shield and theSaharan metacratonis marked by N-S trendingsuture extending from the Bayuda Desert in thenorth to theNuba Mountains to the south. This suture can also beextended southward to the western margin of theMozambique Belt in northwestern Kenya.(Abdelsalam et al., 2003; Abdelsalam and Dawoud, 1991) (Figure 2-4).

The gneisses are exposed as low-lying outcrops, cover in some places by a thin sedimentary cover of Quaternary age. They comprise mainly quartzo-feldspathic gneisses commonly associated with small lenses of concordant amphibolites and local migmatites (Vail, 1978).

The second unit of the basement rocks comprises the low-grade greenschist-facies assemblage (meta-volcanic and meta-sediments) that includes marble, mica schist, quartzites, graphite and chlorite schist's. They occur as low isolated outcrops generally delineating the configuration of the fold structures and forming intercalated bands of meta-sedimentary and meta-volcanic rocks that probably represent different depositional and volcanic eruption phases (Abdelsalam and Dawoud, 1991).The ophiolite zone marks the suture between the low-grade green-schist-facies assemblage (island arc terrain) and the high-grade gneisses of continental origin in the northeastern Nuba Mountains. The rocks of this unit occur as discontinuous lenticular bodies in an imbricate structure (Abdelsalam and Dawoud, 1991).

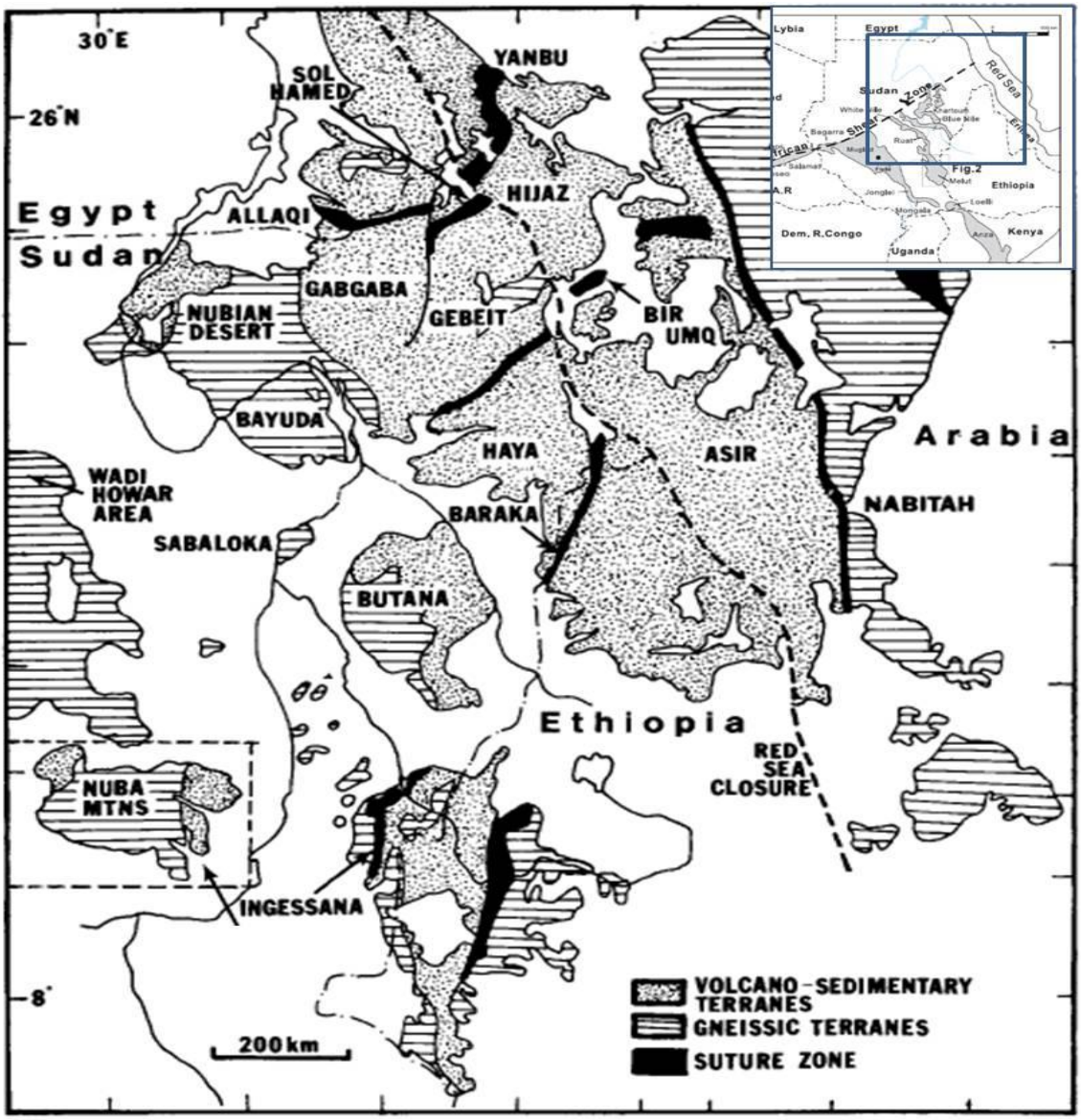

Figure 2-3: Sketch map of the Arabian-Nubian Shield with the Red Sea closed, showing the contact between high-grade gneisses and low-grade green-schist (after Abdel Salam andDawoud, 1991)

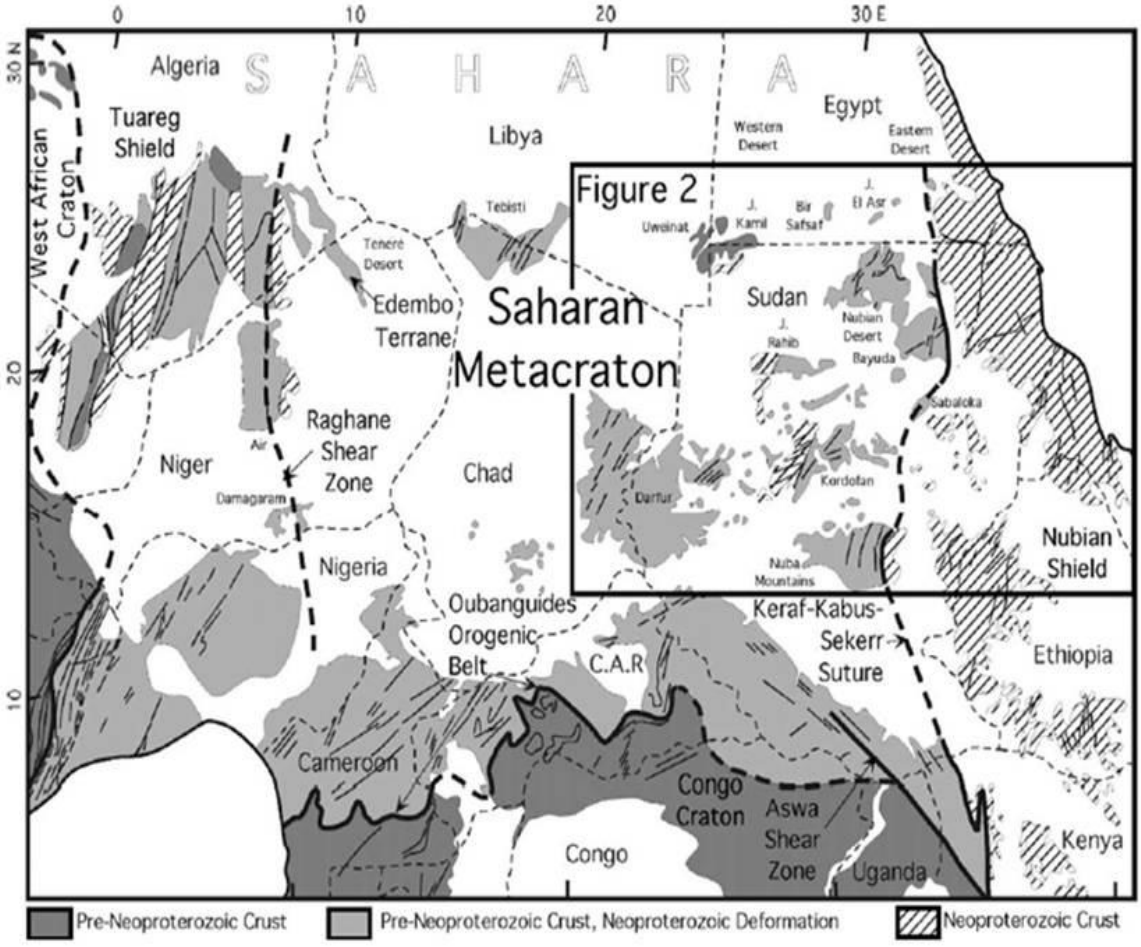

Figure 2-4: The Nubian Shield and the Saharan metacraton marked by N-S trending suture zones (dotted line) (after Abdelsalam et al., 2003)

The older metamorphosed basement rocks were intruded by syn-late orogenic granites, whichpredate the younger post-orogenic igneous complexes of the Sudan (El Ageed and El Rabaa., 1981).The youngest unit of the basement complex is the post-orogenic granite reported from the northern Nuba Mountains. These are non-foliated, shallow-level granitic bodies and volcanics that occur as ring complexes and discrete bodies, intruded during the Paleozoic around 542 Ma (Vail, 1982). The tectonic evolution of the Eastern part of Nuba Mountains occurred in deferent stage through the time, starting from the development of intra- oceanic Island arc over a westerly dipping of subduction zone of oceanic crust and development of the marginal between the arc and the continental crust to the west (Figure 2-5A) then the marginal basin begins to close with the continuity of the compression force and the subduction zone migrates westward with addition to development of Andean type arc over the continental crust (Figure 2-5B) after that the marginal basin totally collapsed and kabusophioliticmelange appeared with period of erosion (Figure 2-5C). El Ageed and El Rabaa (1981) in his correlation of Pan African lithostructural belts in the northeast Nuba mountains implied a twofold subdivision of the basement into a lower cratonized gneissic group, which may represent an older ensialic basement, possibly of earlier Precambrian age, overlain by an upper mobile geosynclinalmetasedimentary and metavolcanic assemblage with late- and post-orogenic igneous phases. Regional correlation with African orogenic belts suggests that the gneissic group may be part of an older, deeply eroded basement succession (probably Mozambiquian), whereas the geosynclinals sequence may be part of an aulacogenic Pan African “basement”.

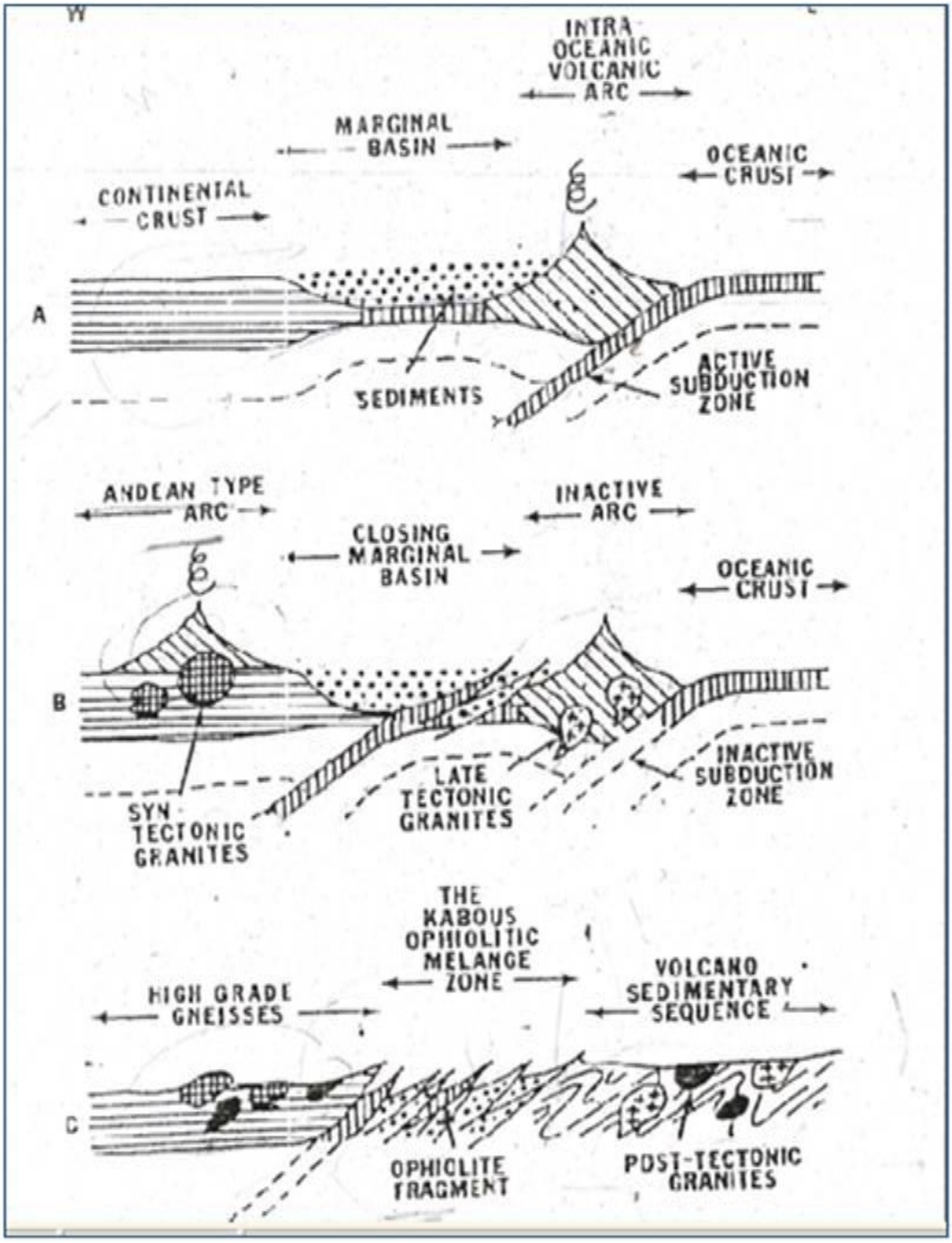

Figure 2-5: Schematic diagram showing the tectonic evolution in East Nuba Mountains (after Abdel Salam andDawoud, 1991)

Ahmed (1984) in his study of the Precambrian lineaments, concluded that, besides the curvilinear features, a strong pattern of Precambrian structures trending mainly N-S, NNW- SSE. As a result of this, the region was dissected into a mosaic of large basement blocks surrounded by tectonic zones of faulting and strong shearing. Faults along the lineaments zones seem to have been rejuvenated several times during the subsequent tectonic events which were active since post-Cretaceous until recent (Gass and Neary, 1975; Qureshi and Sadig, 1967; Vail, 1978).

2.3.2 Basement Complex of Ingessana Hills

The Basement Complex of the Ingessana area consists of quartzo-feldspathic gneisses in which bands of marble, mica-schist and quartzite are developed in places. Varieties of igneous rocks were intruded into the metamorphosed basement. The largest units of the basement rocks are foliated granites and granodiorites, which may be syn-late tectonic intrusions. They are in contrast to smaller cross-cutting unfoliated post-orogenic granite plutons (Vail, 1978). The most striking intrusive bodies are the numerous ultrabasic and basic rocks; the most significant is that of the Ingessana Hills.

2.3.3 Basement Description from Subsurface Data

The results of the petrographic analyses of samples from Ruman N1 and Ruman N2 wells indicate that the mineral composition is mainly composed of polycrystalline quartz and minor mono-crystalline quartz. Considerable quantities of hornblende and some amount of K-feldspar as well as abundant plagioclase, considerable amount of mica (mainly biotite) are also observed, and some amount of iron oxides. These mineral assemblages interpreted as Granodioritic gneiss.

In Ruman NE-1, core was cut and after analysis of the core data it is found two complexes of rocks, meta-sediments and meta-igneous rocks. At depth 1854 m, the meta-sediments was found (Figure 2-6) and interpreted as quartz-plagioclase-biotite-epidoteSchist. The texture isporphyro-blastic, foliated.At depth 2002 m, the meta-igneous was found (Figure 2-7) and interpreted as gneissic biotiteGranodiorite.

In Ruman NNE1, core was cut and after analysis of core data it is found one complex of rock meta-sediments. The meta-sediments were found in (Figure2-8) and interpreted as quartz-sericite Schist. The texture is likeblastic-grained, foliated.

2.3.4 Sedimentary Units of Melut Basin

The Paleozoic sediments were only reported from the far northwestern and northeastern Sudan (Klitzsch and Lejal-Nicol, 1984). Paleozoic sediments were also reported, near the Melut Basin, from west-central Ethiopia.

Mesozoic sediments were only known from the subsurface data within the stratigraphy of the Melut Basin (A brief account will see in Melut basin stratigraphic section). Adigrat Formation is the nearest outcropping Mesozoic unit it located in Ethiopia along the Blue Nile gorge, approximately 250 km east of the study area.

The Cenozoic sediments (Paleogene/Neogene) were found in subsurface in Melut basin, where the Umm Ruwaba Formation is Cenozoic sediments found in the surface. The Umm Ruwaba Formation represents the unconsolidated fluvial deposits of the White Nile drainage system in central and southeastern Sudan. The unit consists of unconsolidated sands, clayey sands and clays with some gravel beds and generally exhibits rapid facies variation (Eisawi and Schrank, 2008).

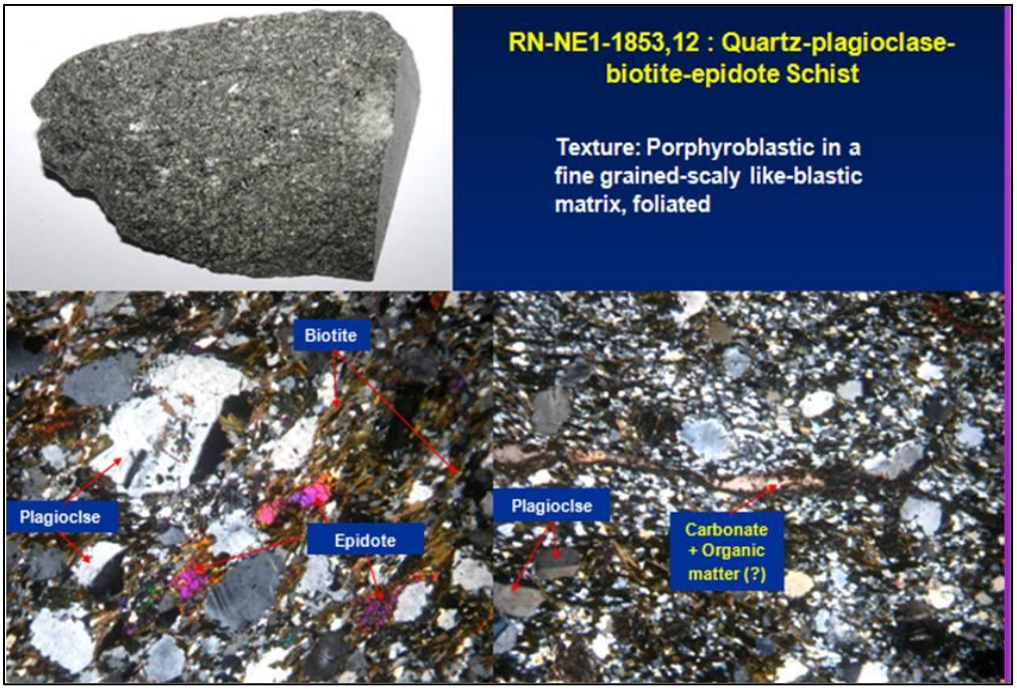

Figure 2-6: Show the meta-sediment rock (Schist) in well Ruman NE-1

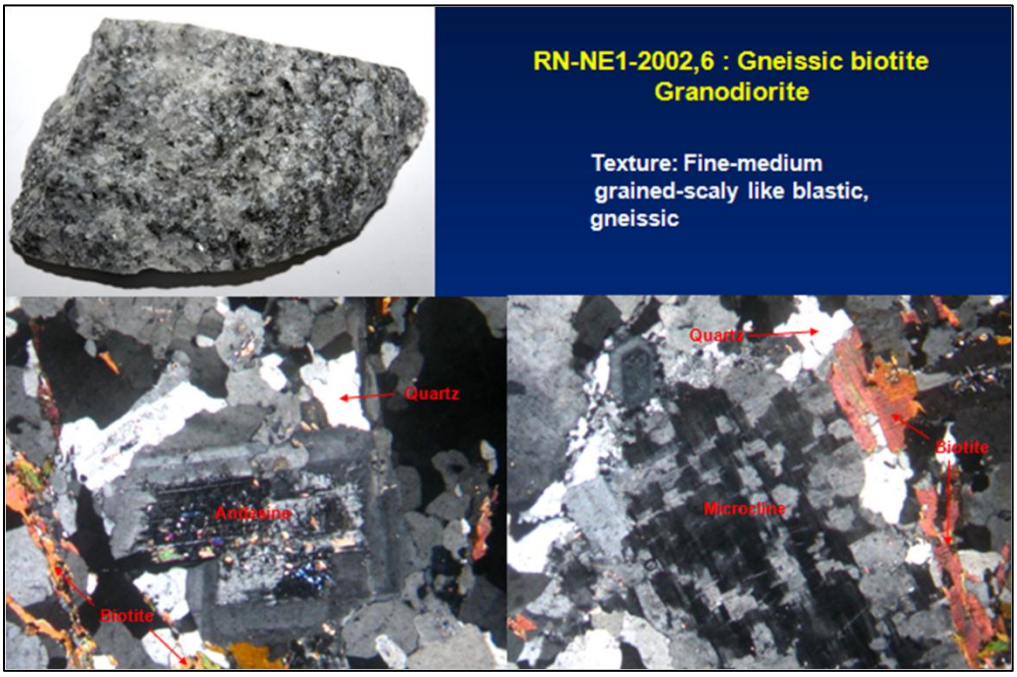

Figure 2-7: Show the meta-igneous rock (Gneissic BiotiteGranodiorite) in well Ruman NE-1

Figure 2-8: Show the meta-sediment rock (Schist) in well Ruman NNE-1

At the type locality (Umm Ruwaba village), the unit is 278.6 m thick but may attain a thickness of 335 m or more in the eastern Kordofan(Vail, 1988).

The Quaternary to recent sediments include all the active alluvial deposits in the south of Sudan and Wadi deposits older Alluvium represented by raised terraces and old channels in the northern part of the region.

2.4 Tectonic Setting

Africa has been affected by a long and complex history of rifting affected Africa since the Proterozoic. According to Browne et al. (1985) and Bosworth (1992), the tectonic evolution of the Sudanese interior rift basins is related to the Mesozoic-Cenozoic movements that reactivated the weak lineaments inherented in the fabric of the Pan-African mobile belts. Major phases of rifting were took place during the Mesozoic time (Jurassic-Cretaceous)resulted in the development of the West and Central African Rift Systemduring Jurassic-Cretaceous times (Figure 2-9) (Bosworth, 1992; Genik, 1993; Guiraud and Maurin, 1992; Schull, 1988). The central and southern Sudan interior rift basins are defined by an extensive rift that began to develop in the late Jurassic to Early Cretaceous time) (McHargue et al., 1992; Schull, 1988). The development of these rift basins attributed to processes operated not only within the central areas of Africa, but also along the eastern and western continental margins of Africa, and associated with the separation of west and east Gondwana. In early Cretaceous (late Jurassic?) and to the west, the African and South American cratons began to separate (Fairhead, 1986; Schull, 1988). As a consequence of these major events, shear reactivations along the central African shear zone developed which has led to the development of a parallel and sub parallel half grabens of predominantly NW–SE orientation in the central and southern

Sudan craton area (Figure 2-9). Sudan rift basins are composed of a complex system of linked extensional and trans-tensionalsub-basins that typically have a half-grabengeometry and modified by subsequent reactivation during younger rift cycles (McHargue et al., 1992).The Central African Rift System exhibits a major ENE-oriented strike-slip zone showing a dextral movement.

The Central African Rift System extends from the Gulf of Guinea toSudan and Kenya (Bosworth, 1992; Browne and Fairhead, 1983; Genik, 1993). The Central African Rift System is represented by the Doba, Doseo, Bagara, Muglad (southern Sudan), Melut (White Nile), Khartoum (Blue Nile) and Atbara rifts (Figure 2-9). The Central African Shear Zone crosses the continent from Cameroon into northern Sudan, marking the northern termination of many basins. Along its track many "pull-apart" basins are observed (Bosworth, 1992) (Figure 2-9).

Multiphase of rifting resulted in a variation in the regional stress field, generally this also is control the evolution and development of individual rift basin with a unique history of each rift basin due to local influences.

According to Schull (1988) the tectonic evolution of the Interior Rift Basins in Sudan can be divided into five phases:Pre-Rift Phase, First Rift Phase, Second Rift Phase, Third Rift Phase and Sag Phase.

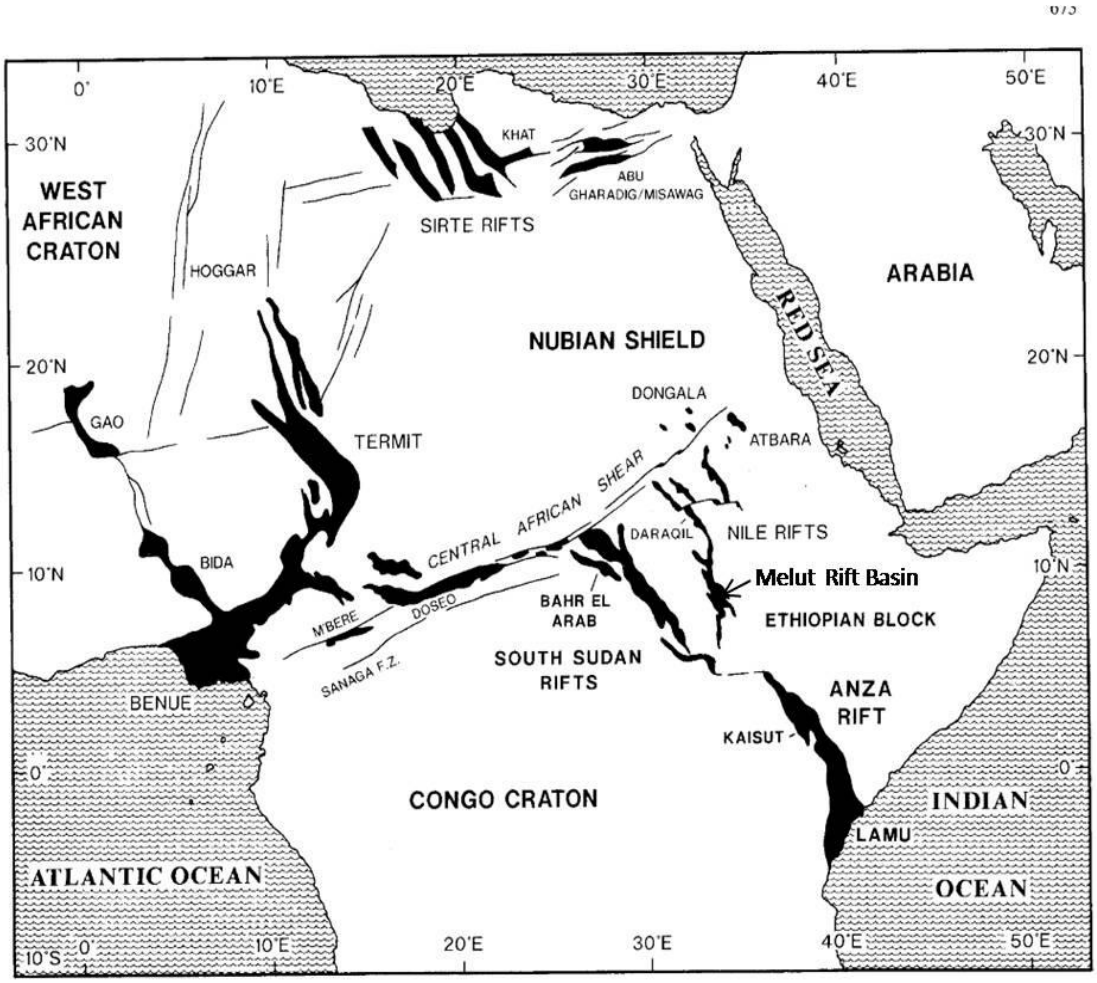

Figure 2-9: Location map of the north-east African rift basins, showing Melut basin (after Genik, 1992)

2.4.1 Rift and Sag Phases in Melut Basin

The Melut Basin located in the south east part of Central African Shear Zone CASZ. It is an intra-continental Cretaceous-Tertiary rift basin formed due to the strike-slip and associate pull-apart structure took place along the CASZ during the Early Cretaceous on the consolidated craton(Binks and Fairhead, 1992; Guiraud and Maurin, 1992; McHargue et al., 1992) (Figure 2-10).

The recognition of the rift episodes is based on identification of three regional correlative depositional cycles which are practically evident in the Melut Basin. Each cycle boundary is regionally or locally expressed by an angular unconformity(McHargue et al., 1992).

As indicated earlier Africa has been affected by a long and complex of rifting since the Proterozoic time. According to Bowne (1985), the tectonic evolution of Melutbasin is related to the effects of Mesozoic-Cenozoic movements which were reactivation of the weak lineaments inherented in the fabric of the Pan-African mobile belts.

Pre-rift phase weakness zones were mainlyresult due to the development of the Late Proterozoic juvenile mobile belts (Arabian-Nubian Shield) in NE Africa. The shield began initially with rifting in proto-oceanic basins followed by the formation of several island arcs, and by later by the growth of Andean-type magmatic arcs. The closure of the oceanic basin resulted in the accretion and coalescence of these arcs. Subsequently the whole system collided with the ancient east African coast.

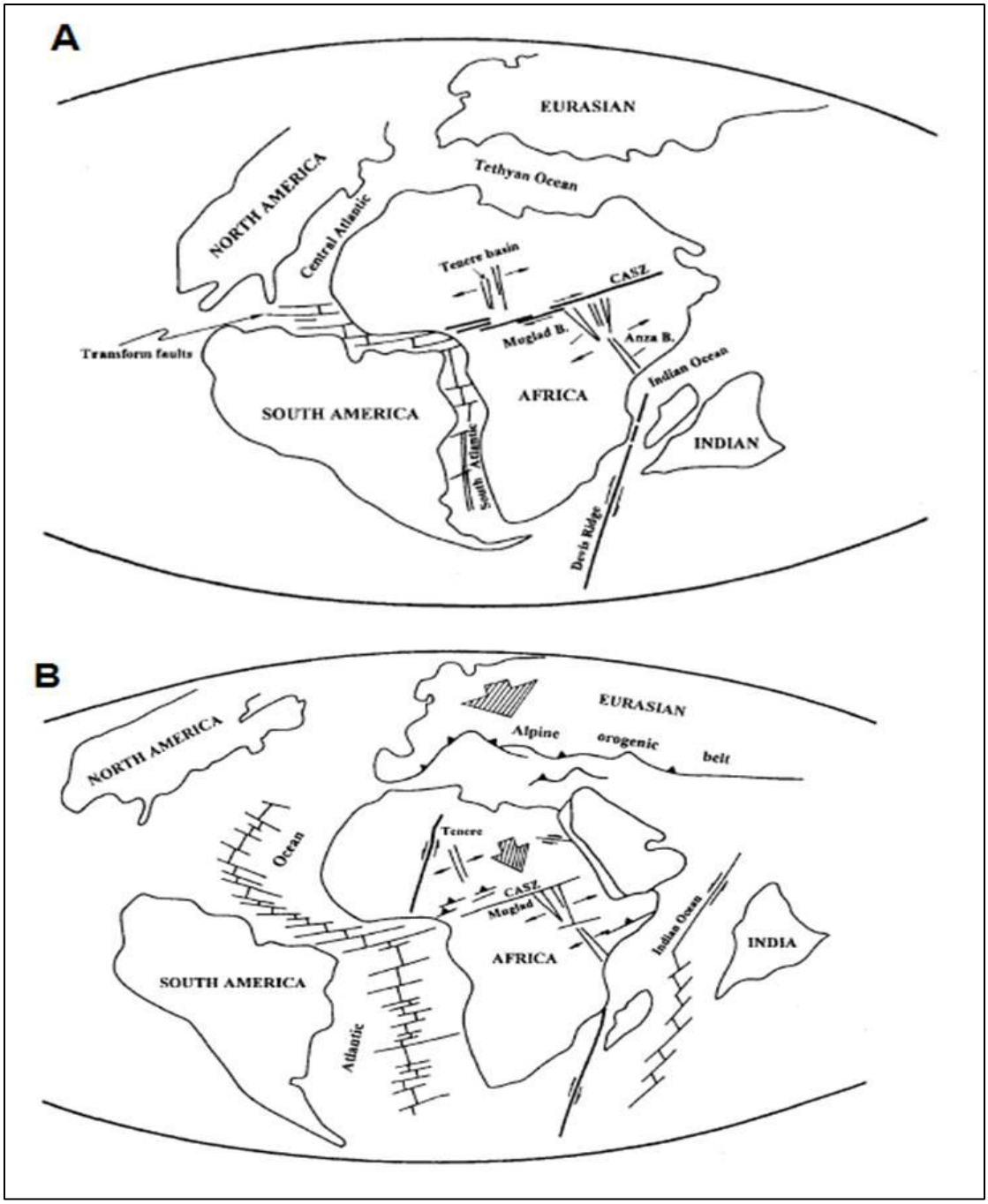

Figure 2-10: Regional tectonic setting of Africa (A) Early Cretaceous. Note that transform faults extend into the African continent, leading to strike-slip faulting of Central African Shear Zone (CASZ) and initiation of Sudanese rifts. (A) Late Cretaceous(B) Late Cretaceous collision of Eurasian and African plate along the Alpine orogencreats NW-SE oriented compressional stress, and induces NE-SW oriented tensile force, leading to subsidence of Muglad basin (McHargue et al., 1992)

These processes led to crustal thickening andshortening, calc-alkaline magmatism, emplacement of ophiolitic belts, thrusting, shearing and strike-slip faulting. The boundary between theNubian Shield and theSaharan metacratonis marked by N-S trendingsuture extending from the Bayuda Desert in thenorth to theNuba Mountains to the south (Abdelsalam and Dawoud, 1991); this represents the N-S weakness zones that reactivate later by Mesozoic-Tertiary rifting. The basement rocks in and around the Melut basin during the end of Pan-African orogeny became a consolidated platform (Schull, 1988).

During the Paleozoic and early Mesozoic, these high areas became the source of sediments of the adjacent lowlands areas.

The first Rifting phase (Early Cretaceous 130-96 Ma)was the most significant rifting episodes. It resulted in the deposition of freshwater large lacustrine basin. The origin of this rifting is generally related to the break-up of Gondwanaland and the opening of the South Atlantic and Indian Oceans starting about 130 Ma (Schull, 1988). Lacustrine shale, which considered beingtheoil source, was accumulated at mid of the lower Cretaceous formation. The termination of the initial rifting is marked by basin wide deposition of lower Cretaceous formation thick sandstone deposits. Two stages of sub-rifting developed during the Early Cretaceous (Fairhead, 1988; Guiraud and Maurin, 1992); (Figure 2-11). The first sub-rift start during the Early Cretaceous (Barremian) the major extension Start by NNW-SSE to N-S (Guiraud and Bosworth, 1997). It caused the development of WNW-ESE to E-W trending lineaments parallel to the Central African Shear Zone (Figure 2-11) EW or ENE-WSW. The second sub-rift was developed during the Early Cretaceous (Albian), a major phase of NE-SW extension occurred in the

Melutarea due to the opening of the South Atlantic Ocean (Figure 2-11) (Guiraud and Bosworth, 1997). It caused the development of NW-SE to NNW-SSE trending lineaments.

The second rifting phase occurred in late Cretaceous (96 Ma to 75 Ma) characterization by the widespread deposition of lacustrine and floodplain claystone and siltstone, and the end of this phase are represented by the deposition of an increasingly sand-rich sequence that concluded thick Paleocene sandstone, the Melut formation. This phase was accompanied by minor volcanism. During this rifting, the NW–SE trending faults were reactivatedby the NE–SW extensional stress (Fairhead, 1988).

The final rifting phase began in the Paleocene and is characterized by thick lacustrine and floodplain claystone and siltstone. The Samma, Yabus and Adar formations were developed during the third rift. Late Eocene basalt flows have been found in the south of Melut Basin near Ethiopia. The third rift was terminated by a regional unconformity which ushered in the post rift phase (Fairhead, 1986, 1988). NE-SW trending faults occurred as a result of Tertiary extension during the opening of the Red Sea.

The sage phase (Neogene - Quaternary) occur after Eocene-Oligocene, the basin entered into an intracratonic sag phase with very gentle subsidence accompanied little or no faulting till the Quaternary.

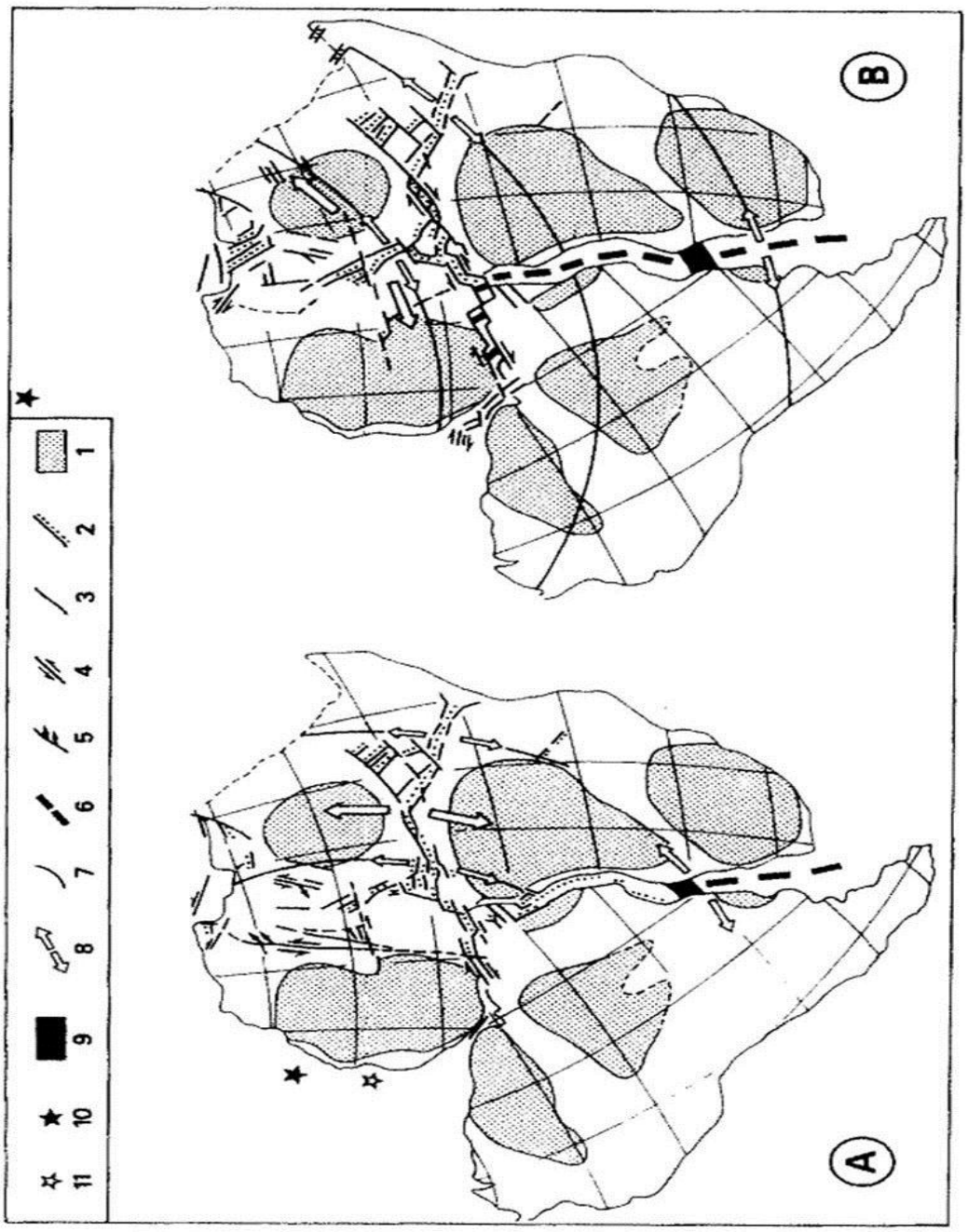

Figure 2-11: Two stage development of African rifts during Early Cretaceous. (A) Barremian. (B) Albian. I = Craton; 2 = rift; 3 = active fault; 4 = major strike-slip fault; 5 = compression zone at the end of wrench fault; 6 = oceanic crust; 7 = flow line; 8 = extension direction; 9 = Walvis-Rio Grande Ridge; 10 = pole of rotation (after Fairhead, 1988; Guiraud and Maurin, 1992)

2.4.2 Structural Style in Melut Basin

Based on gravity, aeromagnetic and seismic data, Melut basin can be divided into the Northern, Eastern, Central, Western and Southern sub-basins and the Central High (Dou et al., 2007).

Thick-skin faults (basement involved,originating within the deep crust or mantle) and thin-skin faults (restricted to sediments only) are responsible for the structural development of half-graben rift-basins in Sudan (Mann, 1989). The low-angle listric normal faulting is responsible for the mostSudanese riftbasins development (Mann, 1989).Thick-skin faults form the basins and providethe half-graben holes, into which thousands ofmeters of sediment are deposited (Mann, 1989). Thin-skin detachment faults are antithetic to thick-skin faults. Thin-skin detachmentshave been recognized in the sediments on passivemargins; termed slumps or growth faults; they areoften associated with salt or shale flowage, activedeltas, or slumping of the shelf sediments.Melut basin exhibit typical rift extensional tectonic feature with strike-slip compressional effects. Major fault trends throughout the basin are NW-SE to NNW-SSE, oblique to the main basin axis (Mann, 1989). The North part of Melutbasin shown in (Figure2-12 and Figure 2-13) illustrates the resulting half- grabenbasin shapes developed by the thick-skin crustal detachment faults, Mann 1989. Extension stress toward the NE- SW directions.The tilting, subsidenceand extension of each sub-basin is developed byseveral listric shaped thick-skinnormal faults (Mann, 1989). The resulting basins are steep half graben, approximately10-15 km wide and several tens ofKms long.

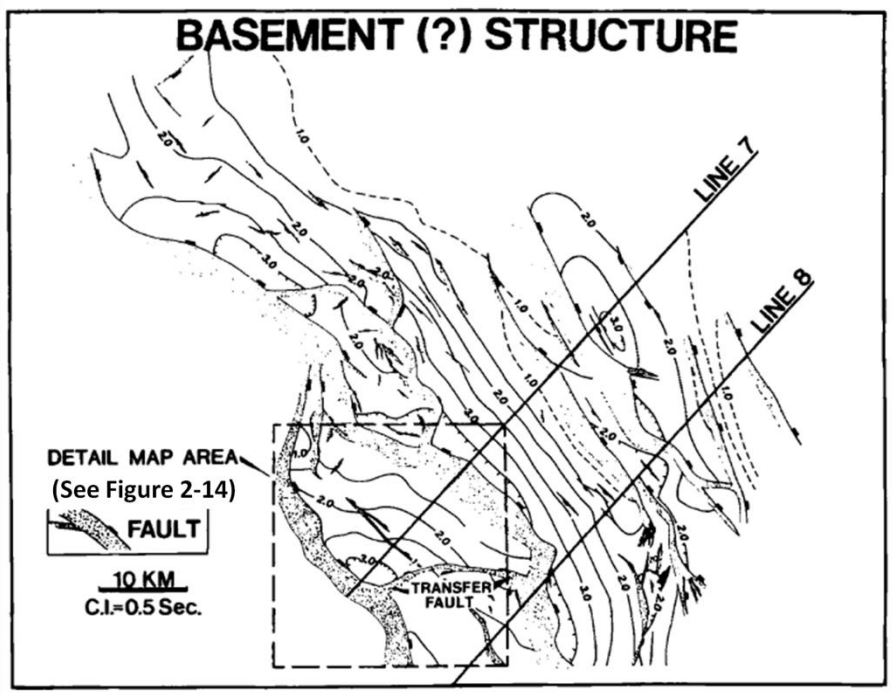

Figure2-12: Basement Time Structure Map constructed from an extensive seismic data illustrates the shapes of the thickskin faults. Faults connect to deep detachment. Fault movement is transferred from one fault to another by means of listric transfer faults (after, Mann 1989)

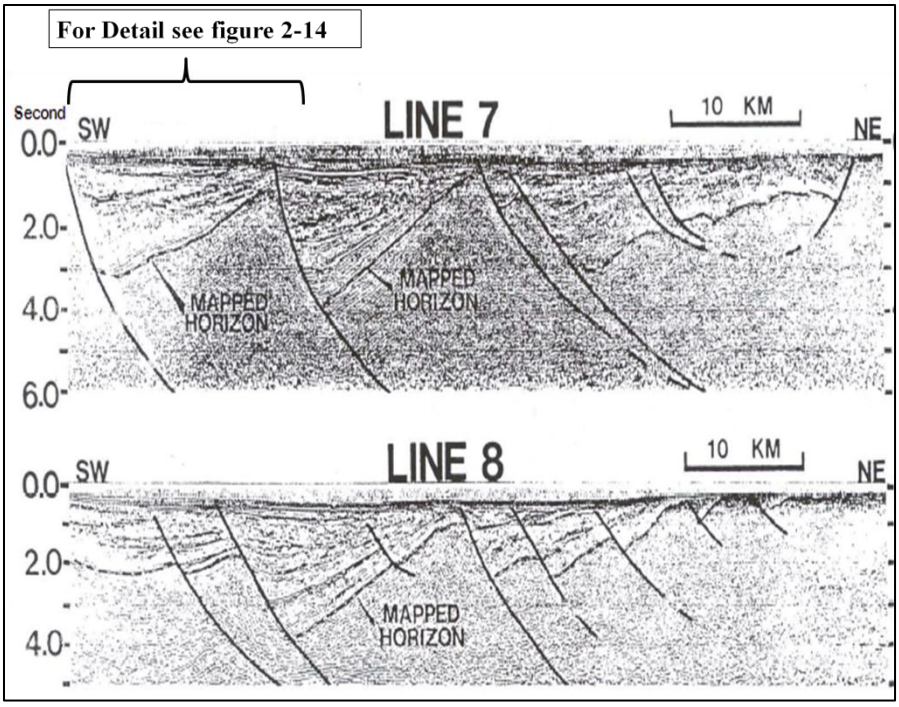

Figure 2-13: Line 7 and Line 8 regional dip linesin the upper map (after Mann, 1989)

The sub-basins typically have a half-graben geometry that was modified by subsequent reactivation during younger riftcycles (McHargue et al., 1992).Two of the large thick-skin faults areconnected by a transfer fault. Figure 2-14shows a detailed area of Figure2-12 with assimple thin- skin detachment. This area illustratesthe relationship between thin-skin and thick-skintectonics. The extension on the thick-skinfault created the half- graben basin (Figure 2-15). Displacement on the thin-skindetachment caused the development ofnumerous secondary antithetic and synthetic normal faults. The thin-skin detachment is an antithetic fault tothe main thick-skin fault(Figure 2-15). The high bedding diphas allowed the antithetic fault to become a bedding-plane detachment. The basin is bounded by normal fault system that experienced predominantly dip-slip displacement that increases at the centre of the fault and decreases toward either ends, with adjacent rider blocks and syn-depositional transverse folds. The preserved present day stratigraphic geometry, architecture and structural styles are strongly influenced by the displacement geometry on the bounding normal fault system. Aspect of the evolution of the fault system including their nucleation, propagation and linkage can be extracted from the sedimentary record. The spatial stratigraphic significant is related to the growth of normal faults in extensional basin, which was established from the fact that cumulative displacement is greatest near the fault center and decreases toward the fault tips and the fault lengthen as cumulative displacement increases.

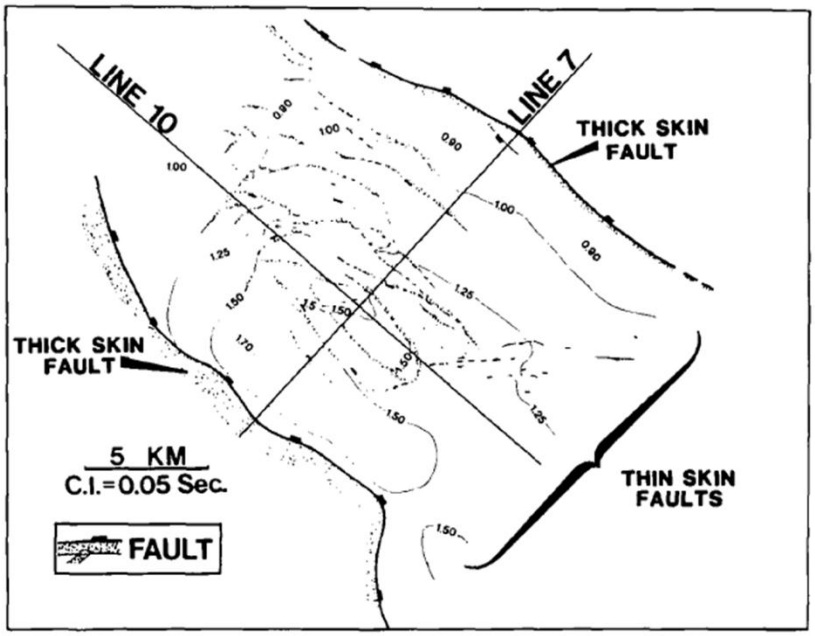

Figure 2-14: Simple thin- skin detachment, Melut basin, showing TWT (Time Structural Map) of Tertiary horizon. Note secondary thin-skin normal faults and their antithetic faults are arculate and rim the basin deep for basement structure) (Mann, 1989)

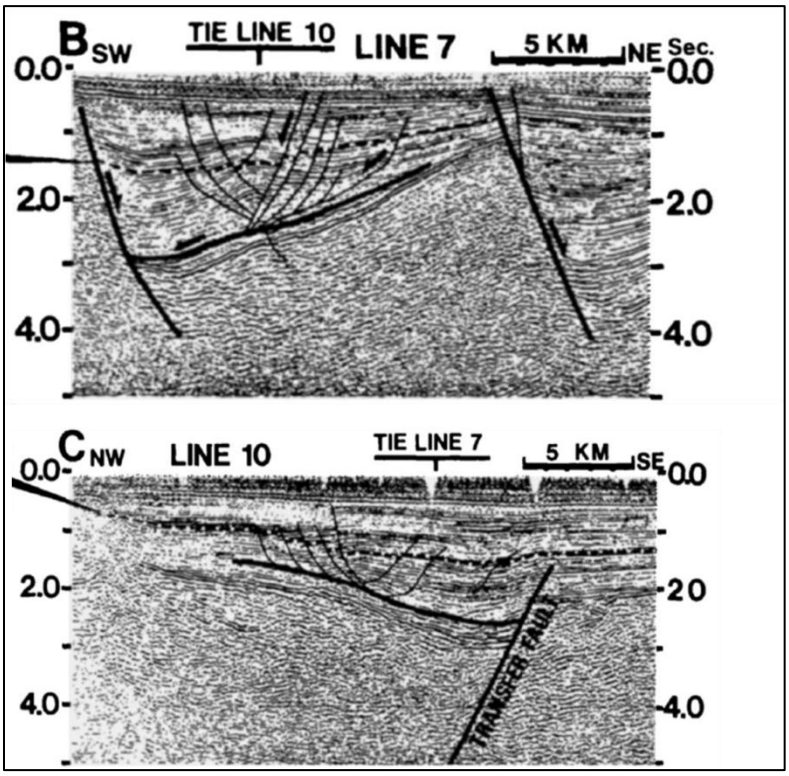

Figure 2-15: Line 7 Dip line to basin forming thick-skin fault. Note antithetic relationship between thin-skin and thick-skin faulting (Mann, 1989)

2.5 Melut Basin Stratigraphy

Schull, 1988 described Melut basin as a deep rift structure filled by thick non-marine Mesozoic and Cenozoic sequences related to the Central African Shear Zone (CASZ).Based on geophysical investigations, geological interpretation and palynological information obtained from boreholes (Dou et al., 2007; Eisawi and Schrank, 2008), the Stratigraphic column (Figure 2-16) of the study area can be summarized as follows:

- Quaternary cover
- Unconformity
- Tertiary strata
- Unconformity
- Late Cretaceous strata
- Unconformity
- Early Cretaceous strata

The stratigraphic column in the Melut Basin can be divided into four units separated by unconformities. These are: Lower Cretaceous, Upper Cretaceous, Tertiary and Quaternary.

2.5.1 The Early Cretaceous Strata

Al-Gayger Formation lies unconformablyon the Basement. The lower interval of Al-GaygerFormation is composed mainly of thin sandstones layers inter-bedded with thin claystones. The main sedimentary environment varied from fluvial-deltaic to shallow

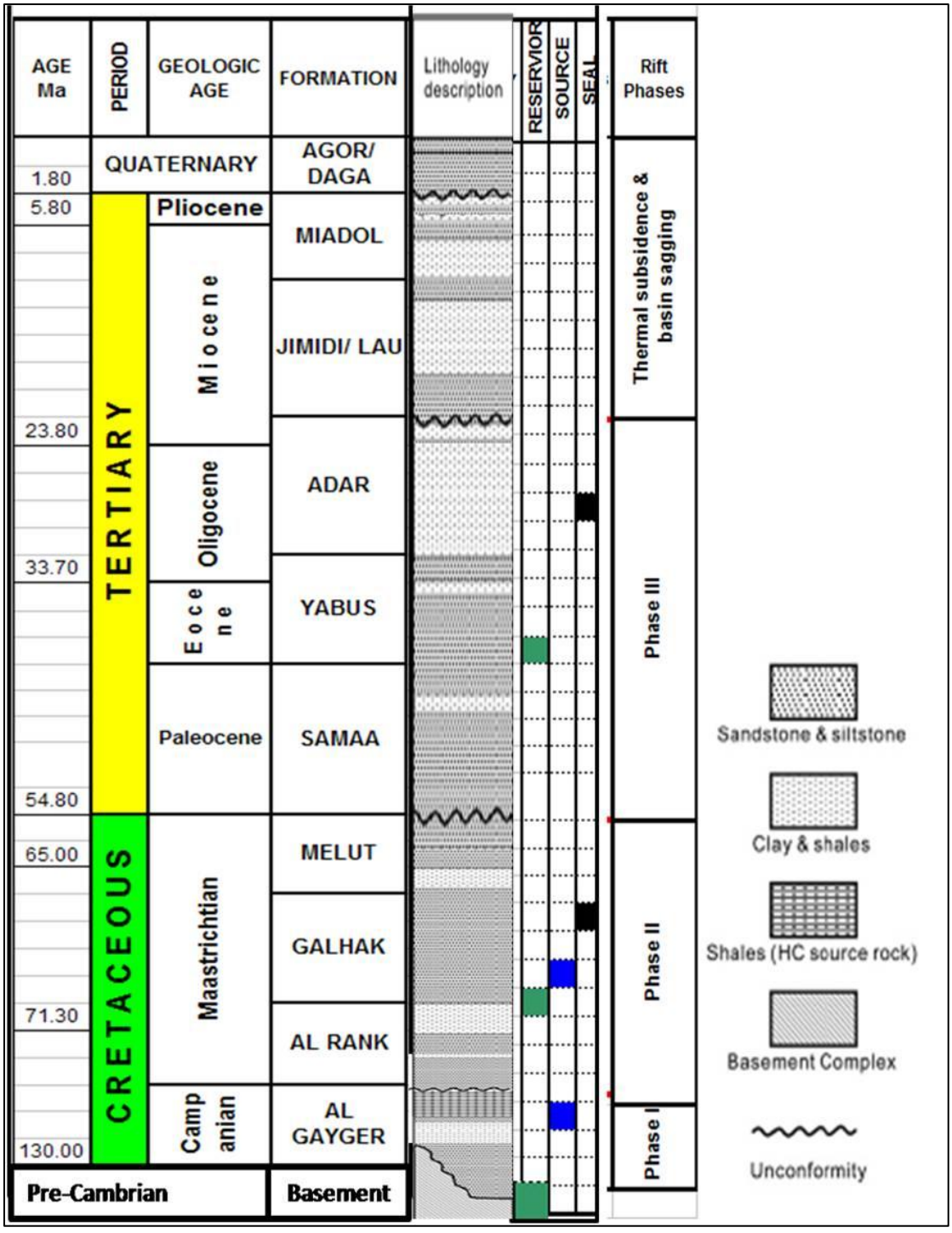

Figure 2-16: Stratigraphic column for the Melut Basin (modified after Dou, L., et al., 2007)

lacustrinefacies upwards. The upper part consists of dark grey and black, thick shales with inter-bedded thin sandstones. The main sedimentary environment of the upper part issemi-deep and deep-lacustrine facies.This formation is interpreted to have been deposited under predominantly non-marine conditions during the first rifting phase related to the opening of the South Atlantic Ocean.

2.5.2 The Late Cretaceous Strata

The late Cretaceous strata in the Melut basin is represent by three formations; Al-Renk, Galhak and Melut respectively. The Al-Renk Formation lies unconformably on Al-Gayger Formation.Galhak Formation is characterized by the medium- to fine-grained sandstones and claystones. The proposed depositional settings are interpreted to have once dominated by fluvial conditions with brief, periodic phases of lacustrine conditions during the second phase of rifting.

2.5.3 The Tertiary Strata

The Paleocene lies unconformablyon the Late Cretaceous. The Samma Formation is composed of thick coarse- to medium-grained sandstones with interbedded thin claystones which were deposited in progressive braided delta, marginal and shallow lacustrine environments during the early stage of the third rifting. This formation typically shows good reservoir quality.

The Eocene Yabus Formation is dominated by channel sandstone that deposited in mouth bars and crevasse splay environment during the third phase of rifting. Yabus Formation is the main reservoir in Melut basin.

The Oligocene Adar Formation was deposited in shallow to semi-deep lacustrine environments. It is characterized by the dominance of shales with thin siltstones and sandstones. In the interior basin Adar Formation deposited during the third phase of rifting which was associated with the opening of the Red Sea.

The Mid Oligocene Lau Formation covers the underlying strata unconformably. It is characterized by an upward fining clastic cycle. It was deposited in shallow lacustrine to braided river environments.

The Miocene Jimidi and Miadol Formations were deposited in shallow lacustrine to fluvial environments. The Jimidi Formation is composed of massive sands, interbedded with more thin claystones upwards.

The Miocene Miadol Formation was deposited in overbank/floodplain and lacustrine environments. The lacustrine facies are often well developed suggesting long lived, stable lake conditions. The Miadol Formation is composed of sandstoneinterbedded with claystones.

2.5.4 The Quaternary Strata

Daga Formation is composed of sandstones in the eastern and central parts of the basin and claystones and interbedded siltstones in the northern and southern parts of the basin.The Daga Formation is interpreted to be deposited in floodplain with humid type vegetation.

CHAPTER THREE

FRACTURE CHARACTERIZATION

As indicated earlier, the main objective of this study is to characterize the fractured basement reservoir. This includes fracture identification from subsurface data, fracture and lineaments delineation from the analogues basement outcrops in the surrounding the study area. Variable information about the length, orientation, intensity and connectivity of those fractures was obtained and helped in fractures characterization.In this section,fractures and lineaments of the basement rocks were interpreted from surface and subsurface data using different sets of data.Fractures and lineaments in the area were identified from regional to local scale using gravity, satellite images, seismic and well data. Orientation analyses were conducted for those fractures and lineaments and major trends were identified and their relationships to geological and tectonic were discussed. The possible origins of the fractures system hosting hydrocarbon in the basement rocks were identified. The study also addressed the possible role of the major faults in hydrocarbon migration.From the in-situ stress analysis, faults and fractures trends were tested for the most susceptible to dilation (open) at present day.

3.1 Fracture Concept

The term fracture is defined by Moores(1992) as: “Fractures along which rocks or minerals have broken; they are therefore surfaces across which the material has lost cohesion”.

Pollard and Aydin (1988) suggested that: “Fractures have two parallel surfaces that meet at the fracture front. These surfaces are approximately planer; and the relative displacement of originally adjacent points across the fractures is small compared to fracture length”.

3.2 Types of Fractures

Stearns (1971) classified fractures into; those observed in laboratory experimentsand those observed in outcrop and subsurface settings. Experimental fracture classified by Stearns into shear fractures,extension and tensile fractures. Natural fractures are also classified into tectonic fractures (formed by surface forces) and regional fractures (formed by surface forces or body forces).

As defined by Lawn and Wilshaw (1975) and suggested by Pollard and Aydin (1988), the term fracture encompasses both joints and faults. In this terminology, fractures were divided into three modes: Mode I, Mode II and Mode III.

Mode I is the extensional fractures and formed by opening with no displacement parallel to the fracture surface, Mode II fractures may exhibit shearing with components parallel to the direction of propagation of the fracture front and Mode III fractures may exhibit shearing with components perpendicular to the direction of propagation of the

fracture front (Figure 3-1). Considering this classification, faults are mode II or mode III, whereas joints are classified as mode I. Therefore joints are fractures along which there has been no appreciable displacementparallel to the fracture and only slight movement normal to the fracture plane.

3.3 Fracture CreationProcesses

According to Pollard and Aydin (1988), naturally created fracture are formed by two processes; primary fractures related to the emplacement and cooling of the magma and secondary fractures related mainly to tectonic deformation.

3.3.1 Fractures Related to the Magma Cooling and Emplacement

Primary fractures are fractures that formed during the emplacement, crystallization and cooling of the magma in the upper crust. This fractures are predominantly mode I fractures. In stocks, fractures usually develop first in the completely solidified outer margin of plutons, while the pluton interior is still mobile. Such fractures are represented by small joints and faults and include four main classes namely; cross joints, longitudinal joints, flat-lying joints, and diagonal joints (Price and Cosgrove, 1990). These classes are based on the relationship between the orientation of fractures and foliation planes in the intrusive body (Price and Cosgrove, 1990)(Figure 3-2). Steeply dipping joints that are parallel or perpendicular to the flow lines (cross joints or longitudinal joints) are tensile fractures. Shear fractures are the steeply dipping joints that strike at angles of about 45 degree to the flow lines (diagonal joints). Flat-lying joints are the horizontal joints are related to volume change of the pluton.

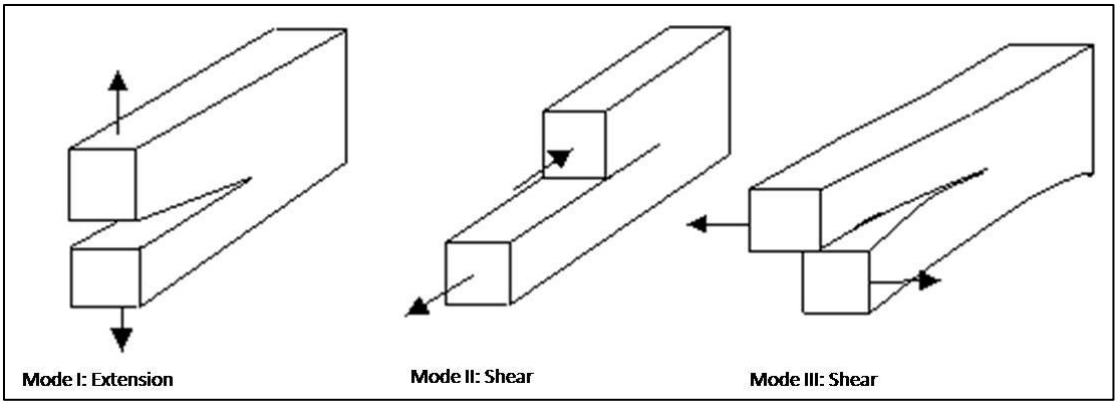

Figure 3-1: Show the three Modes of fractures, Mode I fractures (joints) the extensional fractures and formed by opening with no displacement parallel to the fracture surface. Mode II and Mode III are shear fractures (after Lawn and Wilshaw, 1975)

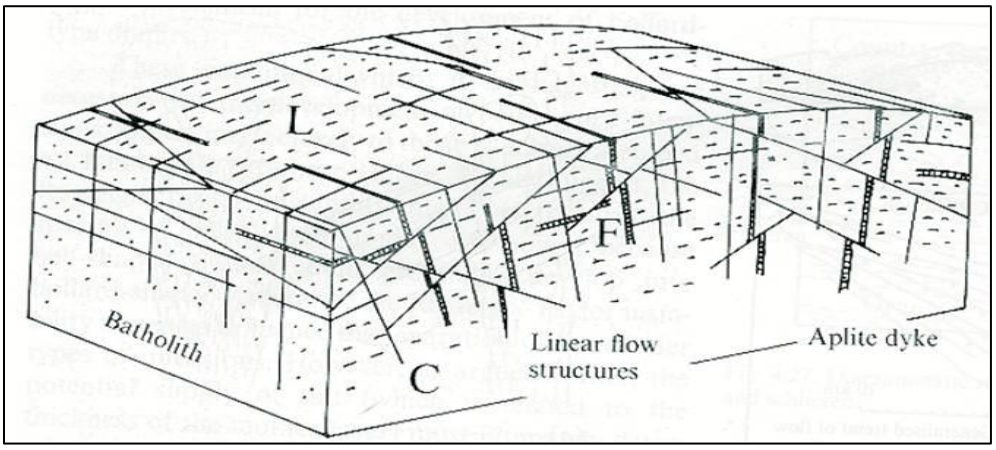

Figure 3-2: Fracture systems related to cooling of large plutonic bodies; C= Cross joints, L= Longitudinal joints; F= Flat – Lying joints (after Price and Cosgrove, 1990)

Secondary fractures that form due to the deformation of the rock mass caused by tectonic forces. Those fractures can be interpreted according to the distribution and orientation with respect to the tectonic event formed them (Nelson, 2003). Tectonic fractures are characterized predominantly by Mode II or shear fractures and showing considerable shear displacement.Tectonic fractures are mainly related to faults and folds (Nelson, 2003).

3.3.2 Fault-Related Fracture Systems

In the vicinity of faults, many parallel fractures to the faults and shear fractures conjugate to the fault are developed (Nelson, 2003).Figure 3-3 illustrates the relationship between fault direction and the associated fractures. Fault related fractures (Figure 3-4) were discussed by many authors such as Van Golf-Racht (1982); Friedman et al., (1972); Norris (1966); Stearns (1971); Tchalenko and Ambraseys(1970). It is possible to determine the direction of the principal stresses at the time of the fault formation because of therelationship between faulting and fracturing. Additionally, the sense of movement of the fault can be determined, if orientation of the fault plane and its relationship to trends is determined. Moreover, the fractures intensity related to faults is controlled by many factors such as distance from fault plane, lithology, amount of displacement, depth of burial and fault type(Friedman et al., 1972).

Faults are generally made up of a damage zone of highly fractures that are roughly parallel to the fault strike. The width of this damage zone has been studied by many researchers and related it to the amount of the fault thrown Nelson (2003). They also reported that the fracture density gradually decreases away from the fault(Stearns, 1971).

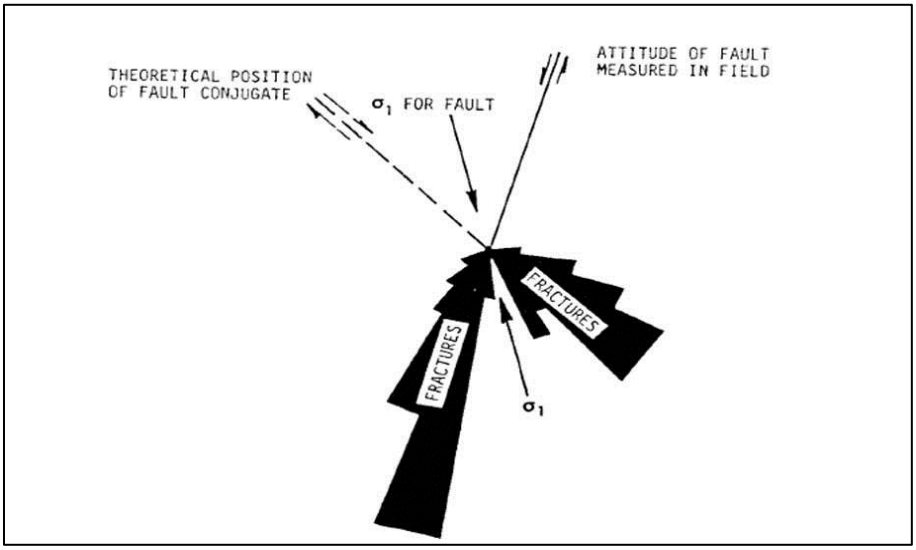

Figure 3-3: Rose diagrams of shear fractures related to faults system. The orientation of the shear fractures are parallel and conjugate to the faults plane (after Nelson, 2003)

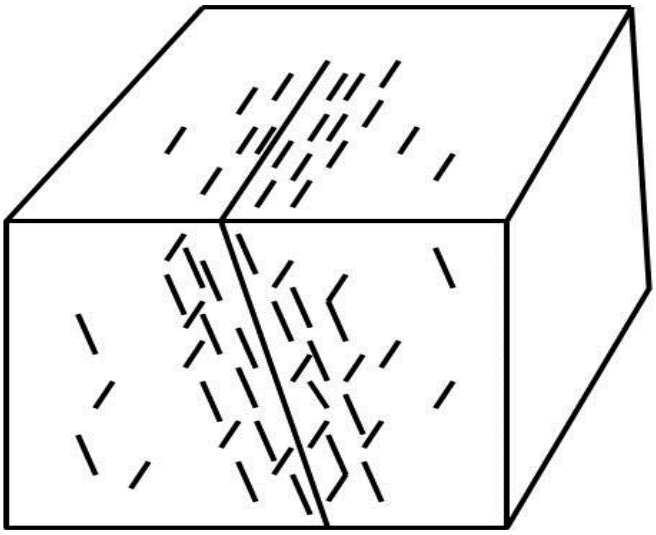

Figure 3-4: Block diagram, Showing 60 degree dipping normal fault and the predicted associated fractures (afterVan Golf-Racht (1982)

Characteristics of faults and associated fractures are generally similar in regard to the dip angle, dip azimuth and trends. This observation Led Van Golf-Racht (1982)to conclude that the orientation of fractures can be predicted if the orientation of the fault is known. Accordingly, he subsequently demonstrated that faults with associated shear fractures sharethe same orientation, and approximately the same dip magnitude (Figure 2-4).

3.3.3 Fold-Related Fracture Systems

Fracture patterns developed within fold are very complex because it is controlled bythe stress and strain history during the foldingdevelopment (Figure 3-5) (Nelson, 2003).

Fracturesassociated with dome structure may exhibit specific patterns as described by Hariri(1995) (Figure 3-6). He demonstrated that in the elongated oval shaped domes such as the Lead-Deadwood dome; two orthogonal sets of fractures may develop in the overlying strata. One of these fracture sets is longitudinal (parallel to the dome axis) and the other is transverse (perpendicular to the dome axis).

Studies conducted on fractures and lineaments for Dammam dome eastern Saudi Arabia also indicated the fractures that the ovalshape dome structure has a great influence on the trend and pattern of the features (Hariri and Abdullatif, 2004). In this study, patterns and trends of fractures were determined in several locations within the Dammam dome and the resulted pattern confirmed the relationship of those fractures to the doming in thearea (Hariri and Abdullatif, 2004). Concentric and radial trends are characterizing the fracture pattern that iscoincided with a pattern produced by an elliptical shape dome (Figure 3-6; Hariri, 1995).

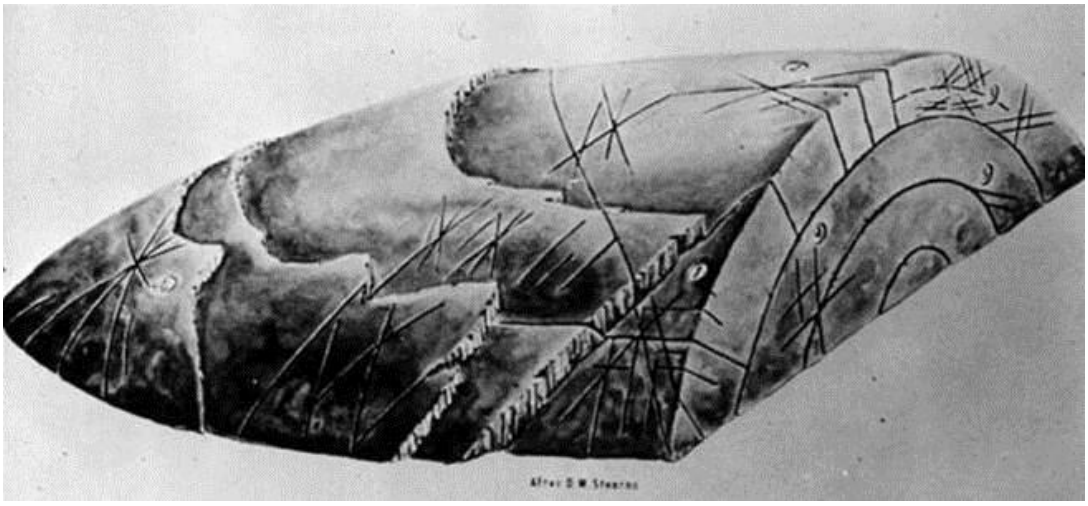

Figure 3-5: A block diagram showing the fracture patternsobserved on folds (Nelson, 2003)

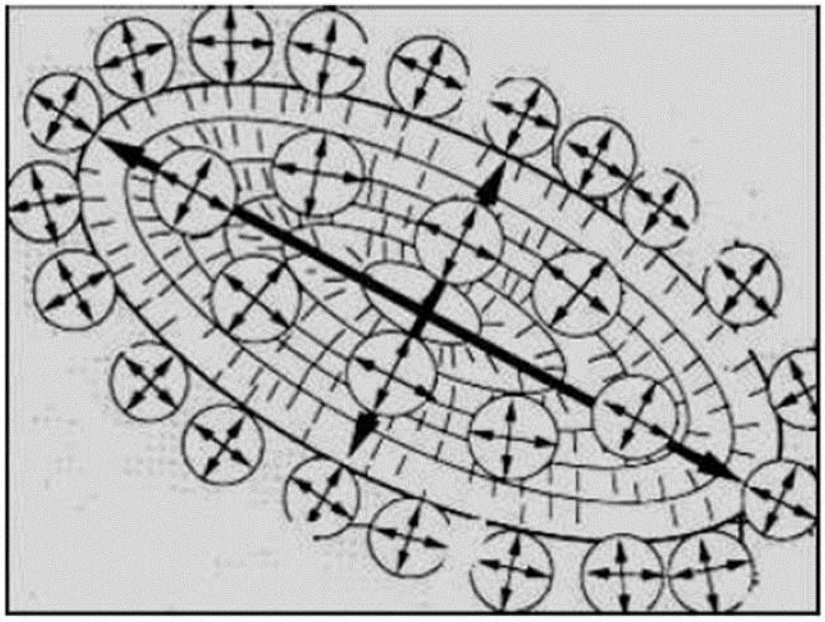

Figure 3-6: Hypothetical model for the radial and concentric line fracture patterns expected to form within an elongated dome. Arrows in circles around the dome indicate the expected fracture trends (after Hariri, 1995)

3.4 Fracturesand Lineaments Defined from Gravity Data

Gravity data represents variations in the Earth's gravimetric field that caused by the variations in density of the underlying rocks. It can alsoprovide information on numerous deep dense sources, such as structure and composition of dense basement and shallow sources such as faults, dykes and sills, as well as textural features. Standard Free-air and Bouguer anomaly images contain information from all these sources. In this study, lineaments represented by gravity were interpreted and delineated from data set of land gravity using Bouguer anomaly of grid cell size of 2km and also by using satellite gravity with low resolution of 5 km.GIS software was utilized to delineate the gravity lineaments features (Figure 3-7).

3.4.1 Lineaments OrientationAnalysis

The gravity lineaments appear primarily in four sets of directions: two major sets oriented in NW-SE and NNW-SSE to N-S, and the minor sets oriented along NE-SW and WNW-ESE to E-W.

3.5 Faults Defined from Seismic Data

Ruman area covered by 3D seismic data acquired in 2008. The 3D seismic data area is about 187 km2 (Figure 3-8) processed in 2008 (Post Stack Time Migration)PSTM. The seismic grid is 200m X 200m and the data quality fair to good. Also, the study area is covered by 2D seismic data.

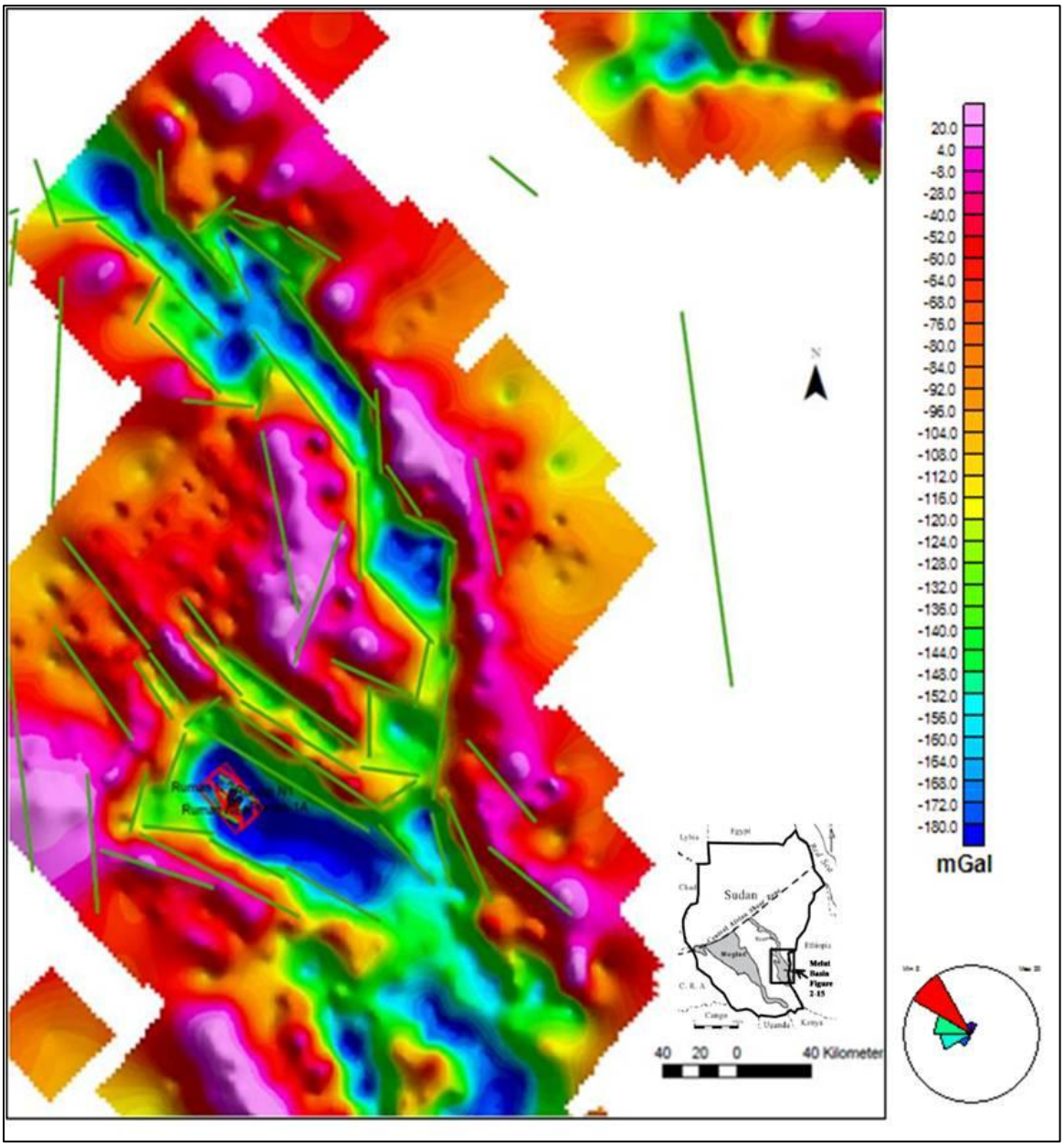

Figure 3-7: Gravity lineament interpreted from gravity image.Gravity image color scale, red represent high gravity (shallow basement) and blue represent low gravity (deepest basement) green and yellow in-between. Rose diagram in the lower right corner represent the general lineaments trends

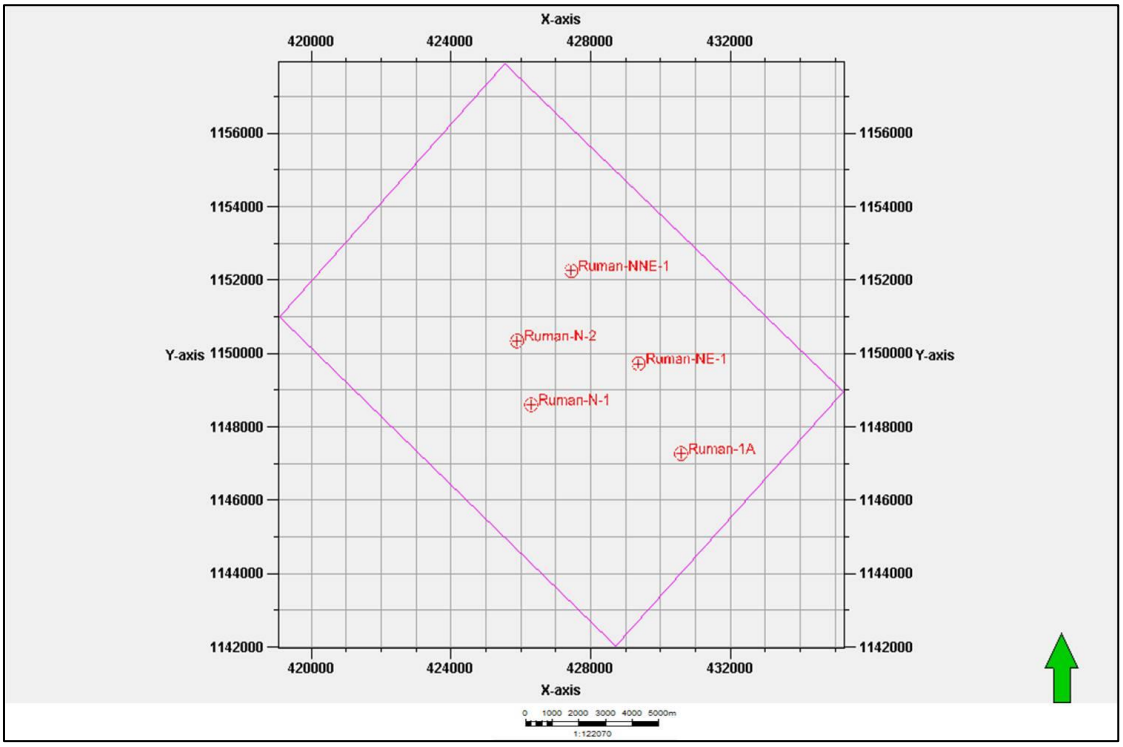

Figure 3-8: Show the area of Ruman 3D seismic survey and wells locations

Given the distribution of the wells over the area of interest, it is possible to validate the horizons picked on the seismic volume using defined well markers. The basement top is represented by a series of high amplitude reflections separating the layered sedimentary sequences above from noisy basement below.Top basement horizon and faults along the seismic section is illustrated inFigure 3-9 and Figure 3-10.

The basement is interpreted and contoured. The basement surface is posted on the seismic section that intersects Ruman-N2 and Ruman-N1 (Figure 3-11). The structural time map for top basement was provided by PDOC (Petrodar Operating Company) (Figure 3-12).

Ruman area is located at the northwest part of Melut basin (Figure3-13)and surrounded by basement outcrops namely,Ingessana Hills in the east and the Nuba Mountains in the west (Figure 3-14 and Figure 3-15).

Figure 3-15 shows a detailed section of Figure 3-14. Thesesections illustratesthe relationship between thesurface basement outcrops (Nuba Mountains and Ingessana Hills) and the subsurface basement.

3.5.1 Faults Orientation Analysis

Orientations analyses were conducted for those seismic scale faults which were digitized from the structural maps showed earlier. The rose diagrams of the strike orientation (faults trend) for those faults shows that, there are four orientations, NW-SE, NNW-SSE to N-S and WNW-ESE to E-W.

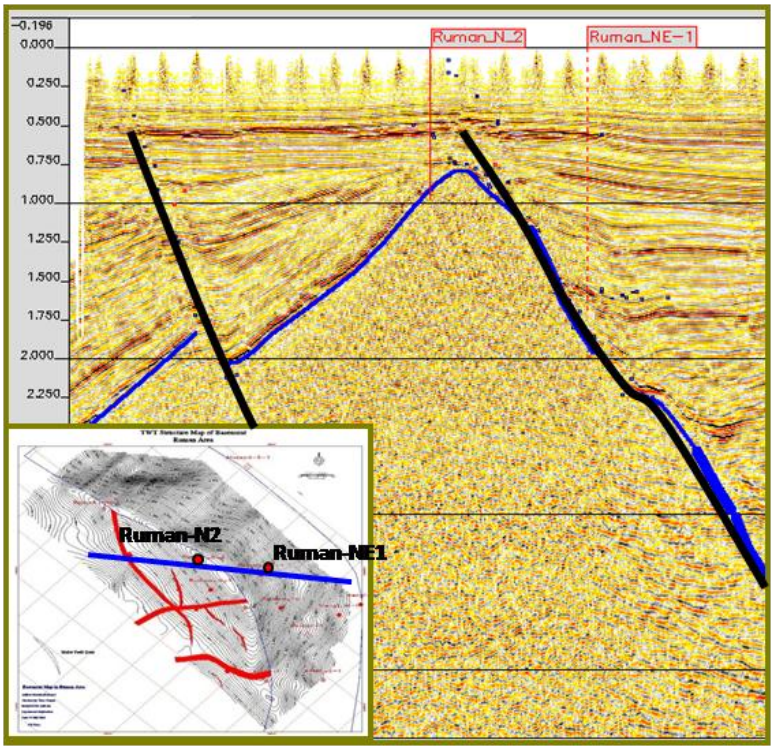

Figure 3-9: Show faults interpretation in Ruman 3D,illustrates the faults identified along the seismic sectionintersects Ruman-N2 and Ruman NE-1

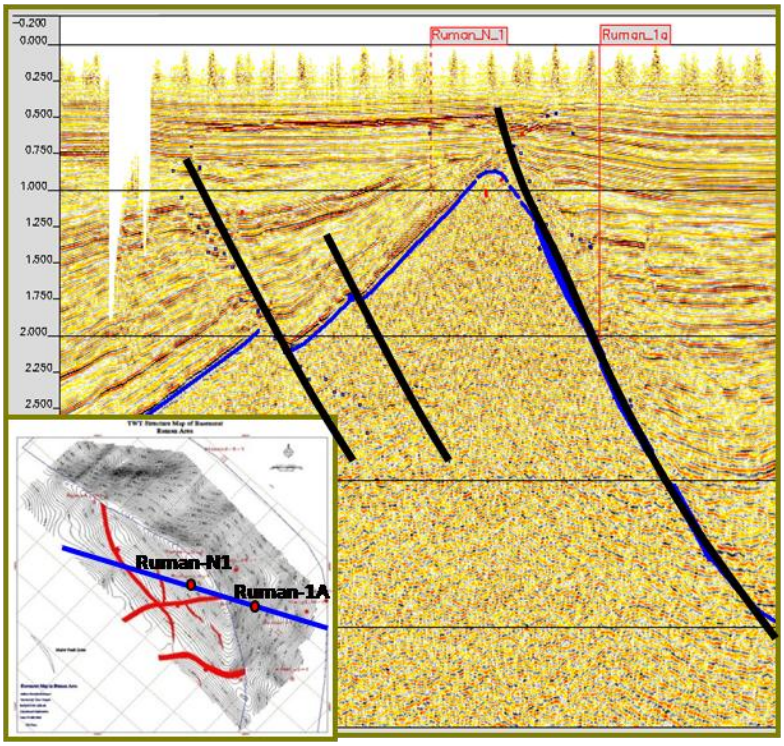

Figure 3-10: Show faults interpretation in Ruman 3D,illustrates the faults identified along the seismic sectionintersects Ruman-N1 and Ruman-1A

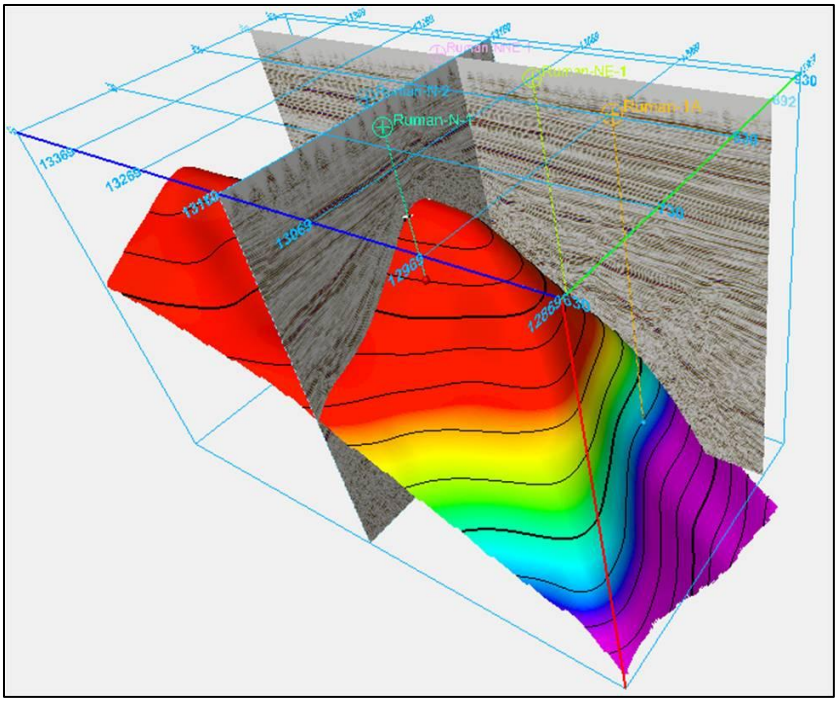

Figure 3-11: Top basement, where the basement surface is posted on the seismic section that intersects Ruman N1 and Ruman 1A basement tops

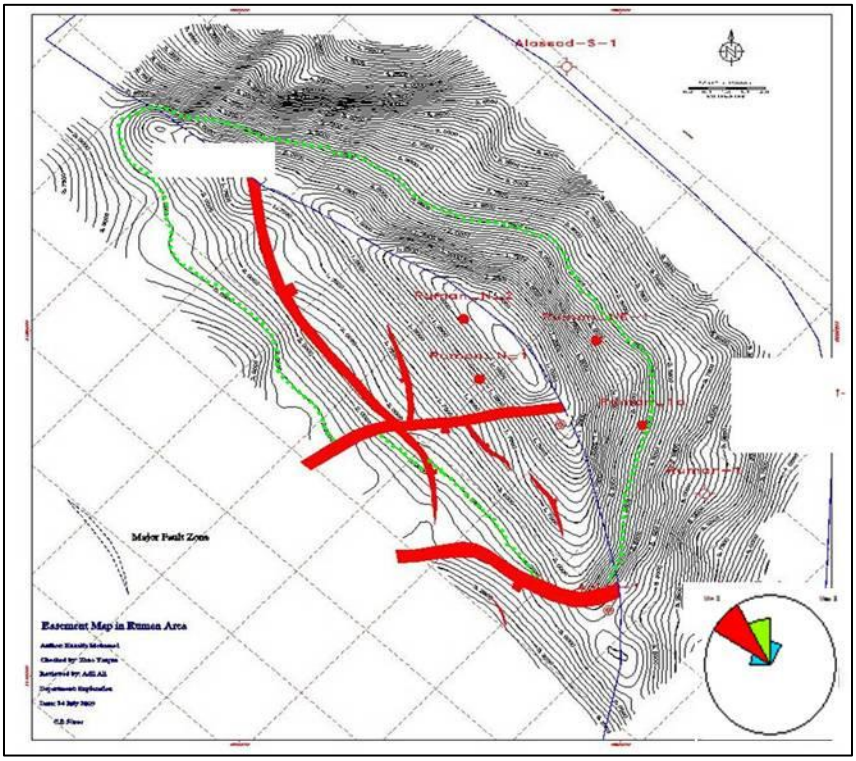

Figure 3-12: Structural map of top basement in Ruman area, showing the faults interpreted from the 3D seismic data. The rose diagram in the lower right corner represent the general faults trends

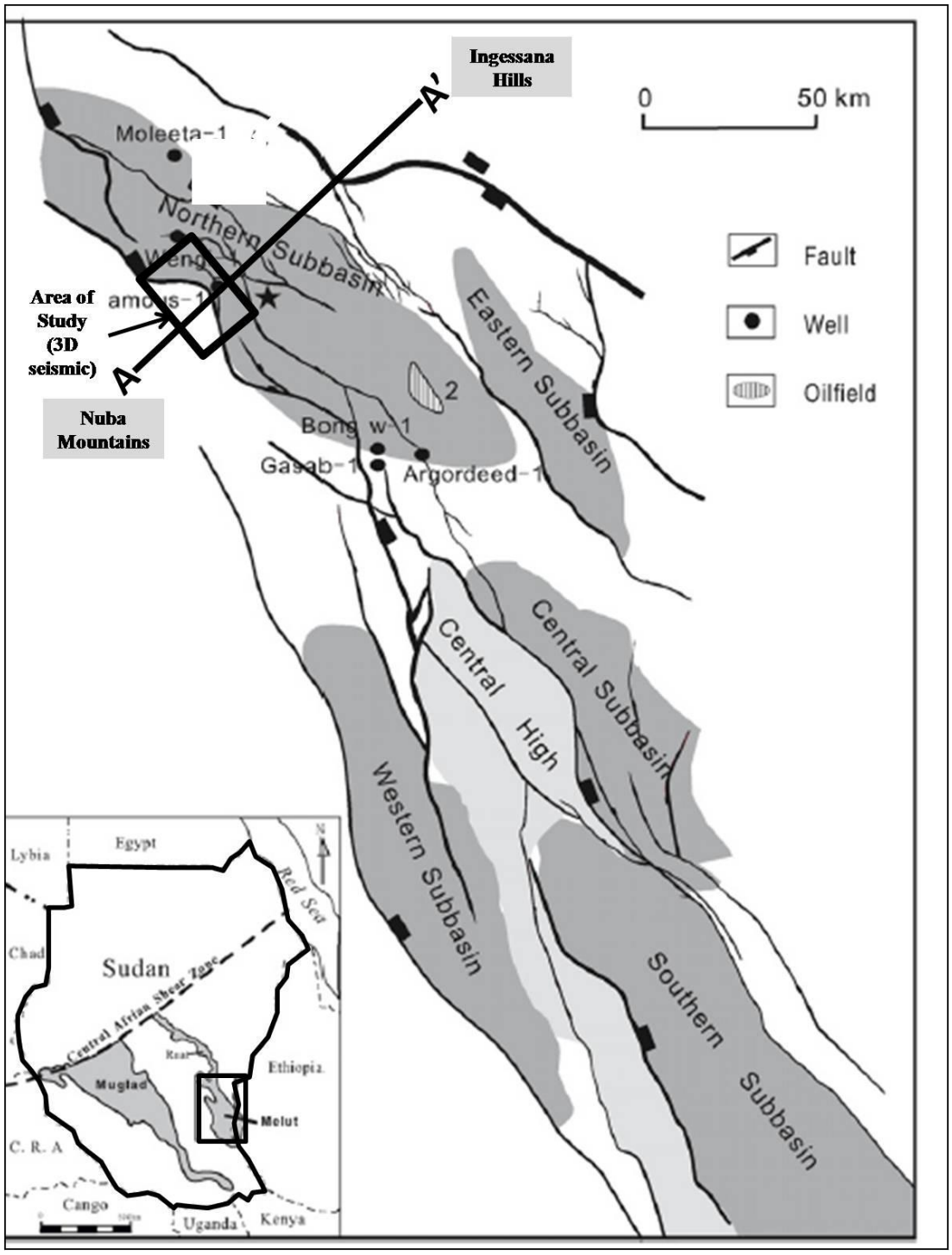

Figure3-13: Simplified structural map of the Melut Basin, showing the major faults interpreted from 2D seismic data. This figure also shows the location of Ruman 3D seismic area and the location of the 2D seismic cross sectionA-A' with relation with Nuba Mountains, Ingessana Hills and the 3D seismic(modified after Dou etal., 2007)

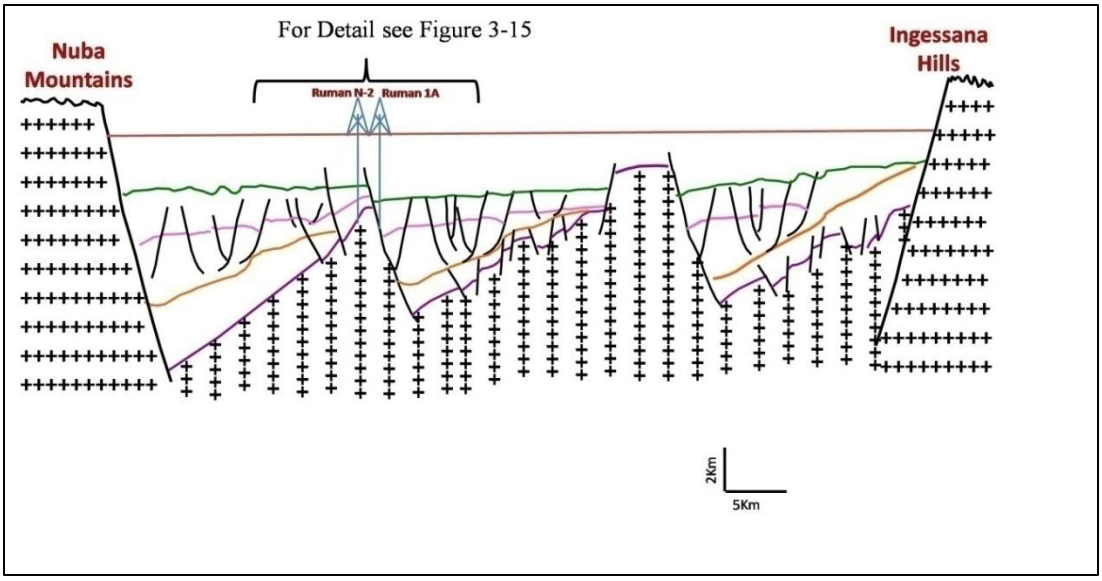

Figure 3-14: Geo-seismic cross-sections showing the relation between the basement rock on the subsurface at the area of study and the surface basement in Nuba Mountains and Ingessana Hills. Locations are shown onFigure 3-13

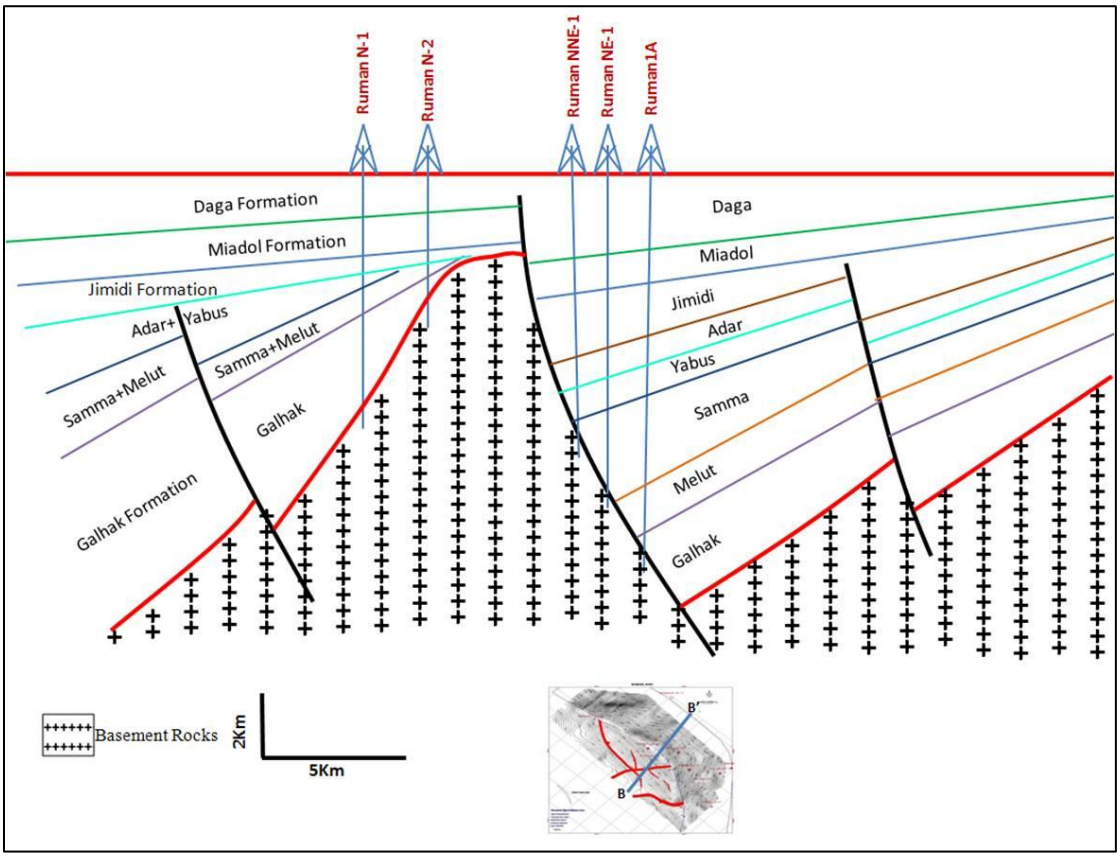

Figure 3-15: Geo-seismic cross-sections showing the major thick-skin (basement involved) faults in Ruman area with relation to the Ruman wells

3.6 Fractureand Lineaments Definedfrom SatelliteImages

Basement outcrops around the area of study; namely Nuba Mountains and Ingessana Hills represent the outcrops analogue of the subsurface basement (Figure 3-13).

Satellite image for the basement rock around the study area were used as analogue for two reasons: The first reason because the subsurface and surface basements have same rock types and the second reason because orientation analysis shows same orientation in the surface and subsurface.

A digital GIS database has been generated for surface lineament using satellite images (Figure 3-16). The satellite images due to its many capabilities such as the synoptic aerial coverage, multi spectral captivity of data, temporal resolution, etc., they can produce better information than conventional aerial photographs (Lillesand, 1979), so the same has been selected for the task of extracting surface lineaments. The final lineament map has been produced by the satellite image data using GIS software (Figure 3-17).

3.6.1 Lineaments Orientation Analysis

The surface linear features in the outcrops around Melut basin (Nuba Mountains to the west and IngessanaHills to the east) were interpreted from the satellite image, four orientations appeared: NW-SE, NNW-SSE to N-S, WNW-ESE to E-W and NE-SW (Figure 3-18). A majority of the surface linear features in the area are oriented in NW-SE, NNW-SSE. On the contrary, those surface linear features oriented in NE-SW are less prevalent (Figure 3-19).

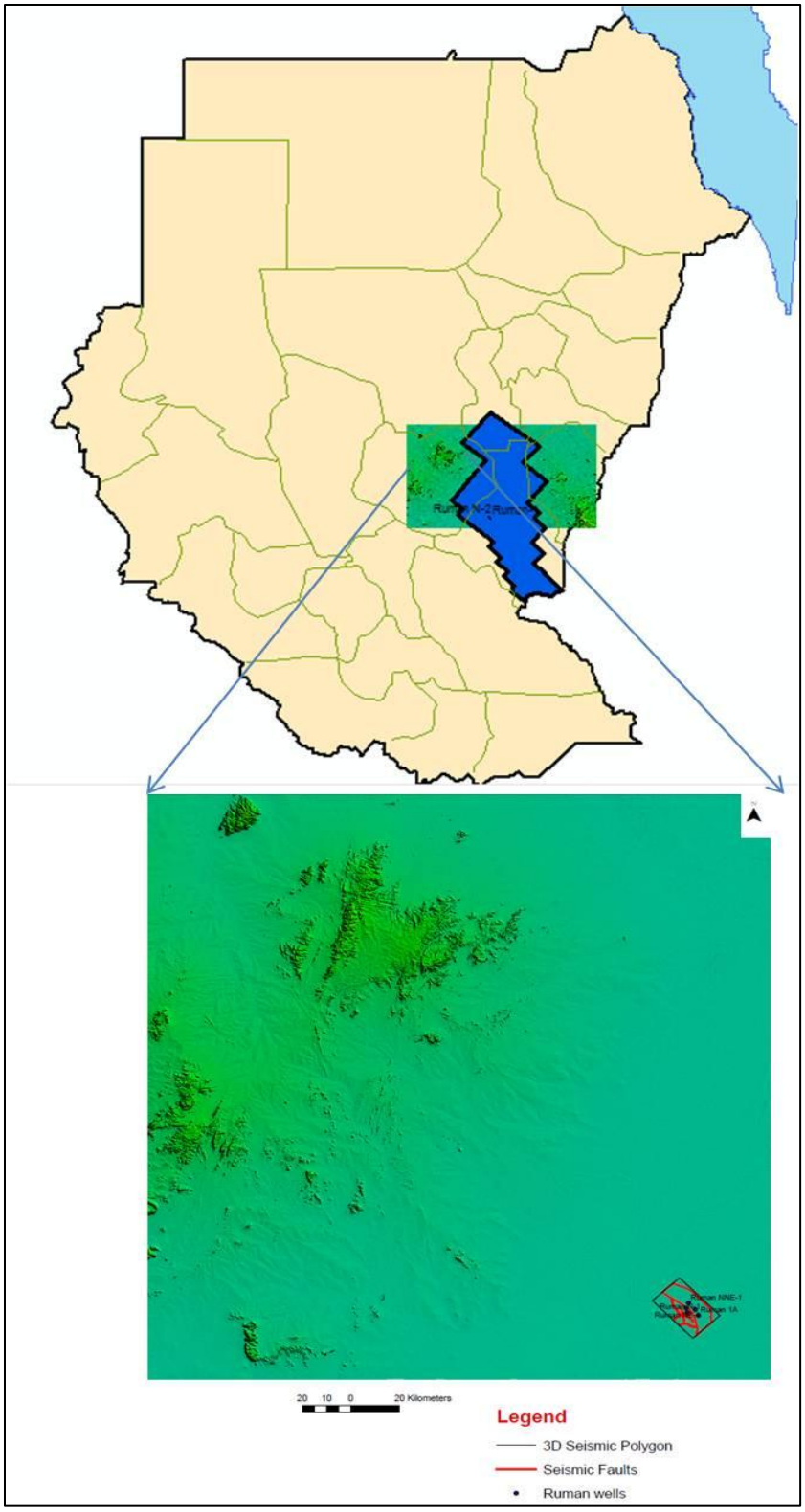

Figure 3-16: Satellite image around Melut basin superimposed over Sudan map, showing lineaments in Nuba Mountains

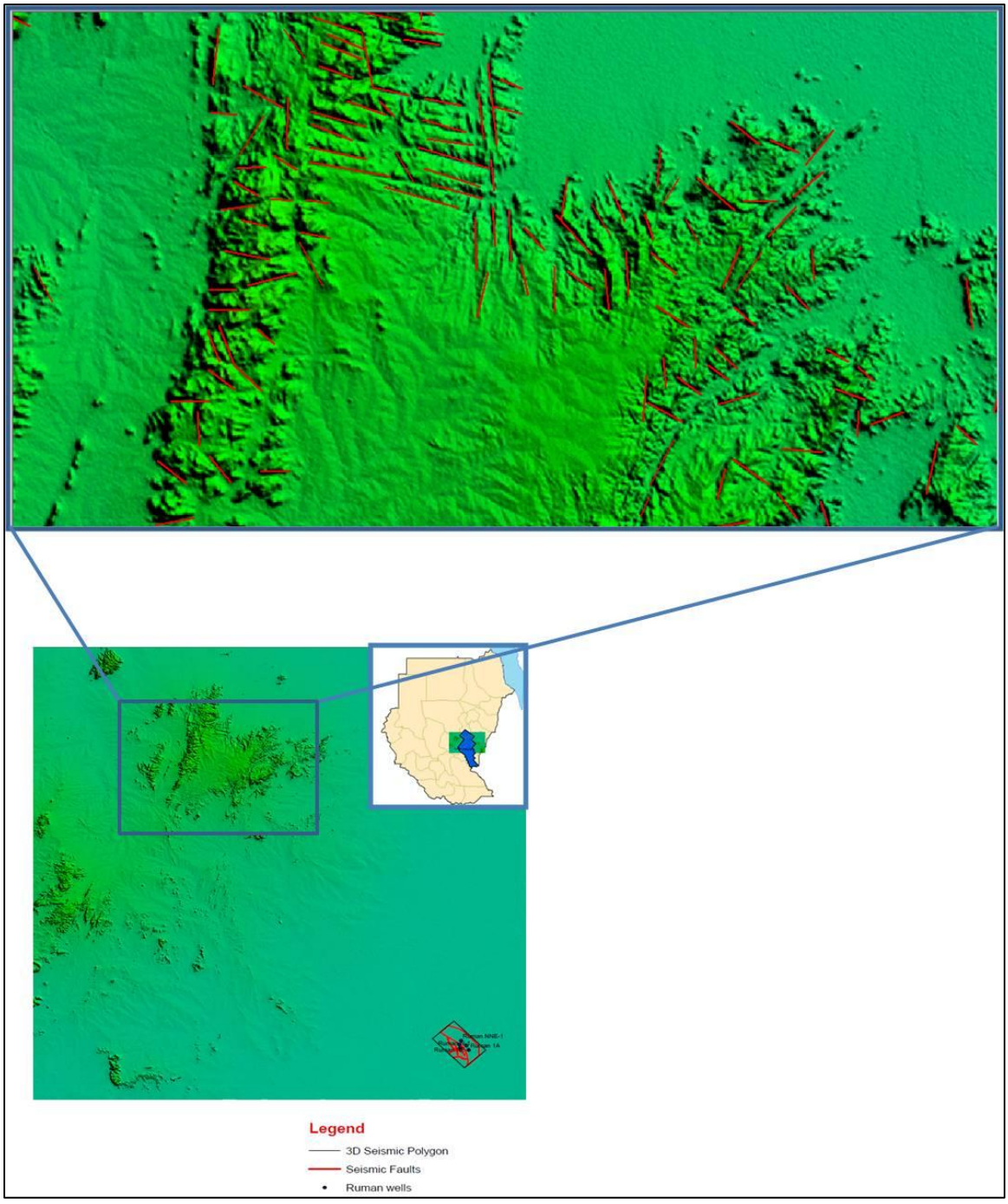

Figure 3-17: Integrated lineament map superimposed over satellite image of part of Nuba Mountains, map scale (1:250,000)

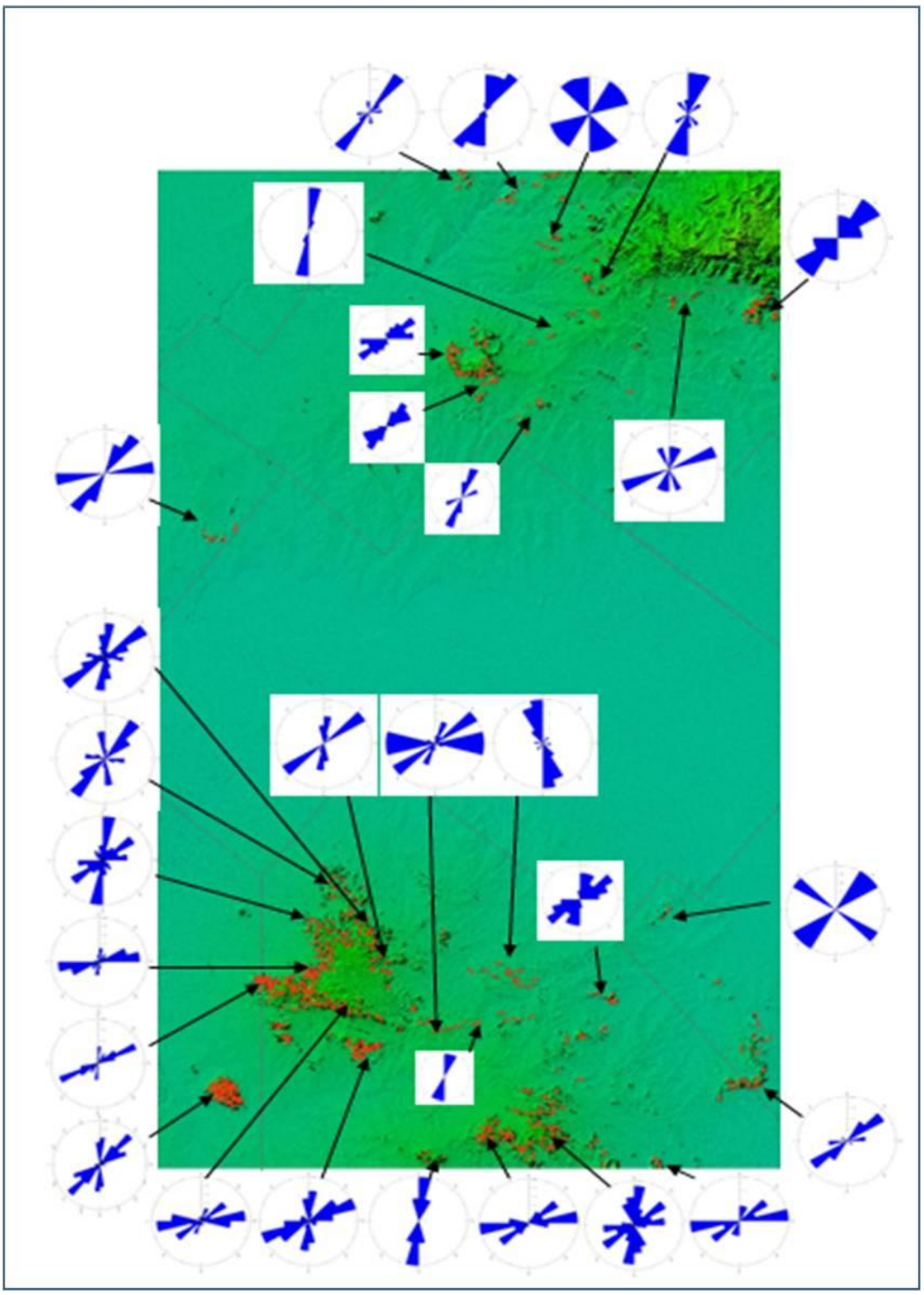

Figure 3-18: Satellite image for Nuba Mountains and Ingessana Hills superimposed by the rose diagrams, showing major trends in different part around study area determined from lineament analysis, map scale (1:1,500,000)

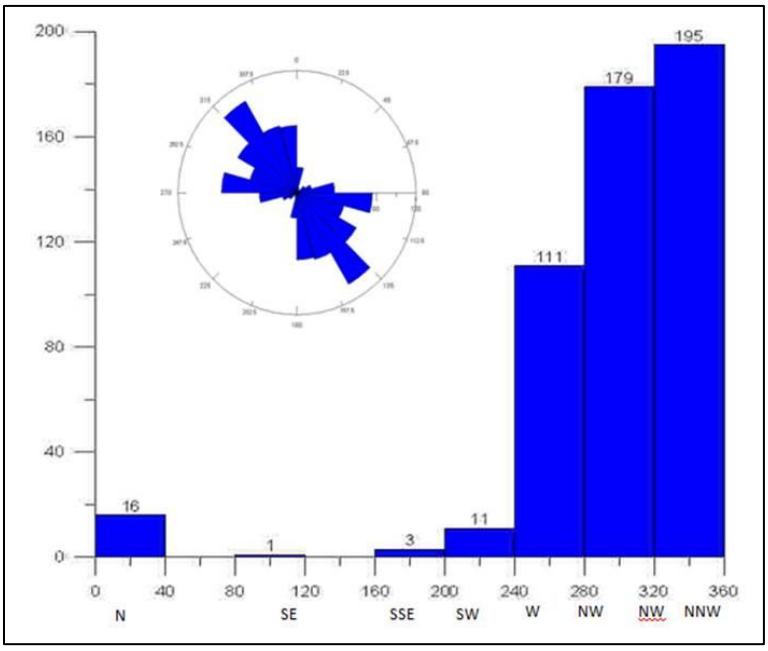

Figure 3-19: Histogram and rose diagram, showing orientation of outcrops linear features around the study area (Nuba Mountains and Ingessana Hills) have four preferred orientations

Lineaments were extracted manually from the satellite images of the basement outcrops around Melut basin (Nuba Mountains). These lineaments were analyzed in a GIS framework, and categorized based on their orientation (Figure 3-20, Figure 3-21, Figure 3-22, Figure 3-23 and Figure 3-24).

3.6.2 Basement OutcropsLength Analysis

As the outcropped basement is used as an analogue of the subsurface basement because they have the same rock types have the same orientation, lengths were measured for all the interpreted surface lineaments from the satellite images. For the purposes of statistical analysis, histogram and cdf (cumulative distribution function)ofthe surface lineaments length at NubaMountain and IngassenaHills were applied (Figure 3-20). The number of interpreted lineaments (fractures) is 672 fractures. The minimum length is 103 m, the maximum length is 4744 m and the mean is 2220 m (Figure 3-25).

3.7 FractureDefined from Well Data

3.7.1 Fractures Identification

Image log analysis at Ruman wells (Ruman-N1, Ruman-N2, Ruman-1A, Ruman NE-1 and Ruman NNE1) detected several fracture types and their orientation, those well were drilled in February 2007, June 2008, June 2009, July 2009, October 2009, November 2009 respectively. The FMI (Formation Micro-Imager) tool produces a high-resolution micro-resistivity image log of the borehole wall, covering 80% of the wall in an 8.5 inch borehole. Each micro-conductivity button can read up to 1 cm into the formation and in combination with adjacent buttons is capable of distinguishing conductivity anomalies smaller than the tool’s effective resolution of 0.2 cm.

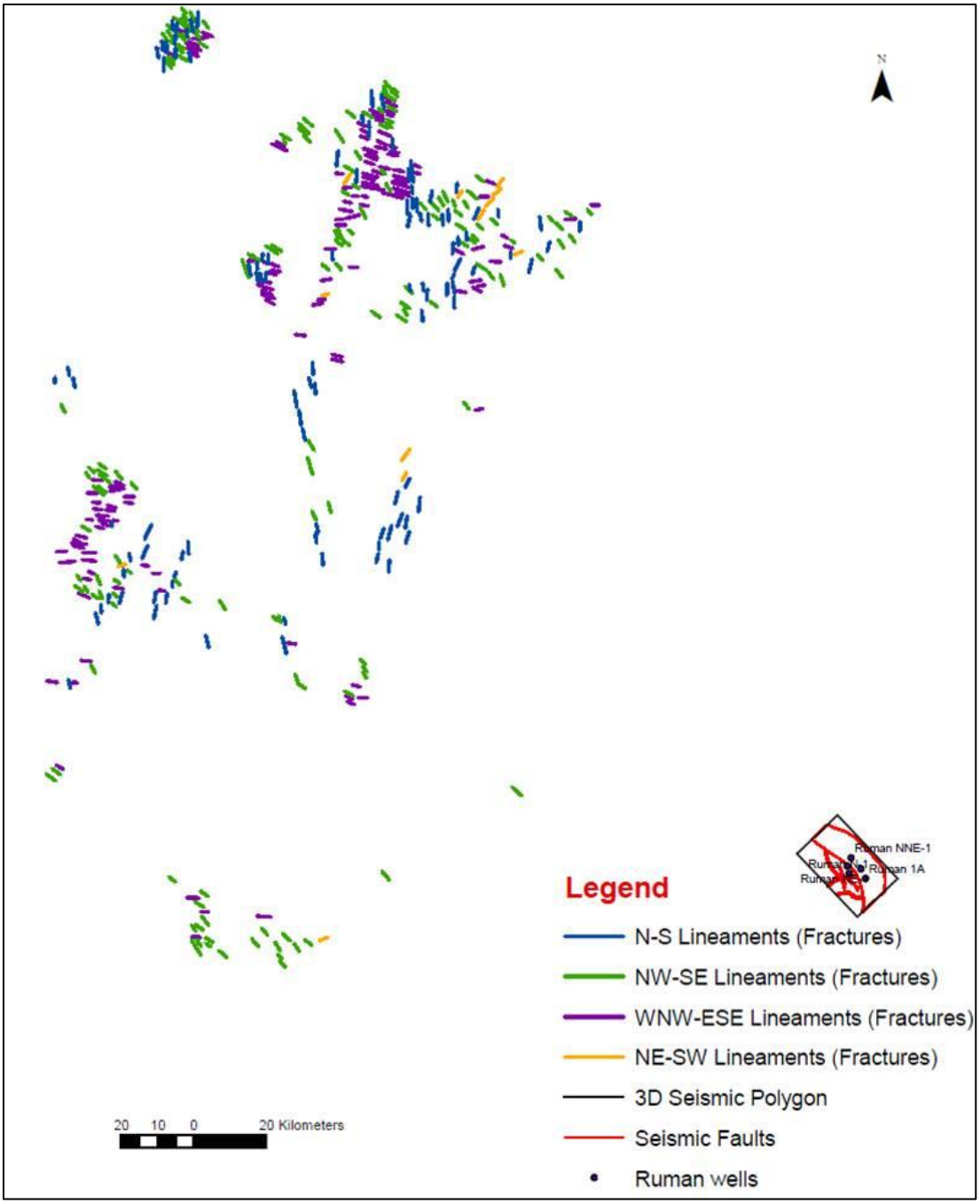

Figure 3-20: Lineaments with different direction interpreted from Satellite image of the eastern part of the Nuba Mountains

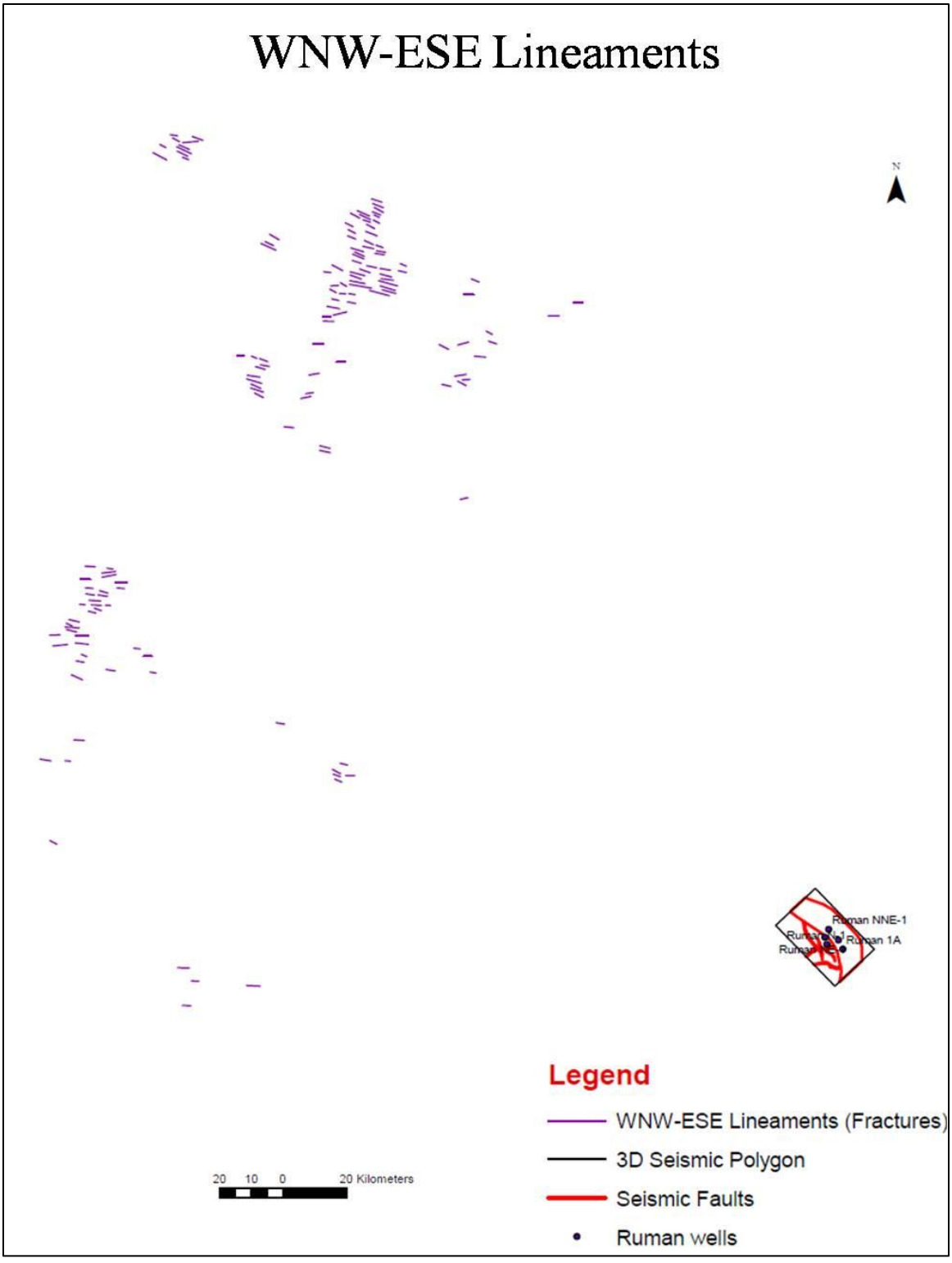

Figure 3-21: Lineaments with WNW-ESE direction interpreted from Satellite imageof the eastern part of the Nuba Mountains

Figure 3-22: Lineaments with NW-SE direction interpreted from Satellite image of the eastern part of the NubaMountains

Figure 3-23: Lineaments with N-S direction interpreted from Satellite image of the eastern part of the NubaMountains

Figure 3-24: Lineaments with NE-SW direction interpreted from Satellite image of the eastern part of the NubaMountains

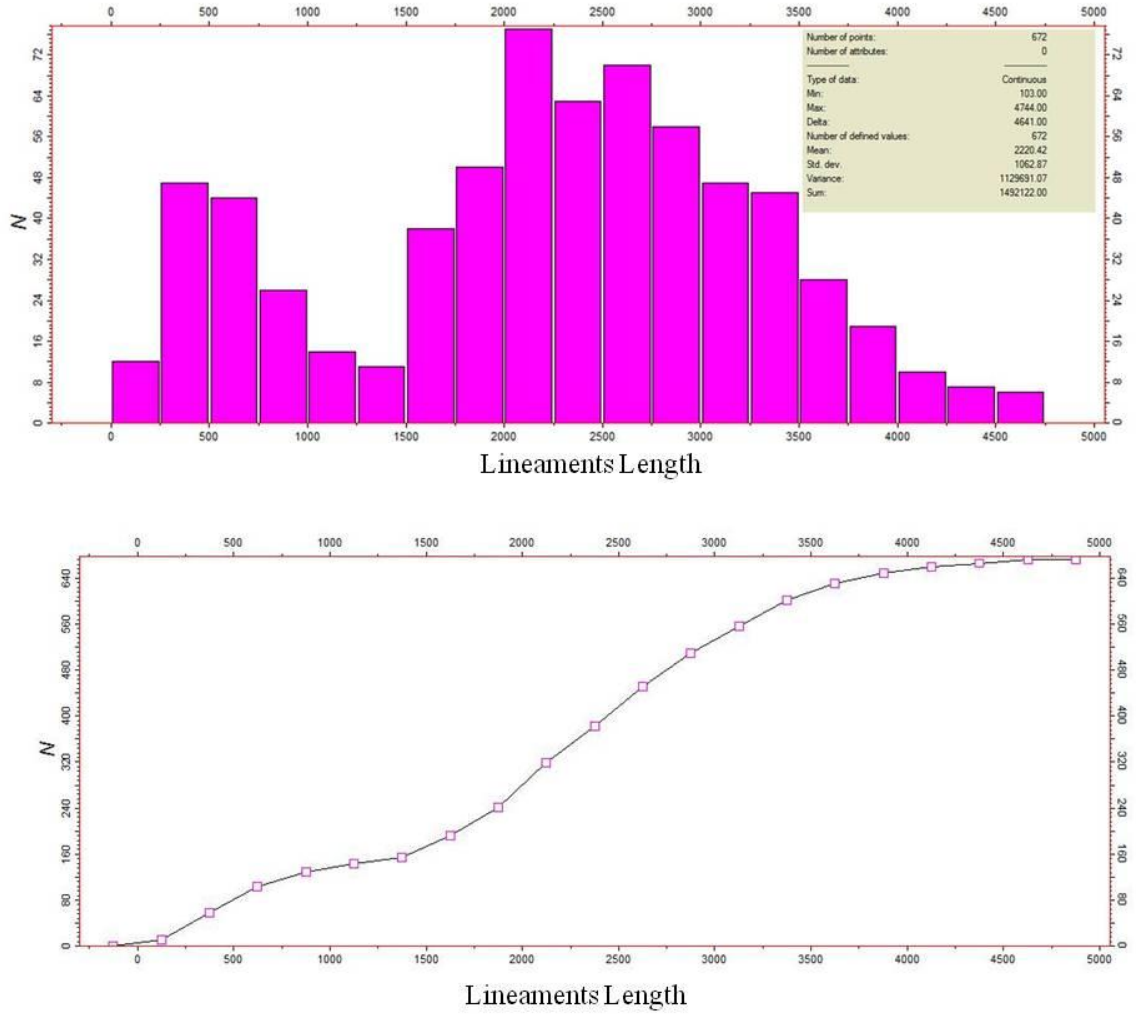

Figure 3-25: Showing histogram and cdf (cumulative distribution function)of surface linear features length around the area of studyarea (Nuba Mountains and Ingessana Hills)

The following fractures classification discussions, and the individual well fracture rose diagrams illustrated in following section, are based on the application of these imaging tools to the Ruman wells.

3.7.2 Fractures Orientation Analysis

Linear feature orientation is considered as one of the most important characteristics as far as petroliferous locales are concerned.

Geological planes are defined by their dip (dip magnitude & dip azimuth) or by their strike, byconvention the dip magnitude is referenced to the horizontal plane and the dip magnitude isreferenced to the North.(Figure 3-26 and Figure 3-27). Dips are presented as tadpoles on a dip track graduated from 0 to 90 degrees. The tail of the tadpole indicates the direction of the dip while the head of the tadpole indicates the magnitude of the dip (Figure 3-28).

In Ruman N-1 well, statistical analysis of the continues conductive fractures scattered range of 10 to 60 degree dip magnitude, the azimuth direction toward SW and minor towards N and S. The major strike direction NNW- SSE and the minor direction E-W (Figure 3-29).

The major fracture orientation between depth 1190 m and 1230 m is NNW-SSE while the major fracture trend between depth 1230 m and 1260 is ENE-WSW. Between depth 1260m and 1281 m the major direction became again toward NNW.

In Ruman N-2 well, statistical analysis of the continues conductive fractures average inclination range between 28 and 38 degrees,the major azimuth direction toward SW and minor towards NE. The main strike direction is NW-SE (Figure 3-30).

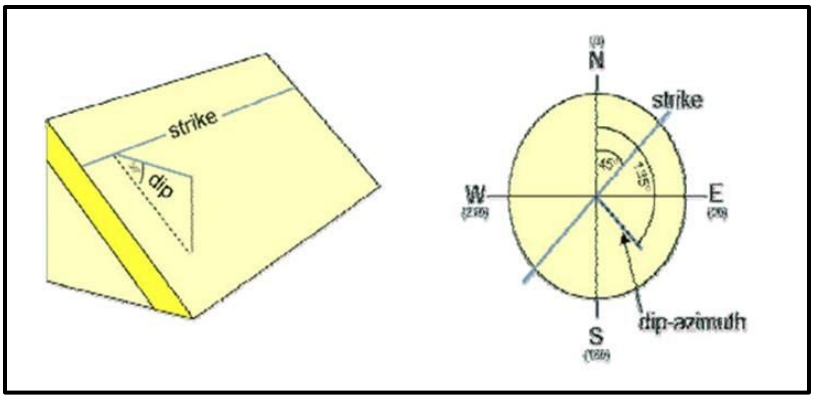

Figure 3-26: Relation between dip angle, dip azimuth & strike

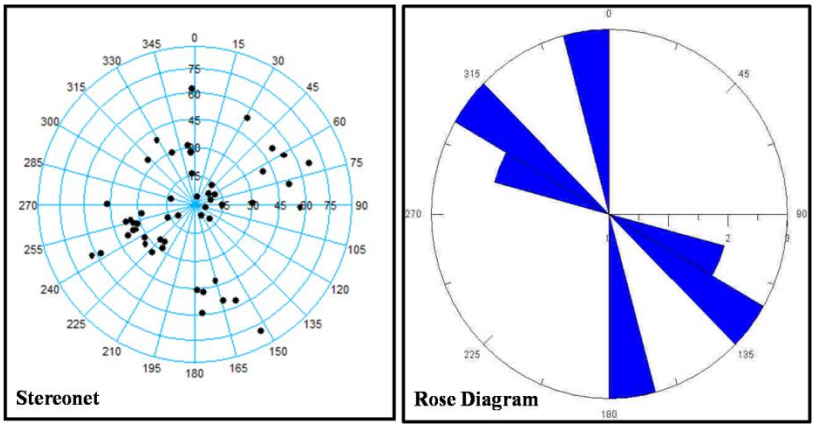

Figure 3-27: Stereonet and rose diagram

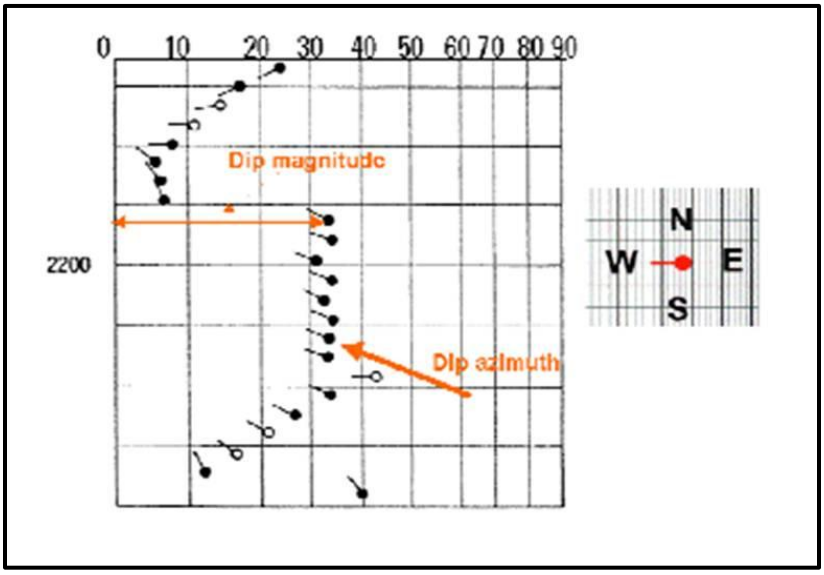

Figure 3-28: Dips are presented as tadpoles on a dip track graduated from 0 to 90 degrees

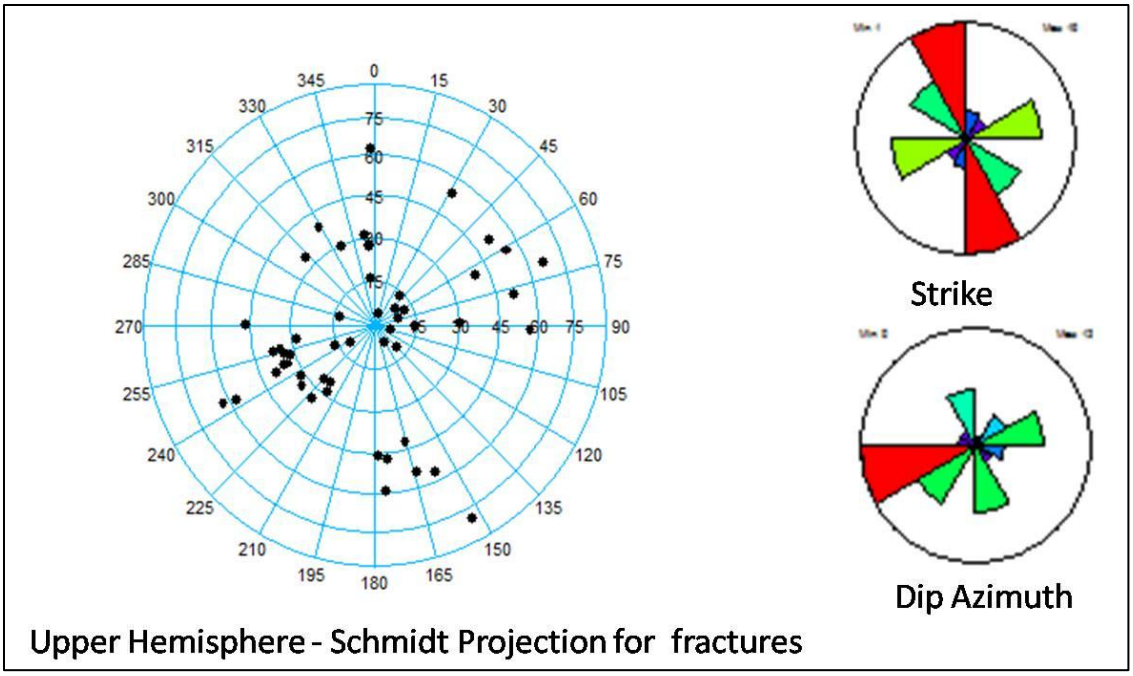

Figure 3-29: Statistical analysis of all basement fracture dip, azimuth and strike in Ruman N-1

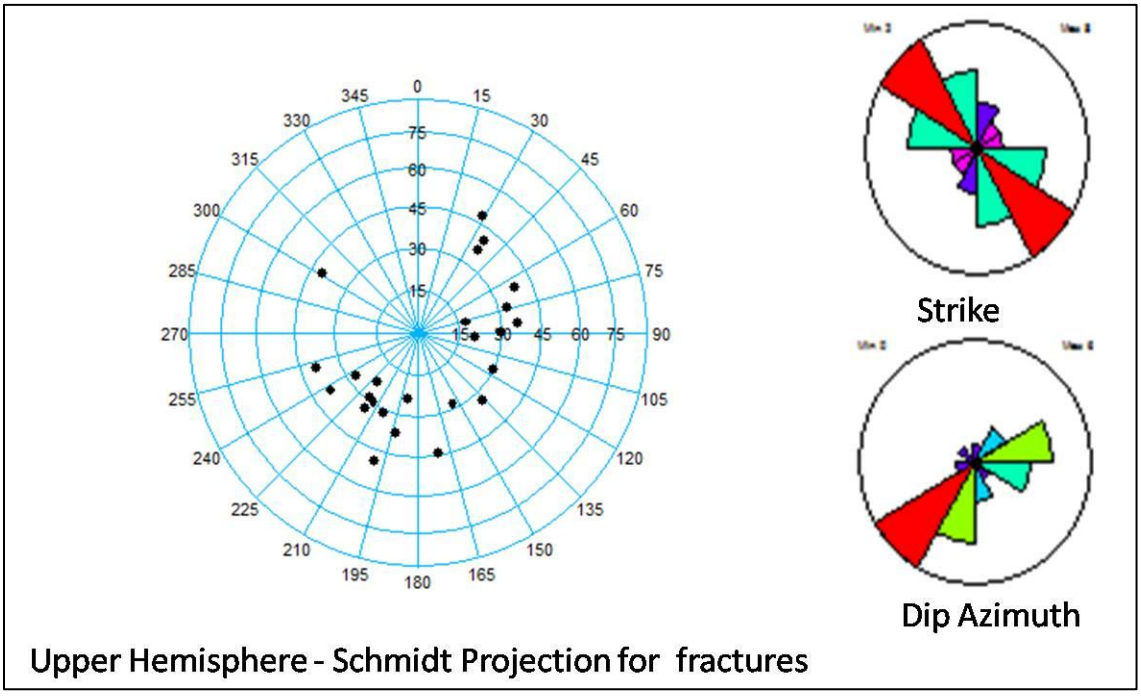

Figure 3-30: Statistical analysis of all continuous conductive fractures in Ruman N-2

The major fracture orientation between depth 863 m and 880 m is NW-SE while the major fracture trend between depth 880 m and 890 is NNE-SSW. Between depth 890m and 900 m the orientation of major fractures mainly NW-SE and NE-SW. In the depth between 900 m and 922 m the major fracture trend toward the NNW-SSE and WSW-ESE.

In Ruman 1A well, statistical analysis of the conductive fractures show that the dip between 20 to 90 degrees to NE and SW with major strikes of NW-SE, and WNW-ESE (Figure 3-31).

The major fracture orientation between depth 2612 m and 2700 m is NW-SE while the major fracture trend between depth 2700 m and 2800 is NNW-SSE, NW-SE and WNW-ESE. Between depth 2800m and 2830 m the major direction became again toward NW.

In Ruman NE-1 well, statistical analysis of conductive fracture dominantly dips 43 degree to the NE and SW with strikes of NW-SE, NNW-SSE, and N-S (Figure 3-32).

The major fracture orientation between depth 1825 m and 1850 m is NNW-SSE and WSW-ESE while the major fracture trend between depth 1950 m and 1975 m is NW-SE. Between depth 1975m and 2006 m the orientation became again toward NNW-SSE.

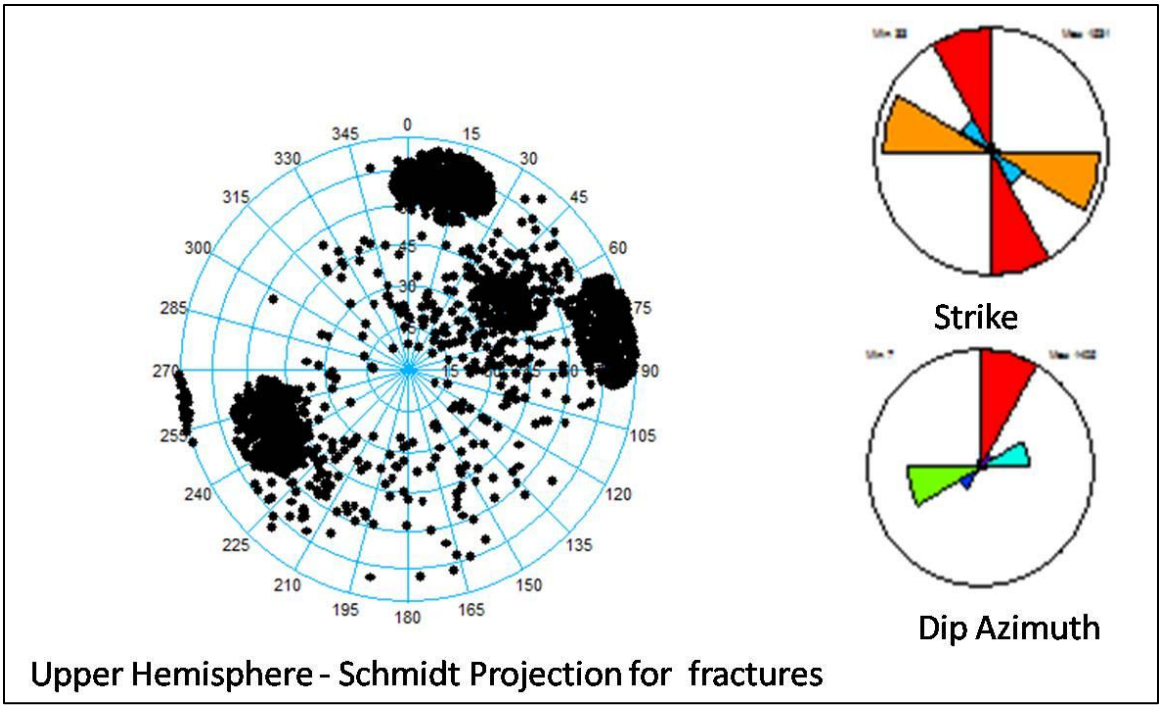

Figure 3-31: Statistical analysis of the conductive fractures in the basement section of well Ruman-1A

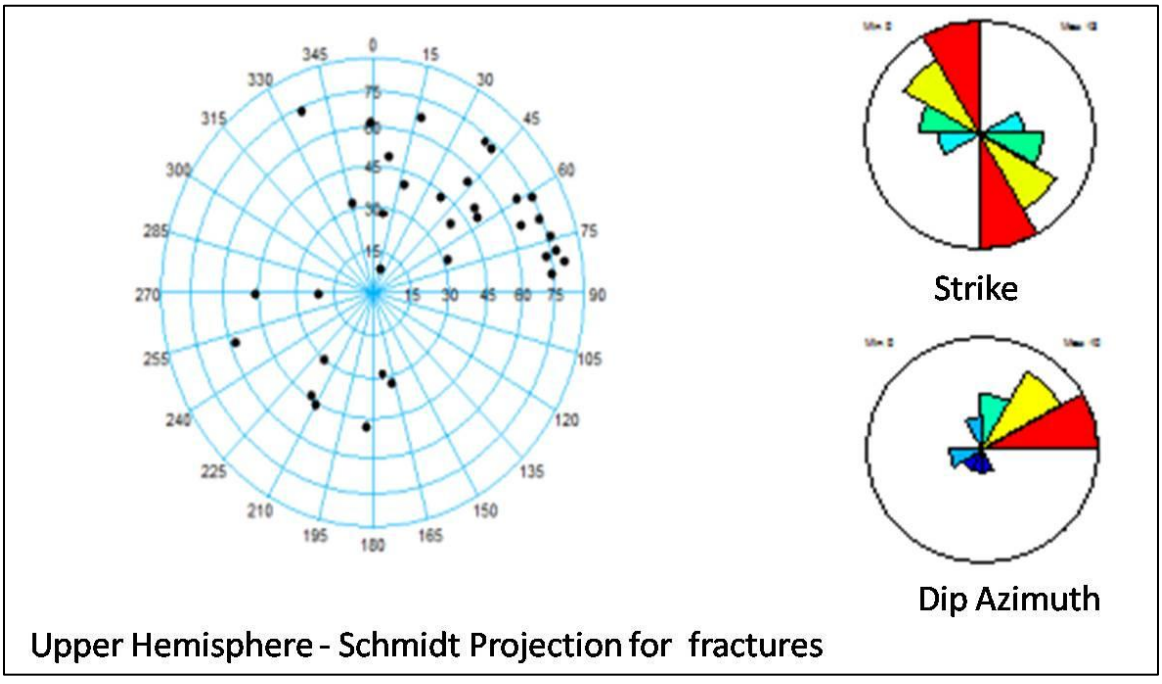

Figure 3-32: Statistical analysis of all continuous conductive fractures dips in Ruman NE-1

In Ruman NNE-1 well, statistical analysis of the conductive fractures dominantly dips 50 degree to the NNE and SW with strikes of NW-SE (Figure 3-33).

The major fracture orientation between depth 1809 m and 1825 m is NW-SE and ESE-WSW while the major fracture trend between depth 1825 m and 1860 is only ESE-WSW. Between depth 1860 m and 1950 m the major direction is NE-SW.

In the depth between 1950 m and 1975 m the major trend toward the NW-SE, NNW-SSE and WNW-ESE. The major orientation between depth 1975 m and 2015 m mainly WNW-ESE.

In all Ruman wells, continuous conductive fractures in Ruman five wells shown in one upper hemisphere-schmidt projection (Figure 3-34). The major fractureorientationsat all the wellsare NW-SE,NNW-SSE to N-S and WNW-ESE to E-W (Figure 3-34) and the minor fracture orientation trend is NE-SW.

3.8 Orientation Analysis Summary

In this study, the lineaments (fractures) and their traces seen on the wells, satellite image, gravityand basement faults from seismic were analyzed for their orientations (Figure 3-35).

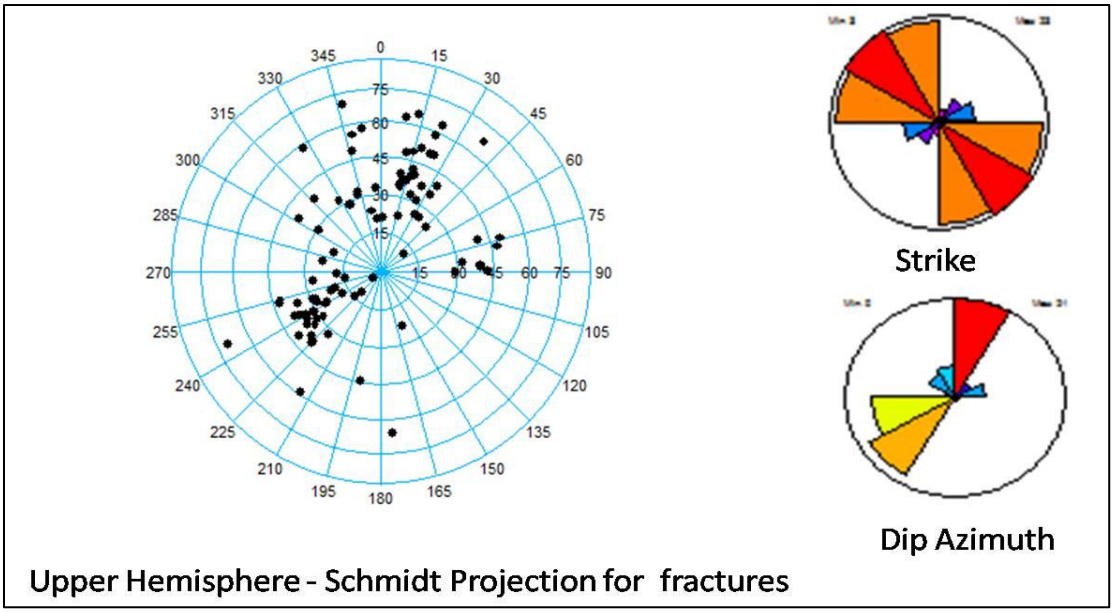

Figure 3-33: Statistical analysis of all continuous conductive fractures in Ruman NNE-1

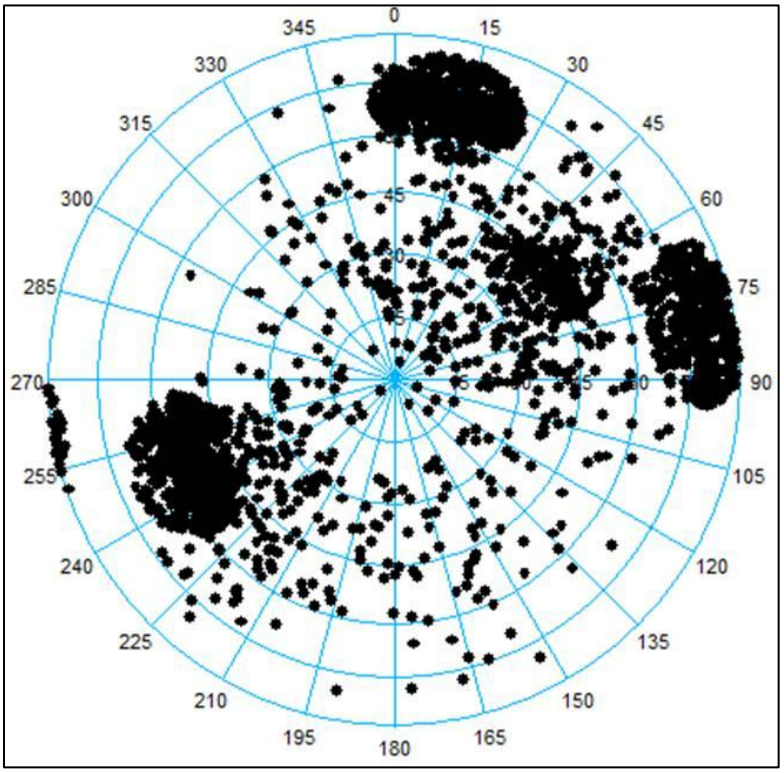

Figure 3-34: Upper Hemisphere-Schmidt projection for fracture, showing all continuous conductive fractures in Ruman five wells

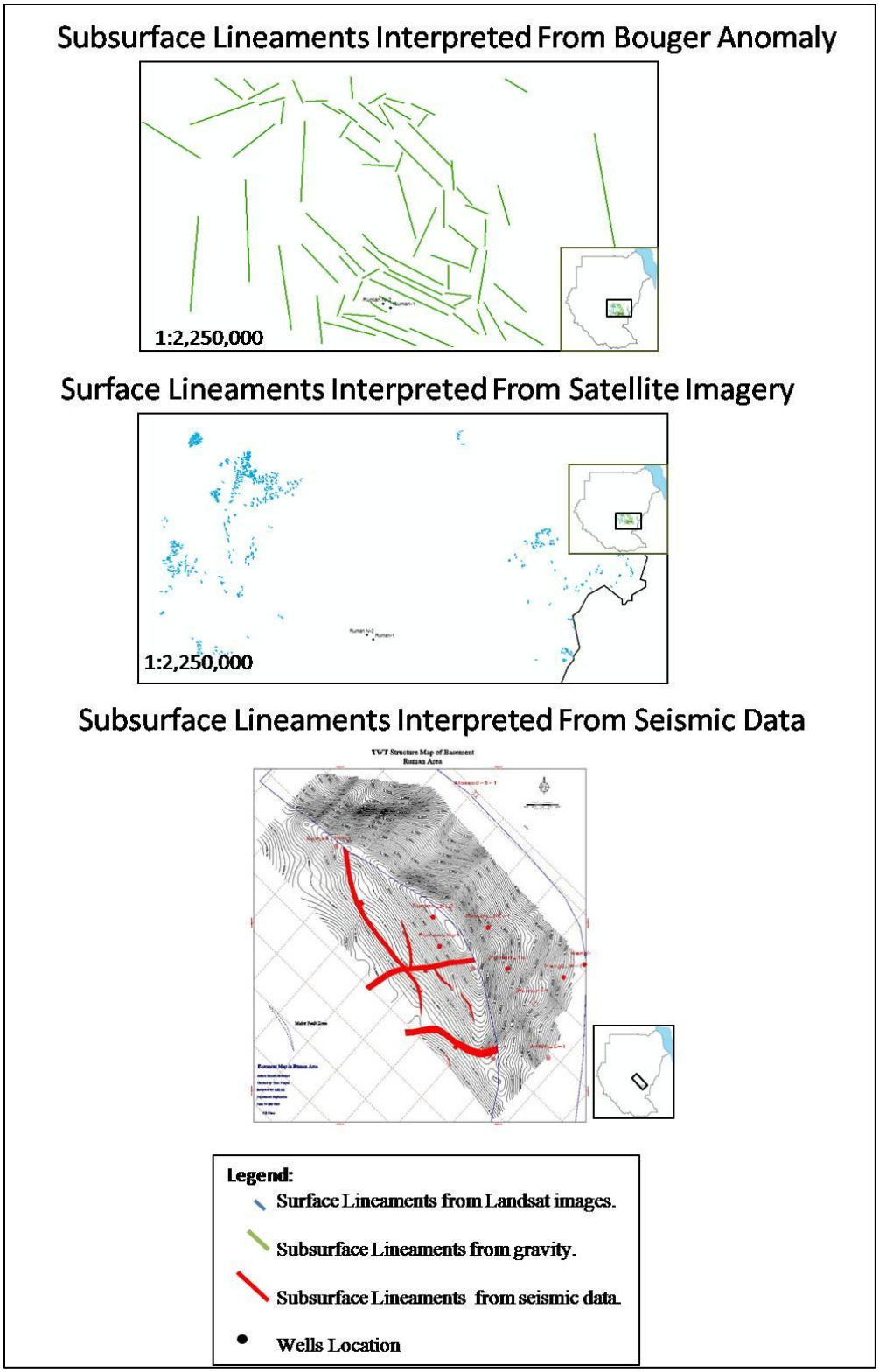

Figure 3-35: Plate showing Lineaments interpreted from Gravity, Surface and Seismic Data

Rose diagrams that generated from all the linear features interpreted in the study area from different sources of data were shown in (Figure 3-36). They were generated based on their trends and frequency.

The surface linear features in the outcrops around Melut basin (NubaMountains to the west and IngessanaHills to the east) show four preferred orientations (NW-SE, NNW-SSE to N-S, WNW-ESE to E-W and NE-SW (Table 1). A majority of the surface linear features in the area are oriented in NW-SE and NNW-SSE. On the contrary, those surface linear features oriented in NE-SW are less prevalent.

The gravity lineaments appear primarily in four sets of directions: two major sets oriented in NW-SE and NNW-SSE to N-S, and the minor sets oriented along NE-SW and WNW-ESE to E-W (Table 1).

The rose diagrams of well data shows that they have four preferred orientations, majority of the fractures and liner features oriented in three directions (NW-SE, NNW-SSE to N-S , WNW- ESE to E-W) and minor directions toward NE-SW (Table 1).

Major and minor faults and fractures within the basement were interpreted from seismic data. The rose diagrams of the strike orientation for those faults and fractures shows that, there are three orientations NW-SE, NNW-SSE to N-S, and WNW-ESE to E-W. The majority of the fractures and liner features toward NW-SE (Table 1).

When we compare the rose diagram generated from the satellite, gravity wells and seismic data; it became apparent they have similar trends (Figure 3-36).

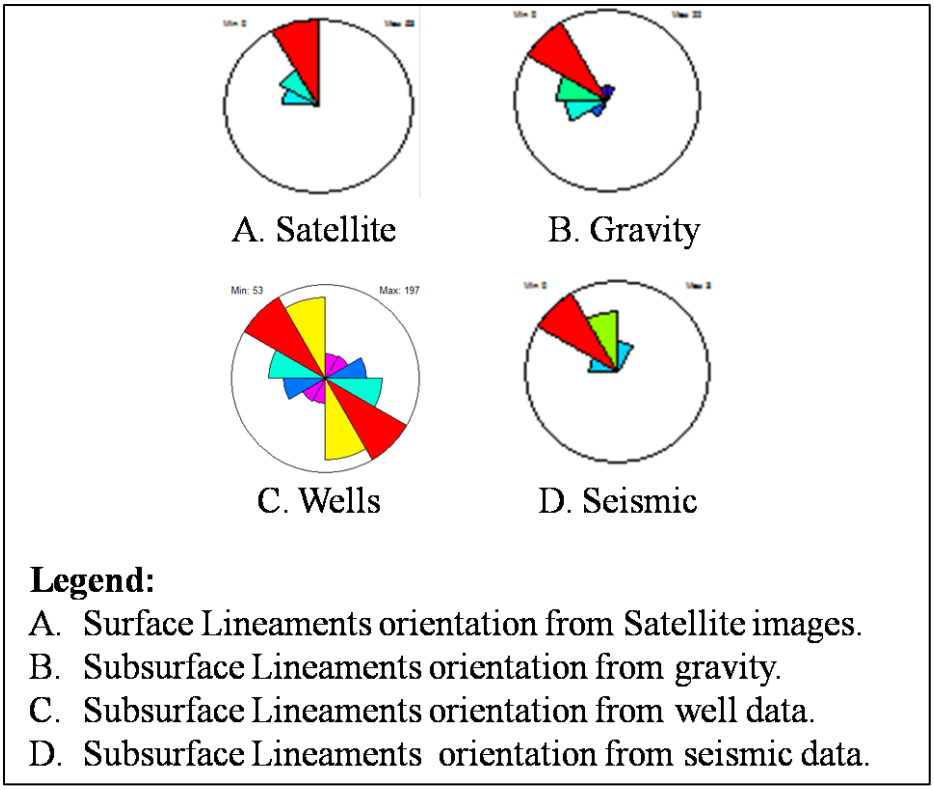

Figure 3-36: Rose diagrams A, B, C and D shows orientations of lineaments derived from outcrops (satellite) and subsurface (gravity, wells and seismic data)

Wells	Seismic	Satellite	Gravity
NW-SE	NW-SE	NW-SE	NW-SE
NNW-SSE to N-S	NNW-SSE to N-S	NNW-SSE to N-S	NNW-SSE to N-S
WNW-ESE to E-W	WNW-ESE to E-W	WNW-ESE to E-W	WNW-ESE to E-W
NE-SW		NE-SW	NE-SW

Table 1: Orientations analysis (fractures strike) using different source of data

3.9 In-situ Stress Analysis

"An additional step which is often of value in basements is to determine whether present day in-situ stress is acting to dilate apertures and hence promote fracture permeability on particular fracture orientations" (Figure 3-37; Hansen, 2008).

Drilling induced fractures dips in Ruman NNE-1 shows the maximum horizontal stress direction around the borehole and Borehole breakouts in Ruman NNE-1 shows the minimum horizontal stress direction around the borehole (Figure 3-38).

The maximum horizontal stress direction (NW-SE) represent the present day in-situ stress at the study area.

The major orientation for all continuous conductive fractures in Ruman five wellsis NW-SE to NNW-SSE (Figure 3-39); so that it is believe that the NW-SE and NNW-SSE fractures will enhanced and opened during the present day.

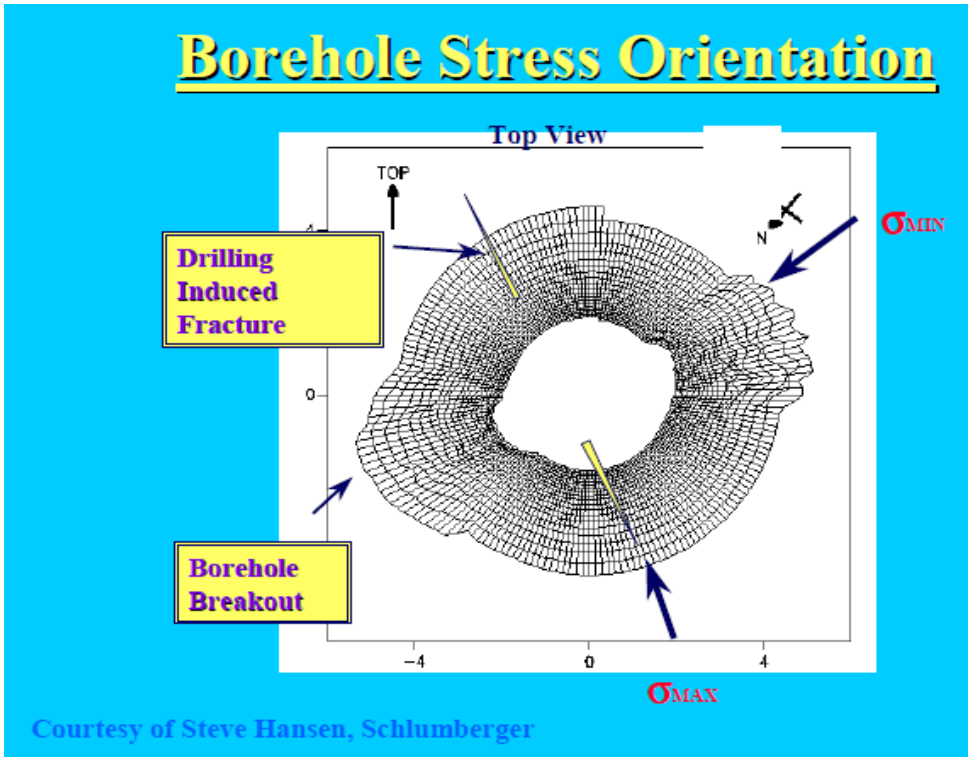

Figure 3-37: Borehole stress orientation (after Steve Hansen, 2008)

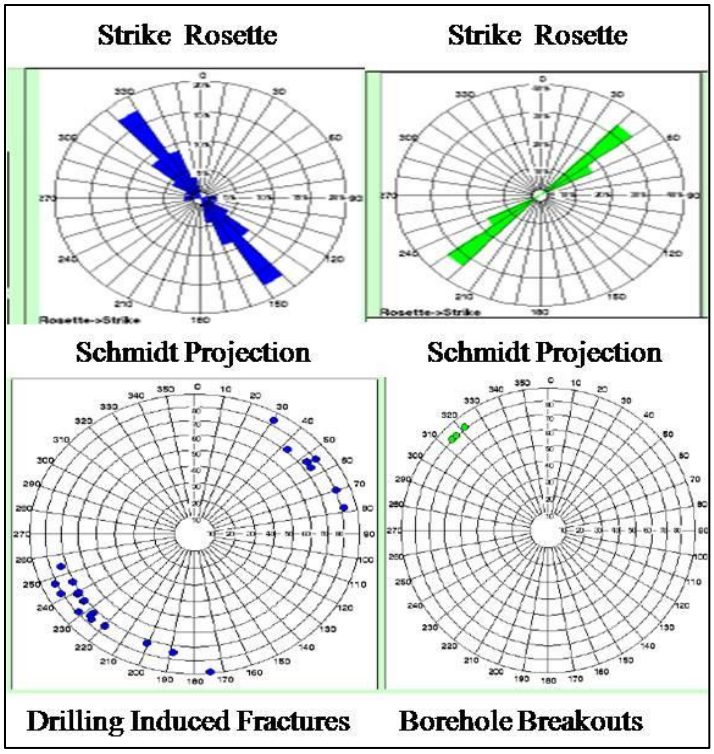

Figure 3-38: Drilling induced fractures dips in Ruman NNE-1 shows the maximum horizontal stress direction around the borehole and Borehole breakouts in Ruman NNE-1 shows the minimum horizontal stress direction around the borehole

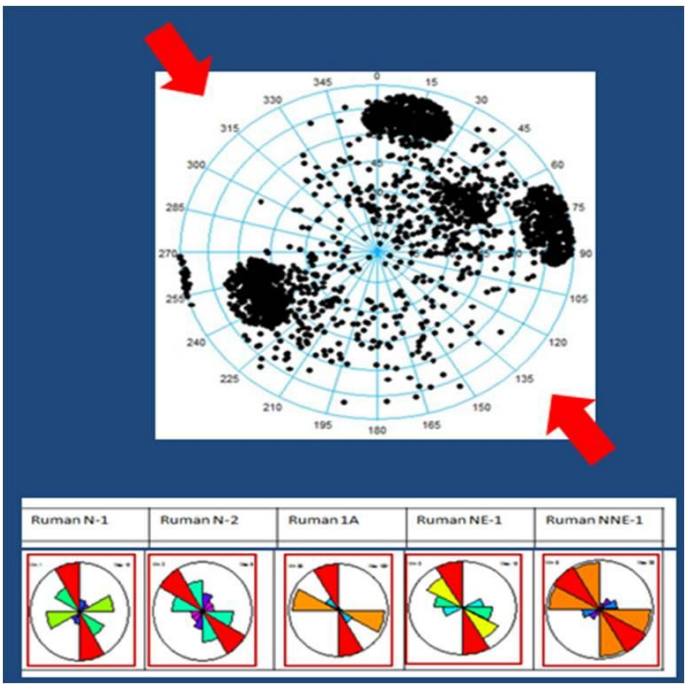

Figure 3-39: Upper Hemisphere-Schmidt projection and rose diagrams for fracture, showing all continuous conductive fractures in Ruman five wells. The red arrows represent the present day in-situ stress and it is acting to dilate apertures and promote fracture permeability on NW-SE to NNW-SSE fracture orientations

3.10 Model of Fracture Origin

The outcomes and findings of this study suggest different origin for fractures associated with basement. Moreover fractures formation can be related to a sequences of chronological geological events that acted or affected the area. The section discusses each event and the possible fractures pattern associated with it. Three stagesmodel were proposed for the origin of the fractures associated with the basement; fractures related to basement formation, fractures related to the Proterozoic tectonic events and faults related fractures (developed during Melut basin rifting).

3.10.1 Fractures Related to Basement Formation

The first set of fractures was developed during the basement origin. Primary fractures or 'cooling fractures' arefractures formed during the emplacement,crystallization and cooling of the magma in theupper crust.

Fractures related to basement formation arecharacterized by evenly spaced joint sets often orthogonal to each other. Thefractures are predominantly Mode I fractures and often filled by pegmatites,volatile-rich melts formed by late-stage segregationof the crystallizing magma. As such, thesefracture sets can be identified as having formedearly in the history of the igneous basement,prior to the onset of regional extension. Allintrusive rocks are expected to have primaryfractures, but their spacing and orientation mayvary greatly within the magma body. For purposesof exploration and production, the geometryof primary fracture sets is hard to predict. However, the presence ofthese fracture sets may have a significanteffect on the porosity and connectivity behavior of hydrocarbon reservoirs.

Fractures related to basement formation are represented by small joints and faults and include four main classes namely; cross joints, longitudinal joints, flat-lying joints, and diagonal joints (Price and Cosgrove, 1990) (Figure 3-2). In Ruman area, the longitudinal fractures are parallel to the body elongation axis (NW-SE trend) (Figure 3-40) and the cross joints are perpendicular to the longitudinal fractures (NE-SW trend).

Fractures related to the basement formation are most probably of the age of Proterozoic as the age of basement rocksin Sudan meanly identified as Pre Cambrian rocks.

3.10.2 Proterozoic Tectonic Fractures

Melut basin is underlain and surrounded by Precambrian rocks, which were almost reactivated during the Neoproterozoic Pan-African tectono-thermal event (from 1200 Ma to 500 Ma) and developed many weakness zones. These weakness zones were mainly developed during two periods, the first period was the Early Proterozoic and it reworked during the Pan African tectono-thermal episode (Schandelmeier et al., 1987a; Vail, 1978). The second period was during of the Late Proterozoic juvenile mobile belts (Arabian-Nubian Shield).The area of Melut basin characterized by suture zone between the Pre Neoproterozoic crust and the Neoproterozoic crust, however the deformation created some lineaments parallel to the suture zone with SE orientation.

Parts of the Precambrian crust have been remobilized by the Pan-African thermo-tectonic rejuvenation episode between 900 and 550 Ma.

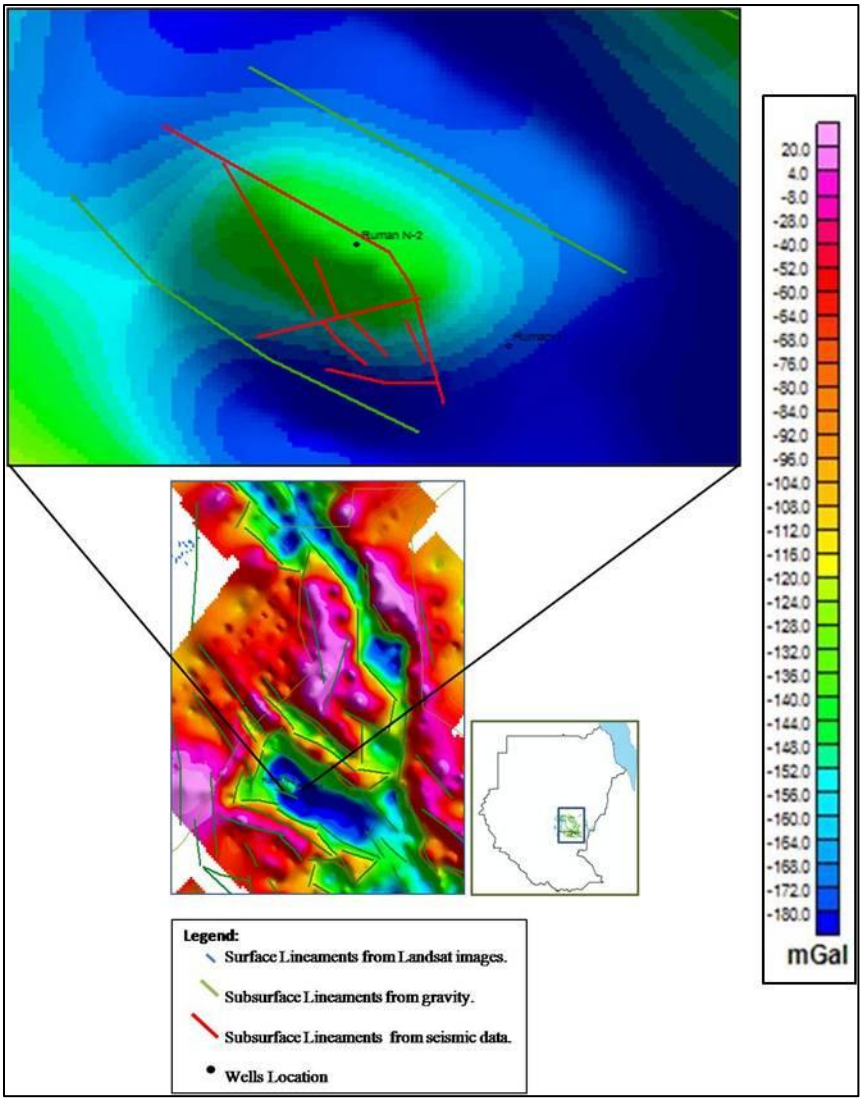

Figure 3-40: Bouguer anomaly images, showing Ruman area wellelongated oval shaped, superimposed by lineaments interpreted from seismic and gravity data

These basement rock formationsoutcrop in five uplifted Precambrian blocks separated by deep depressions which are filled with Phanerozoic sedimentary sequences.

In the eastern Nuba Mountains in central Sudan a NE-SW to NNE-SSW striking belt of low-grade volcano-sedimentary rocks is exposed, which contains fragments of highly dismembered ophiolites and basic to acidic plutons. These arc ophiolitic assemblages were metamorphosed at about 700Ma, with post-tectonic magmatism ceasing at around 550Ma.

The metamorphic rocks are intruded by Neoproterozoicgranitoids ranging in age between 750 and 550 Ma and the mediumto high-grade metamorphism suggests that these terrains could bePaleo-proterozoic or even Archean continental crust.

The final deformation along the Keraf Suture is also defined by N-trending upright folds and NNW-trending sinistral strike-slip faults.

Ar/Ar ages obtained from a granitic body deformed by sinistral strike-slip shearing along the Keraf suture indicates an age of 560 Ma for the end of this deformation.

The origin of the N-trending upright folds and strike-slip faults is far-reaching stresses due to E–W directed crustal shortening which related to collision between the Saharan Metacraton and the Arabian-Nubian Shield(Abdelsalam et al., 2002).

Largely undifferentiated crystalline igneous and metamorphic rocks form the Proterozoic ‘basement complex’ that underlies large parts of Sudan. Pre-

Neoproterozoicrocks include gneisses of Paleo-proterozoic age and are part of the ‘Saharan Metacraton’ (Abdelsalam et al., 2002).

The basement rock in and around the area of study undergone various crustal deformation events in Early and Middle Proterozoic, completed under the Late Proterozoic Pan African Tectono Thermal Episode. These deformational events comprise the early three-stages deformation events during the Early to Middle Proterozoic (Schandelmeier et al., 1987a), characterized by an initial folding at about 2100 Ma, drift and rotation of Gondwana at around 2000 Ma and the subsequent formation of transcontinental shear zones.

The collision of North African continental plate with the West African craton during the Late Pan African Episode generated a compressive stress at the margin of the plate which resulted in the formation of transcontinental shear zones during that time.

During the Late Proterozoic juvenile mobile belts, crustal thickening and shortening, calc-alkaline magmatism, emplacement of ophiolitic belts, thrusting, shearing and strike-slip faulting were resulted from the high tectonic events.

According toAbdelsalam(2003)the main deformational phases of the northeastern part of the Saharan Meta-craton were due to the collision of Arabian Shield and East Sahara Meta-terrain.

The development of N to NW trending sinistral strike-slip faults at about 590 Ma –550 MA due to collision between Saharan Metacraton and the Arabian-Nubian Shield (Figure 3-36). And the development of N-S trending normal-slip faults as a result of

extensional collapse about 550 Ma of northeastern part of the Saharan Metacraton and Arabian-Nubian Shield (Figure 3-41).

To summaries the Proterozoic tectonic events, the area of study was characterized by suture zone between two different basement types to West and to the East. The Proterozoic tectonic events in this zone caused the development of N-S trend lineaments parallel to the suture zones.

In schist metamorphic rocks, the foliation can provide primary transmissibility and exert a control on the subsequent development of tectonic fractures that influence porosity and permeability.

In Ruman NNE-1, foliations were observed from depth 1812 m to 2018 m (Figure 3-42). The foliations trend mainly WNW-ESE and the azimuth direction toward NE.

In Ruman area, those fractures trending N-S might be related to the Proterozoic tectonic events and reactivated later by the faults during Cretaceous and Tertiary .

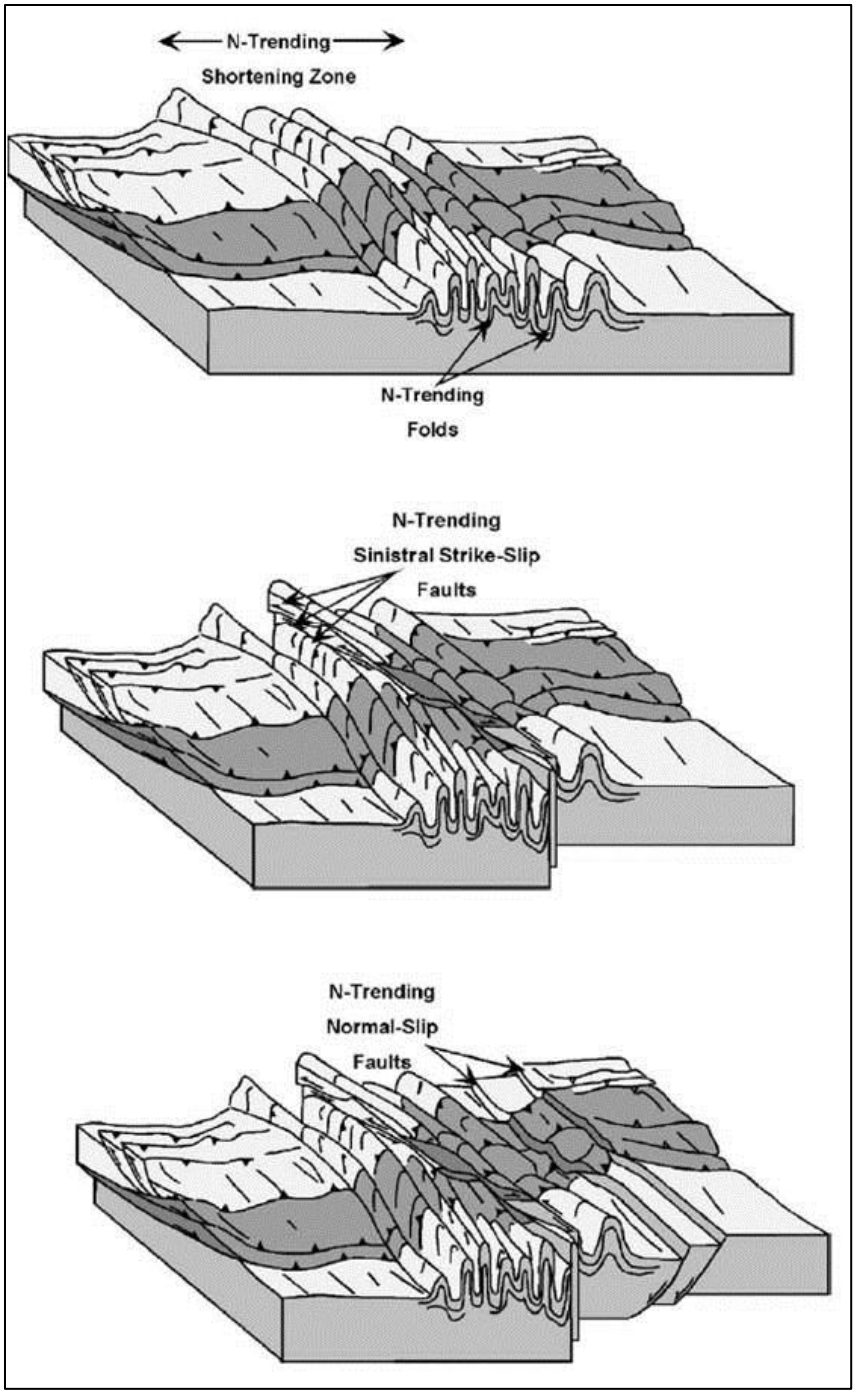

Figure 3-41: Three-dimensional cartoon illustrating structural evolution of the northeastern part of the Saharan Metacraton (after Abdelsalametal., 2003)

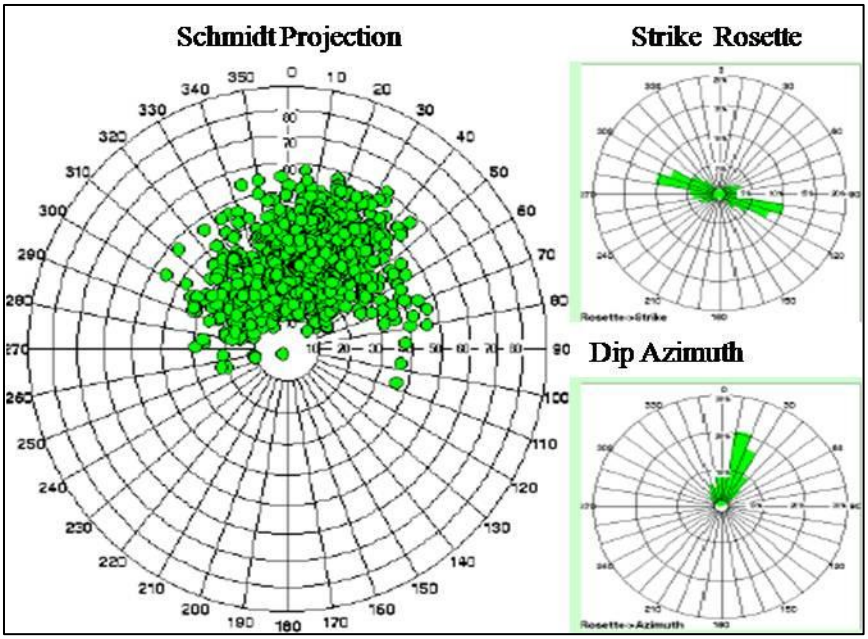

Figure 3-42:Statistical plots in Ruman NNE-1 well from depth 1812 m to 2018 mof the foliation formed within basement and detected the main trends are WNW-ESE and NE-SW

3.10.3 FaultsRelated Fractures

Faults and Fractures developed and/orreactivated during the Melutbasin formation represents the third stage of fracture origin model. To determine the faults and fractures evolution during the Melut basin formation; fractured from well data and faults from seismic data were analyzed base on orientation. These orientations have been classified according to the direction of the kinematic forces in the rock mass(Figure 3-43).The major fracture orientation at all the wells is NW-SE to NNW-SSEand WNW-ESE and the minor orientation is NE- SW (Figure 3-44). The major faults orientation from seismic structural map is NW-SE to NNW-SSE and WNW-ESE to E-W (Figure 3-45). It is believe that many of those fracturesdeveloped during the first and second phases and re-activated again during the third phase.

During the Early Cretaceous (Barremian) the major extension Start by NNW-SSE to N-S (Guiraud and Bosworth, 1997). It caused the development of WNW-ESE to E-W trending lineaments parallel to the Central African Shear Zone (CASZ) (E-W and/or ENE-WSW). During the Early Cretaceous (Albian), a major phase of NE-SW extension occurred in the Melut area due to the opening of the South Atlantic Ocean (Guiraud and Bosworth, 1997). It caused the development of NW-SE to NNW-SSE trending lineaments.

During the late Cretaceous the NW–SE trending faults were reactivatedby the NE–SW extensional stress (Fairhead, 1988).

During the final rifting phase began in the Paleocene NE-SW trending faults occurred as a result of Tertiary extension during the opening of the Red Sea.

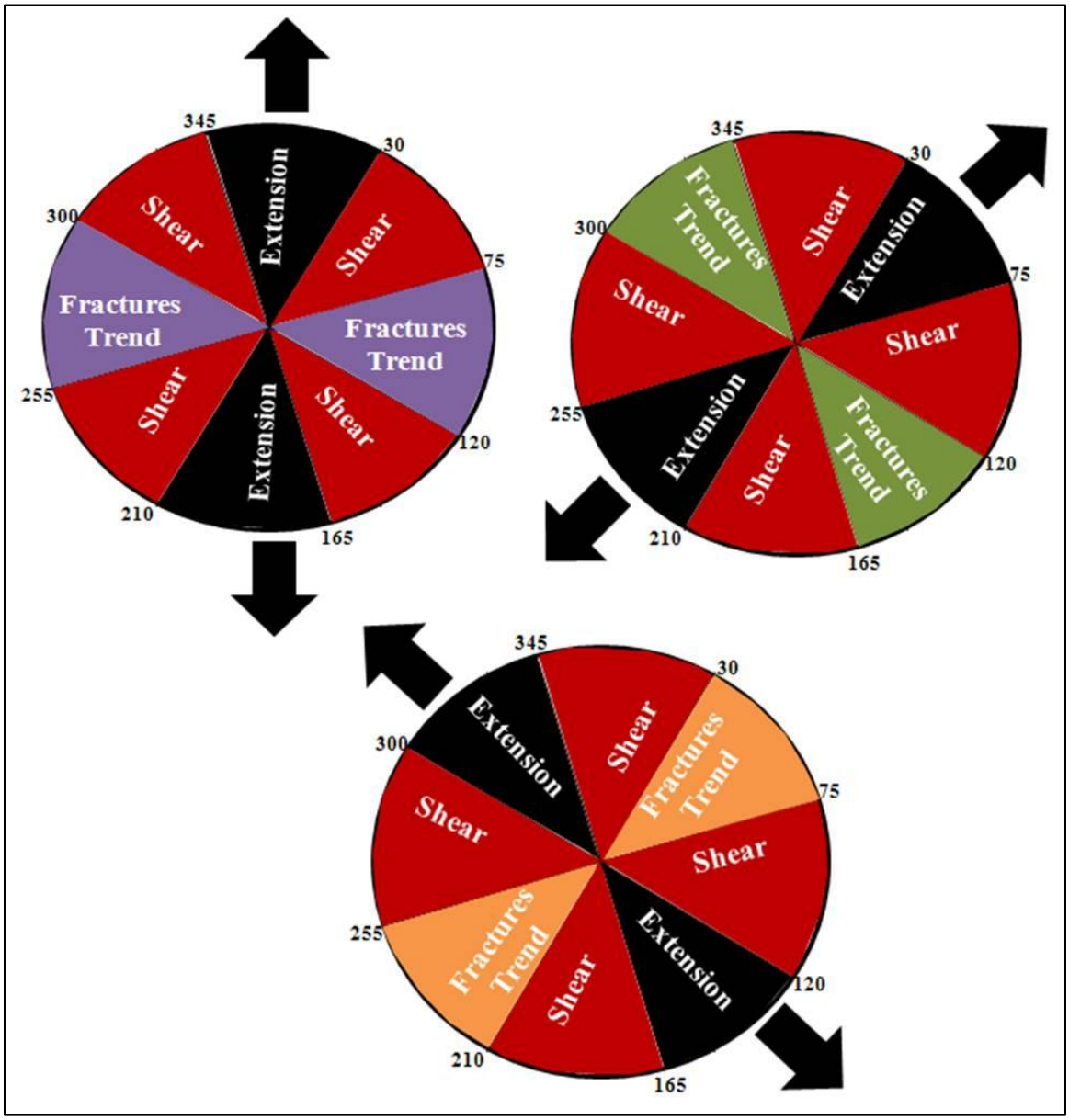

Figure 3-43: Rose diagrams showing the classification of fractures pattern based on the proposed extensional direction in Melut basin

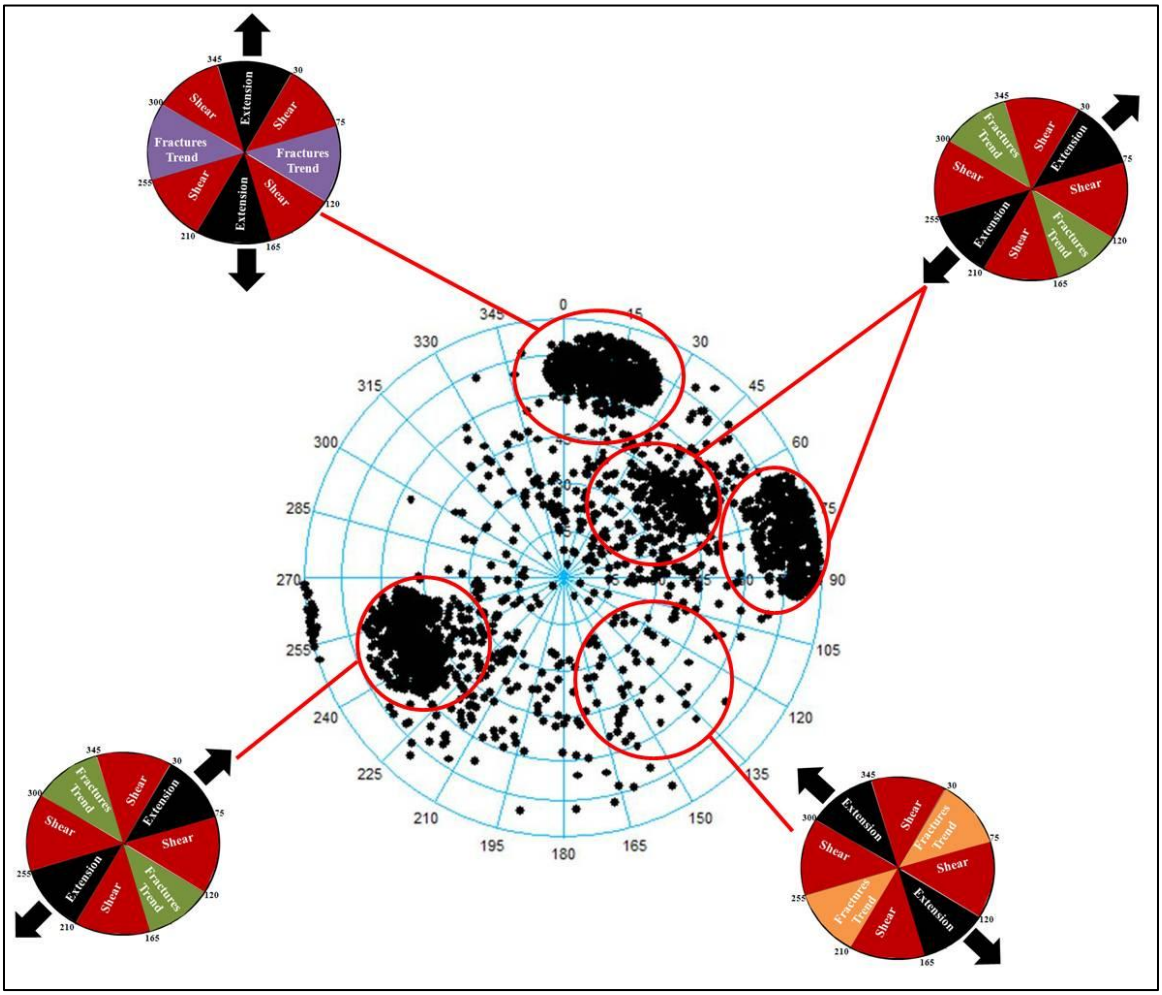

Figure 3-44:Upper Hemisphere-Schmidt projection for all fractures in Ruman five wells and Rose diagrams classification of fractures pattern based on the proposed extensional direction in Melut basin

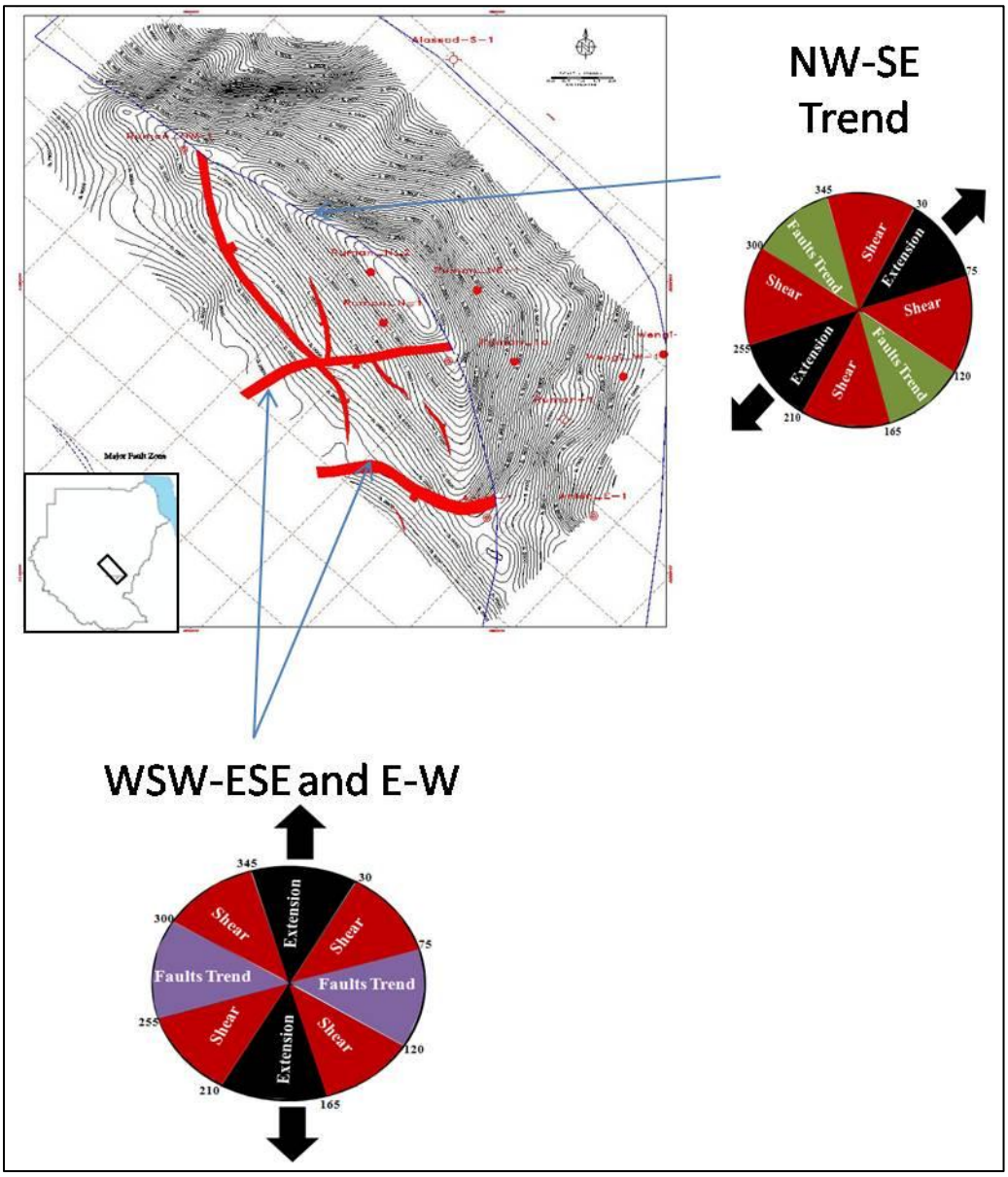

Figure 3-45: Structural map from seismic, showing the different faults orientation as a result of tectonic regimes

3.11 Hydrocarbon Migration

Basement prospects are usually structural highs, with substantial vertical relief. Fractured basements are commonly believed to be charged through the flanks or through thetop of the basement structure.

From hydrocarbon analysis of Ruman five well; Ruman N-2 tested oil (Prove oil), Ruman N-1 no oil in basement (Figure 3-46);Ruman A-1, Ruman NE-1 and Ruman NNE-1 have oil shows and encountered mud losses during drilling. These evidence prove that the oil come throw Ruman A-1, Ruman NE-1 and Ruman NNE-1 throughout the fault zone and pass away toward the basement crest (Ruman N-2) (Figure 3-46).

Ruman traplink with the source rock (Galhak) by the fault zone, this provides very good charging mechanism (Figure 3-45 and Figure 3-47).

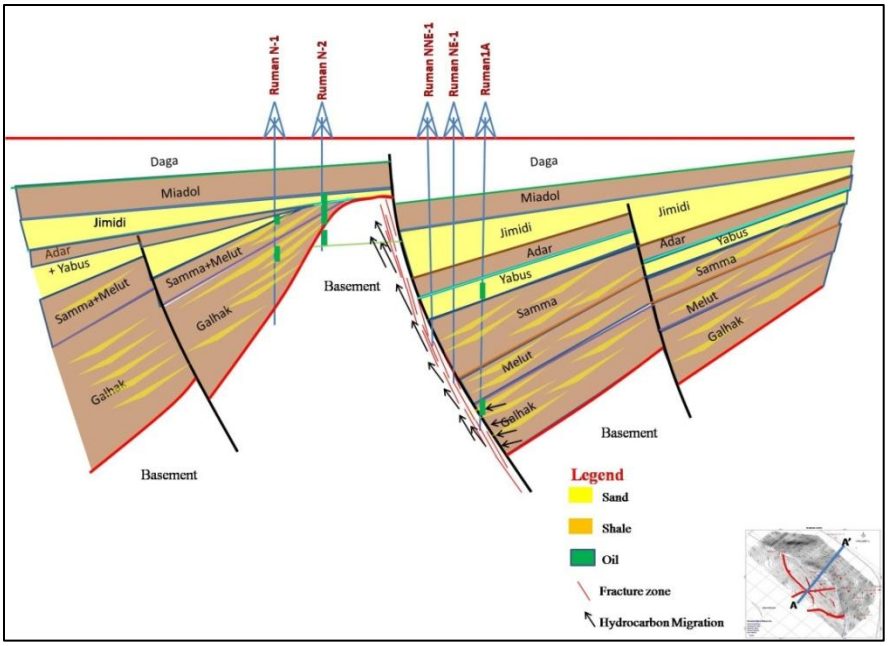

Figure 3-46: Geo-Seismic Cross-section, showing Ruman basement migration pass way throw fractures zone related fault, not scaled

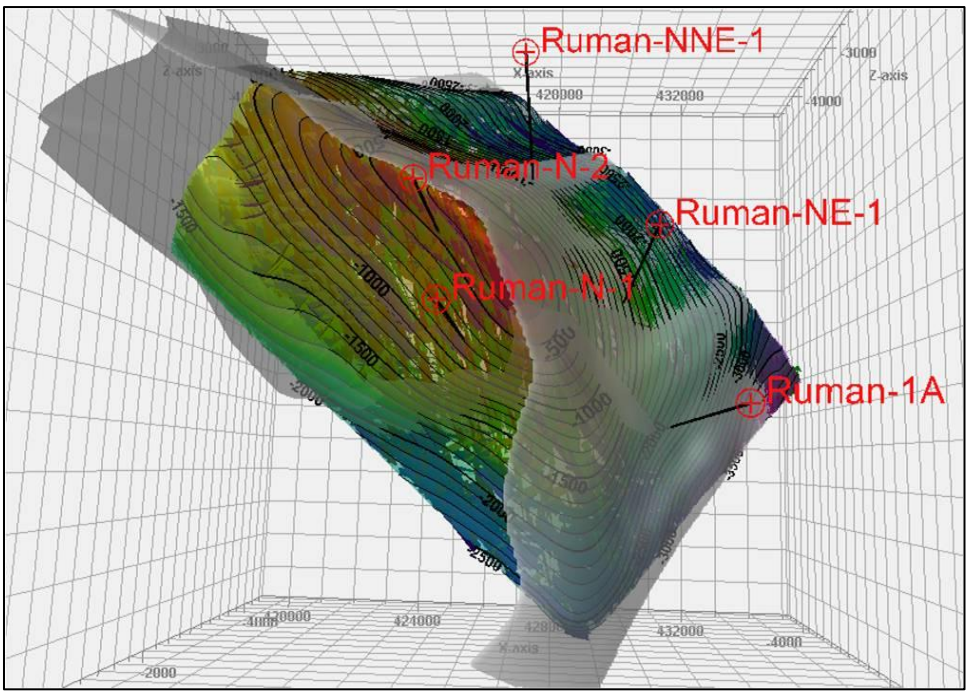

Figure 3-47: Ruman structural map, showing Ruman traplinked with the source rock by the fault zone, this provides very good charging mechanism

CHAPTER FOUR

FRACTURE MODELING

Fracturemodeling consists of many steps starting by analyzing thefracture properties and defining different fracture sets, generating theintensities of the different fracture sets and finally generating the discrete fracture network.

4.1 Geo-cellular Model Description

For better representations of fractured reservoir, model geometry was built based on the basement tops from wells and the seismic interpretation of the basement horizon. The size of the study area is about 124 sq km (dimensions are 9,500 m by 13,100 m) as shown in Figure 4-1. The uppermost surface of the model corresponds to the basement top. The elevation ofthe bottom surface was set to 250 m from the basement top. Therefore, basement model has an equal thickness of 250 m.Figure 4-2, shows a structural map for the top and base of the basement at the study area. Figure 4-3, shows a 3D view for the top and base of the basement that were used in the model.

The lateral dimensions of the cell size is 50 X 50 m. Based on that, the model areal dimensions is 314 cells wide by 320 cells long (Figure 4-4). The model domain has one layer and divided into 25 zones each zone thickness is 10 m. These zones were defined based on the mechanical deformation represented by the fracture intensities. The total number of cells in the model is 2,512,000 cells.

4.2 Analyzing Fracture Properties

Data from the five wells were imported and analyzed inPETREL software (Schlumberger, 2009).Figure 4-5 displays the elements representing the attitude of thefractures intersecting the well. Fractures orientation (dip angle and dipazimuth) were imported, together with their positions into the wells.

4.3 Fracture Sets Identification

The fracture data were analyzed in a stereonet, which plots the poleto the fracture plane characterized by its dip and azimuth. The numbers of 543 fractures were measured on the five wells. The different sets of fractures were identified by visualizing all the fracturesfrom all the wells in the stereonet. Figure 4-6 shows that seven different fracture setswere generated base on their orientations.

The different fracture sets were modeled separatelyto generate as several discrete fractures network (DFN) groups. AllDFN groups were combined into a global DFN model.

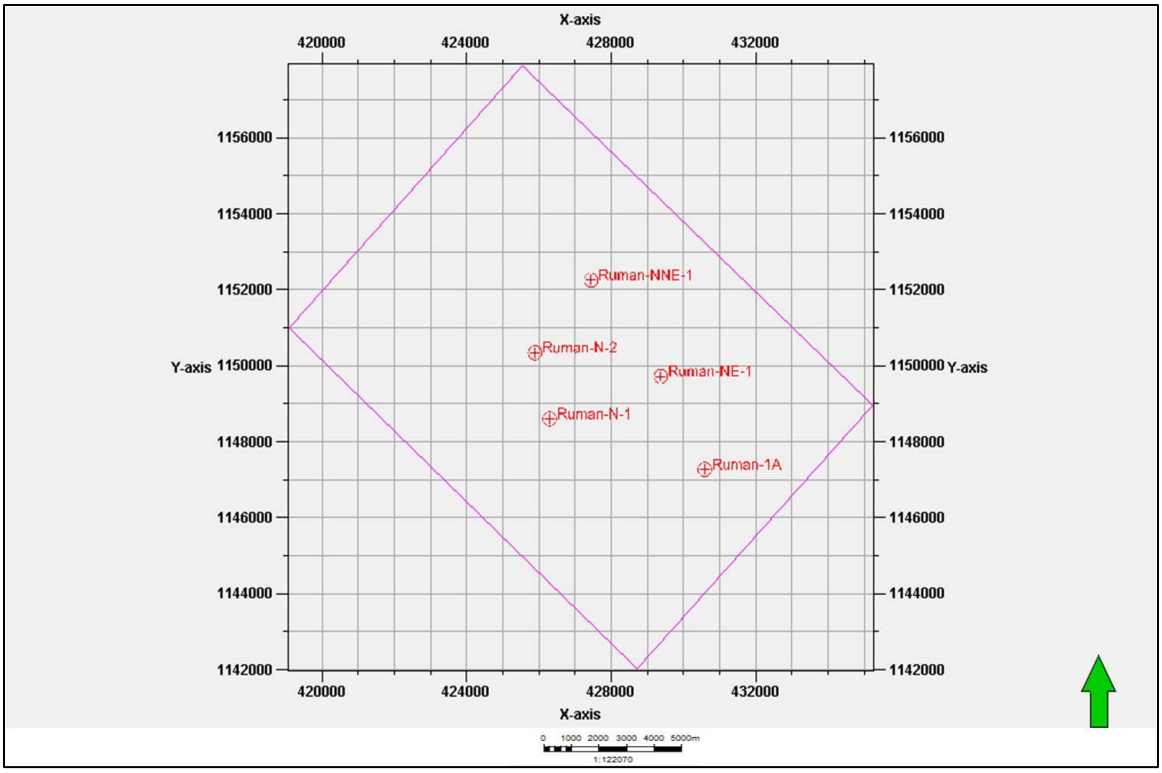

Figure 4-1: The base map of the modeled area shows the well locations and the size of the study area is about124 sq km (Dimension 9,500 m by 13,100 m)

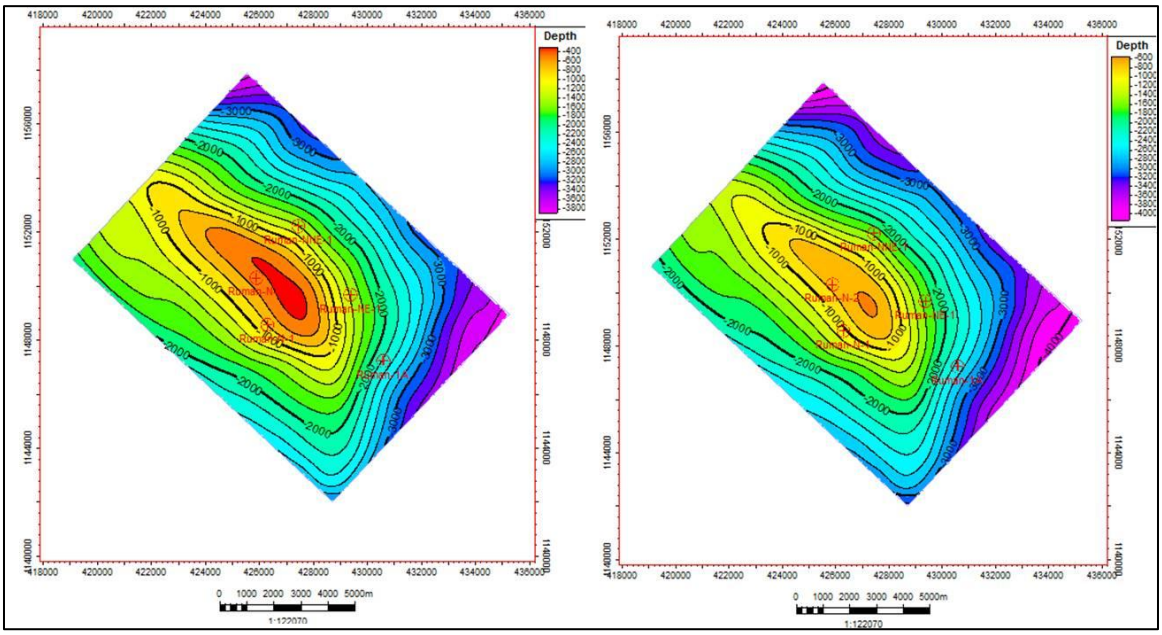

Figure 4-2: The structural maps of the top and base basement surfaces. The upper right legend represents the elevation in meters. The bottom legend represents the map scale in meters

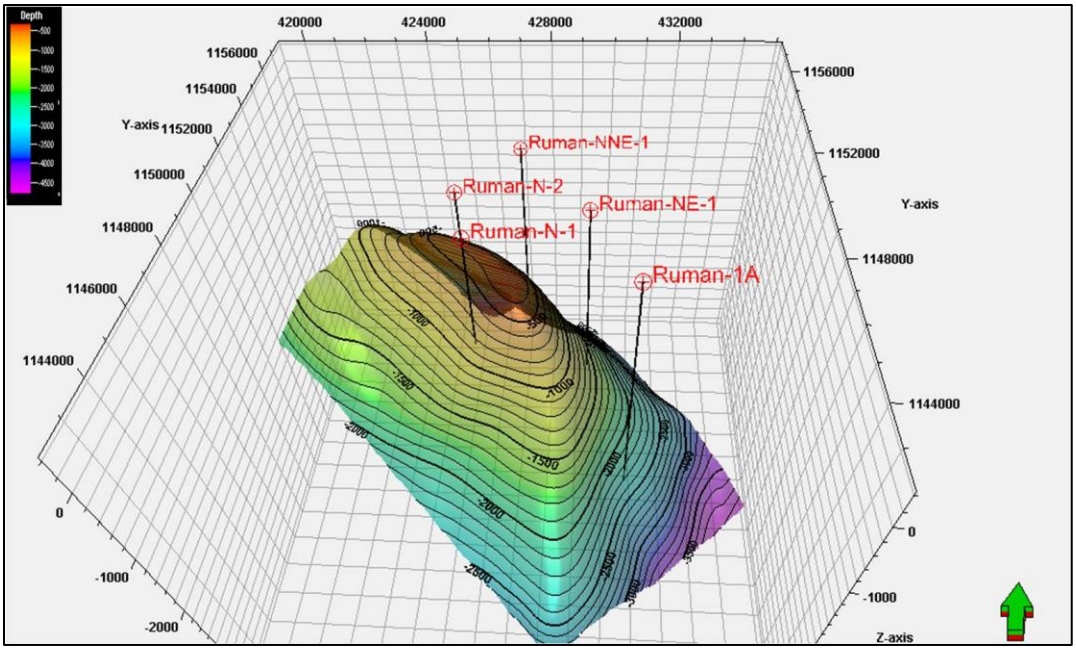

Figure 4-3: The structural map of top basement. The grid coordinates in this view are UTMs and the upper left legend represents the elevation in meters

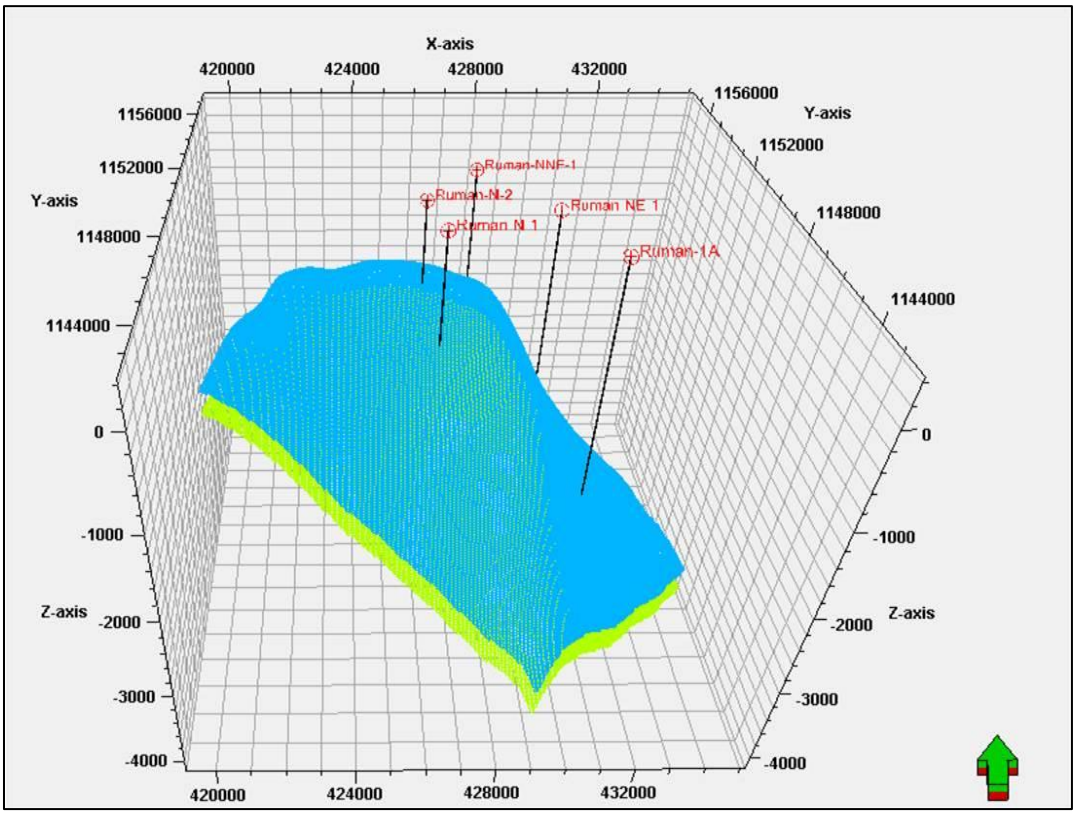

Figure 4-4: The generated 3-D grid of the model

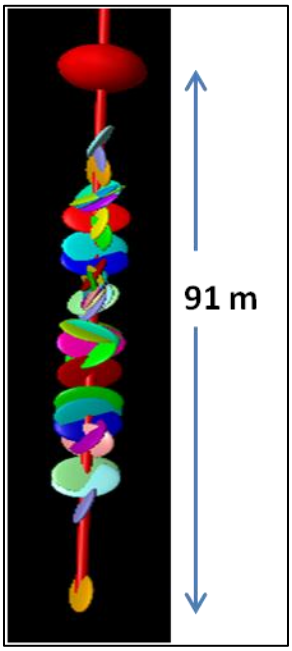

Figure 4-5: Elements representing the attitude of the fractures intersecting Ruman N-1 well

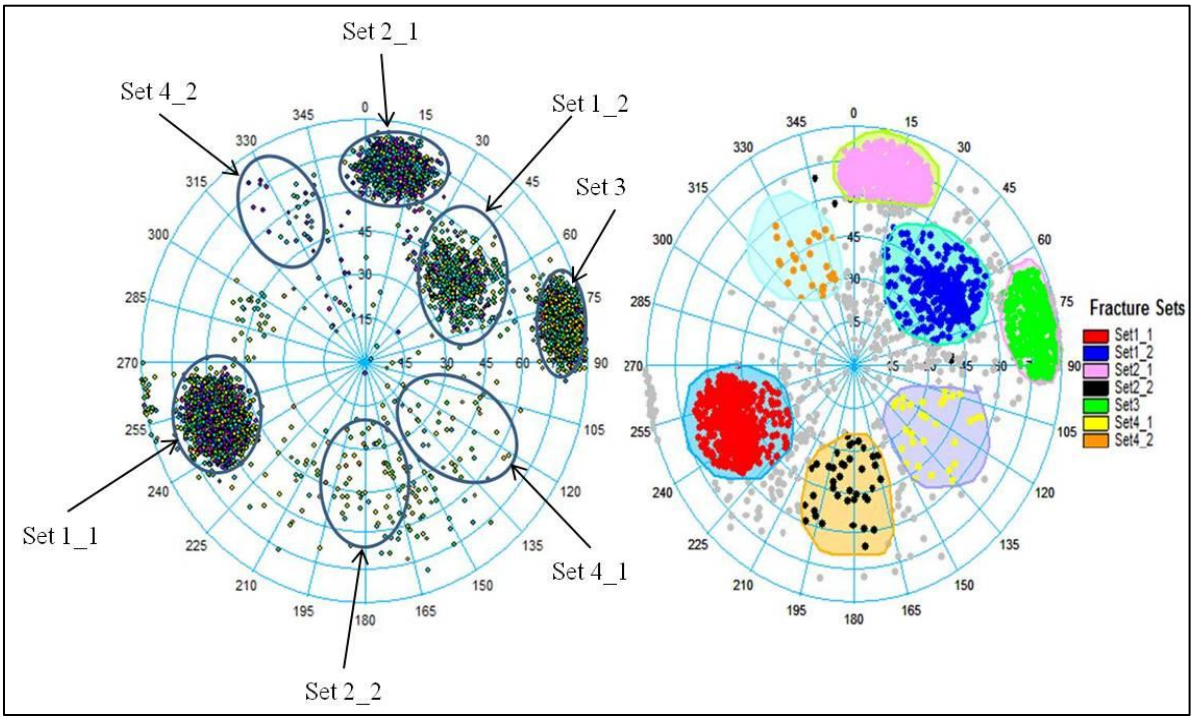

Figure 4-6: The schmidtstereonet, visualizing all the fracturesfrom all the wells. Seven fracture sets were generated

4.4 Fracture Intensities Generation, Upscalling and Simulation

Using the fracture sets identified in the previous step, the next step was to find how fracture intensity varies vertically and horizontally in the area of study. This was accomplished through an upscaling process forfracture intensity followed by interpolation.

Fracture intensities were calculated for each fracture set at each well.Intensity is defined as the number of fractures per unit length. Fracture intensityis calculated by sliding a triangular window along eachwell. Inorder to obtain a good estimate of the intensity along eachwell, alog sample interval of 1 m and a window length of 5 mwere chosen.In this way, the effect of single fractures is removed and the averagefracture intensity is shown over the specified interval around eachpoint. The results for the five wellstotal intensity and the total intensity upscaledinto the 3D gridare presented in Figure 4-7 and Figure 4-8 respectively.

The fracture intensity logs were generated for each set at each well thenupscaledinto the 3D grid (Figure 4-9 and Figure 4-10). During the upscaling process, thefracture intensity is averaged for the segment of the well thatintersects a particular model grid cell, and that value is applied to thecell.

The upscaled intensity values are then interpolated over thedomain; Sequential Gaussian Simulation (SGS) algorithm from GSLIB was used for interpolation as it provided a reasonableinterpolated dataset. The Sequential Gaussian Simulation is a stochastic method of interpolation based on Kriging. It can honor input data, input distributions, variograms and trends.

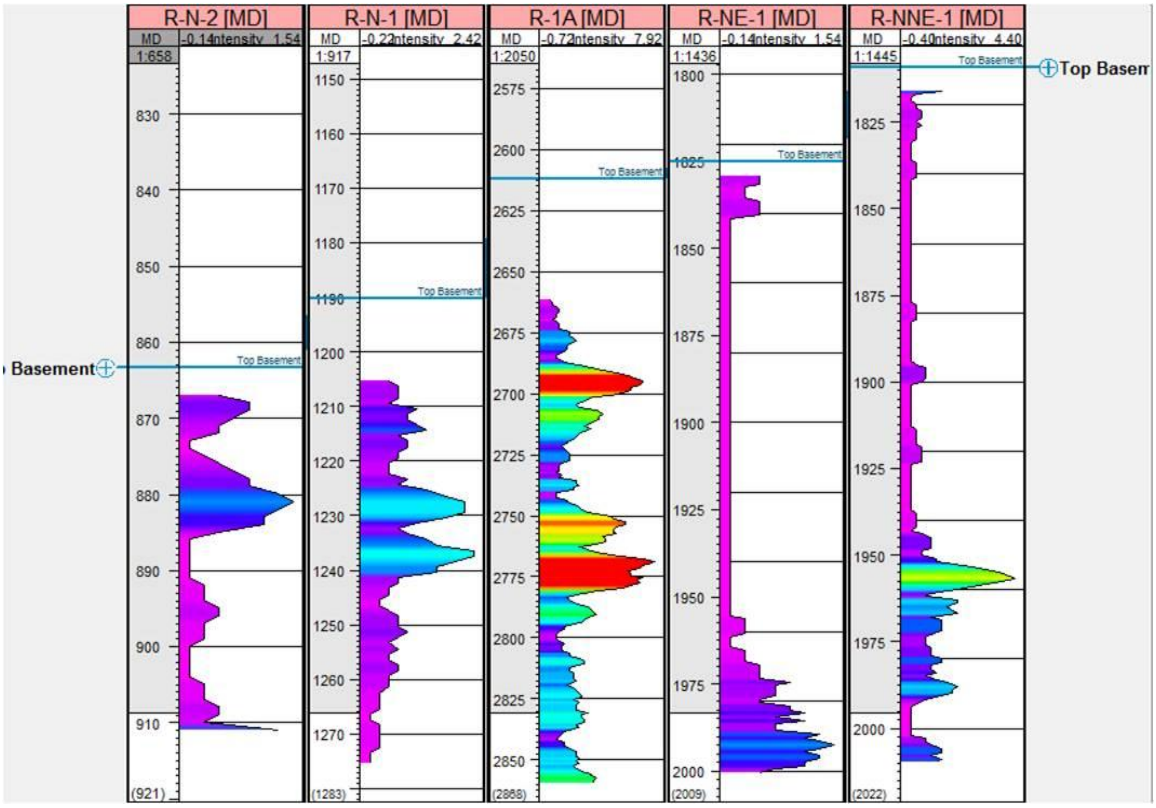

Figure 4-7: Total intensity logs (curves). Intensity logs represent the number of fractures intersecting the well per unit length. The vertical axis (MD) is the measured depth along the wells. The figure represents the five well

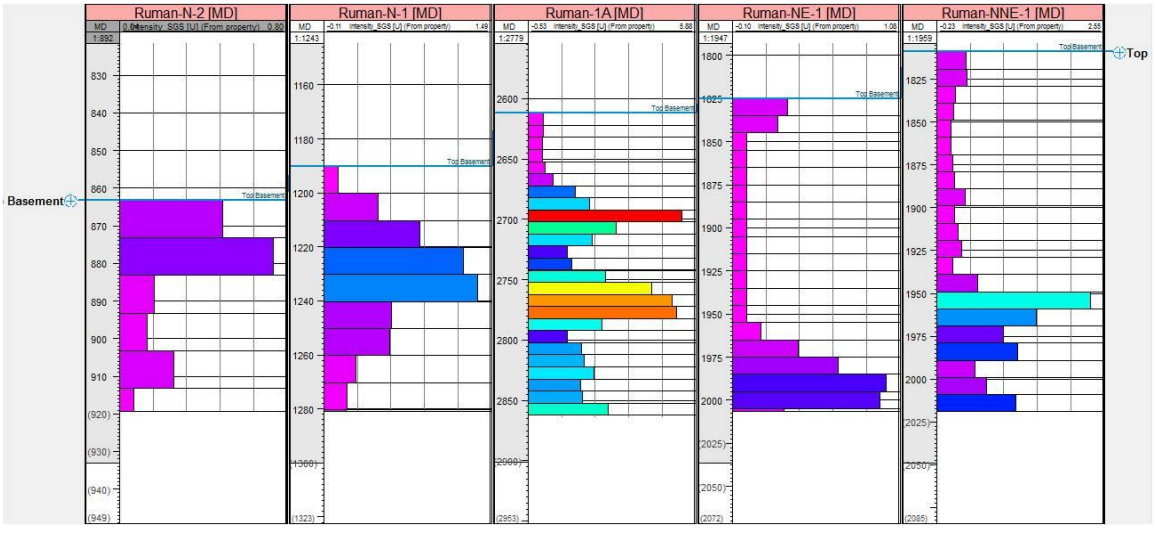

Figure 4-8: Upscaled total intensity for the five wells

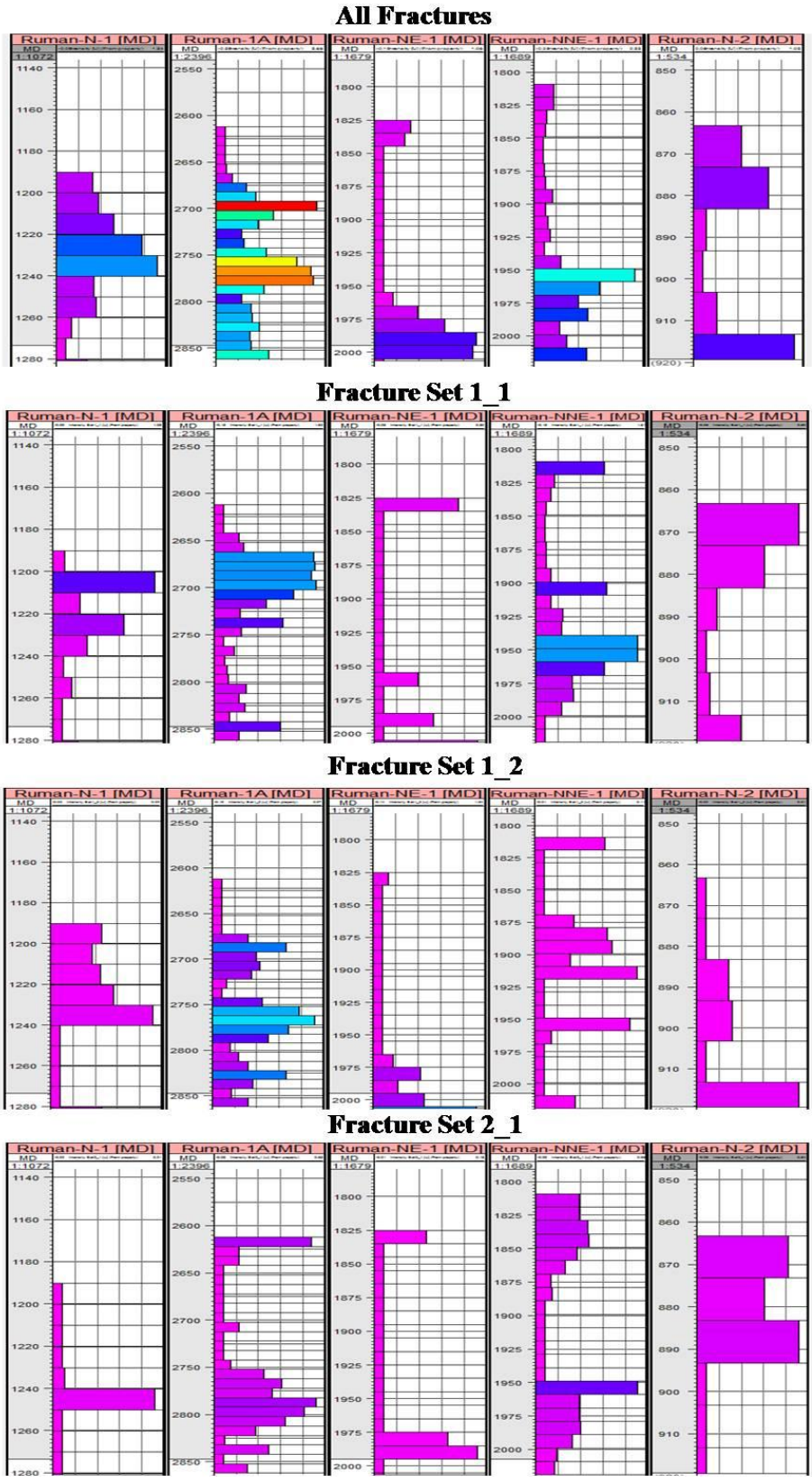

Figure 4-9: Upscaled fracture intensities for each fracture set at all the wells

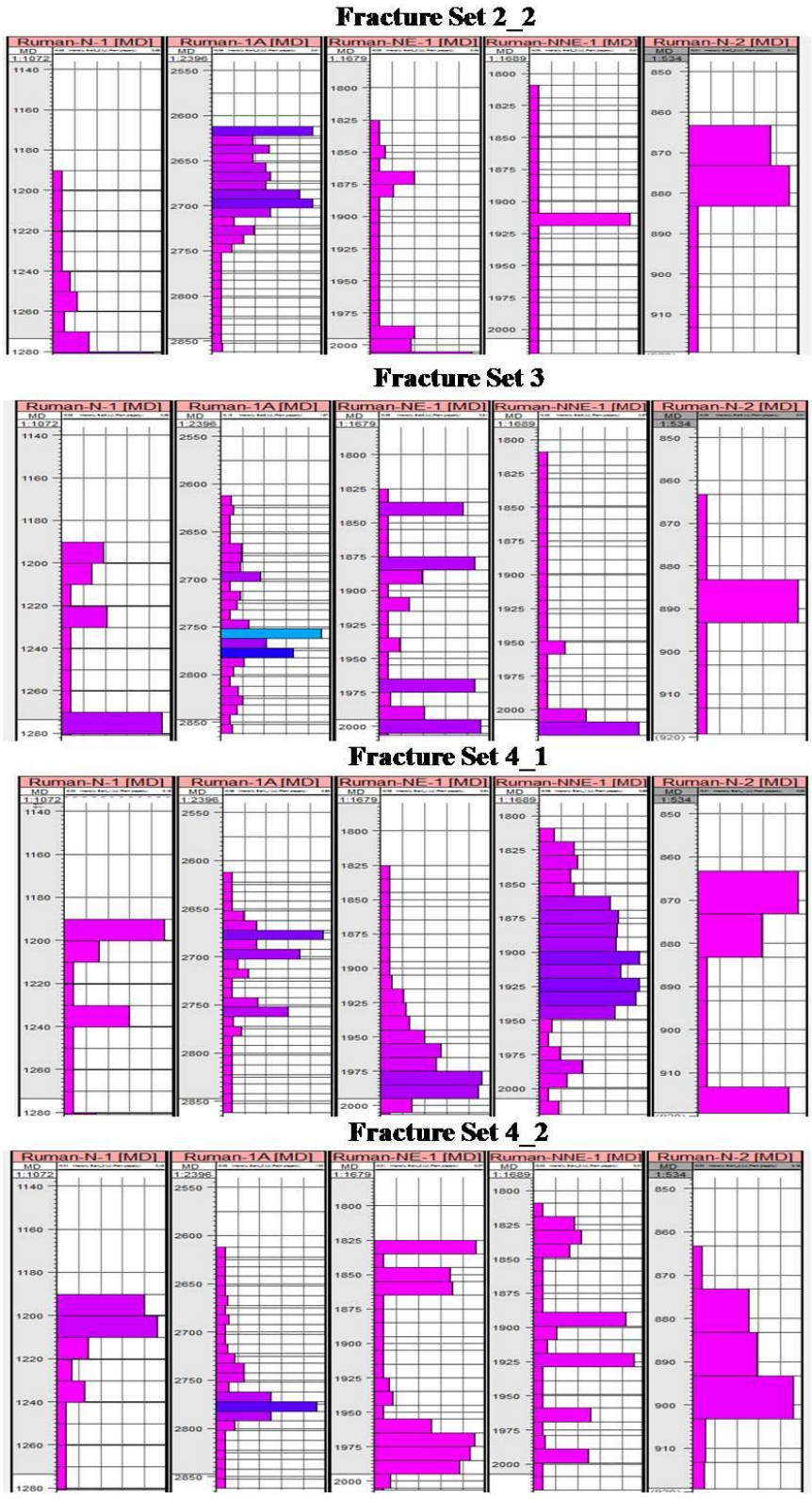

Figure 4-10: Upscaled fracture intensities for each fracture set at all the wells

In the presence of limited information, any description involves the use of statistics. Geostatistics takes advantage of the fact that, in many natural phenomena, variable values measured close to each other are similar. As the distance between the measured values increases, the similarity between the two measurements decreases. On the basis of this similarity, geostatistics captures the spatial relationship through certain correlation functions. Geostatistical procedures were used basically in two aspects: interpolation and extrapolation of fractures intensity values at unsampled locations; spatial-distribution analysis that provides the quantitative relationship describing the spatial variability of fractures intensity. In this sense, the variogram is the most widely used tool to investigate and model spatial variability of the reservoir properties. Furthermore, the variogram reflects our understanding of the geometry and continuity of reservoir properties.

Variogram, an intrinsic stationary process, is used for visualising, modeling and exploiting spatial continuity and spatial variability of regionalized variables (Cressie, 1991). Variogram is also a generalized variable characterized by both generalization andrandomness. It is used widely in geostatisticalmodeling, especially in spatial distribution modeling (Deutsch and Journel, 1999). Experimental variogram vector γ (h) provides quantitativemeasurements for spatial variability. It takes into consideration the separation vector (h), measuring the difference on average asseparation distance increases along a given direction. In general, separation vector is specified with some direction and lag distance tolerance (Figure 4-11).

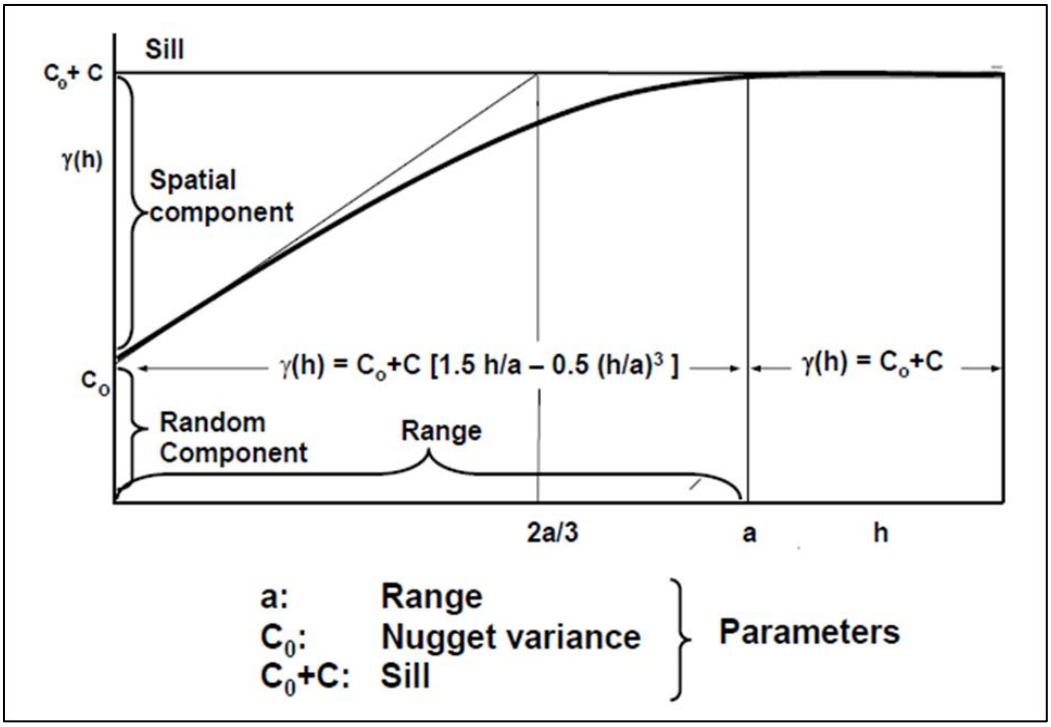

Figure 4-11: Variogram simple spherical model (afterCressie, 1991)

In this study, the data points in the plots have shown in Figure 4-12 and Figure 4-13represent the experimental variograms. For modeling purposes the data is fitted to certain known models (continues lines in plots). In this case I have fitted the data with a “Spherical model” since the data tend to follow that kind of behavior.

A variogram analysis (Figure 4-12 and Figure 4-13)was applied; rather SGS parameters were based on the variogram. Fracture total intensity model is presented in Figure 4-14. The results obtained for each fracture set are presented in Figure 63.

4.5 Discrete Fractures Network (DFN) Model Construction

A fracture network is a group of planes representing fractures. Fractures are two scales, seismic scale and sub-seismic scale fractures. Inthis study, the sub-seismic fractures of the same type and generated at the same time are grouped into a fracture sets and then modeled stochastically using statistical and geostatistical discrete modeling methods based on the fractures properties. The seismic scale (faults) were interpreted from seismic data, and then modeled deterministically as a separated fracture set.

4.5.1 Stochastic Model

The main propertiesto create the Discrete Fracture Network (DFN) model stochastically are the fracture distribution, geometry and orientation.

Total Intensity Variogram
- Major Direction 315 degree
- Minor Direction 225 degree
- Major Range 4113.4
- Minor Range 3715.7
- Nugget 0
- Sill 0.985
- Spherical

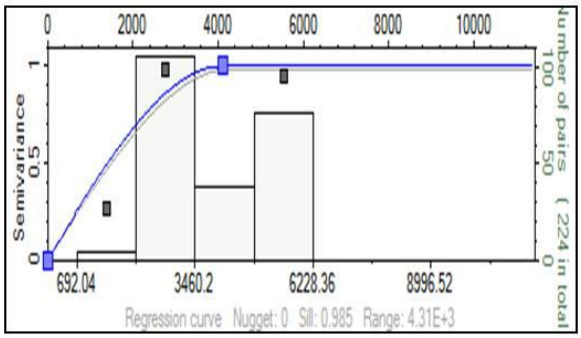

Set 1_1 Intensity Variogram
- Major Direction 315 degree
- Minor Direction 225 degree
- Major Range 5001.1
- Minor Range 4271.4
- Nugget 0
- Sill 2.36
- Spherical

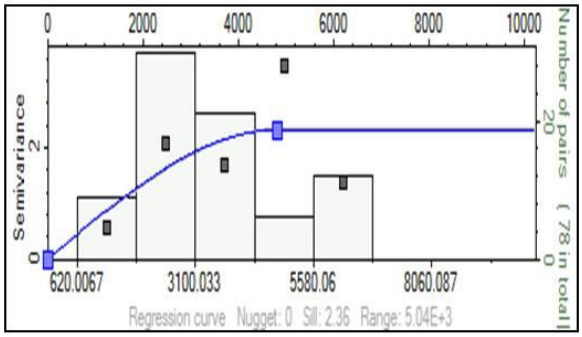

Set1_2 Intensity Variogram
- Major Direction 315 degree
- Minor Direction 225 degree
- Major Range 5699.3
- Minor Range 35334
- Nugget 0
- Sill 1.43
- Spherical 0

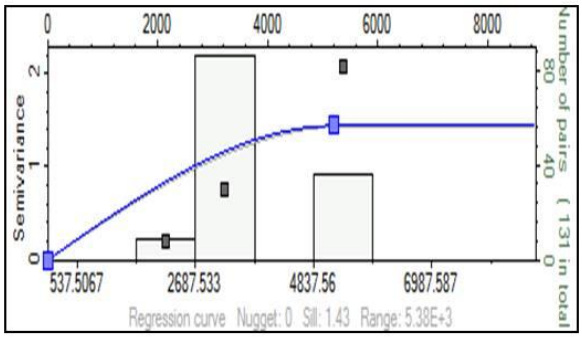

Set2_1 Intensity Variogram
- Major Direction 270 degree
- Minor Direction 180 degree
- Major Range 3615.3
- Minor Range 3408.4
- Nugget 0
- Sill 1.05
- Spherical

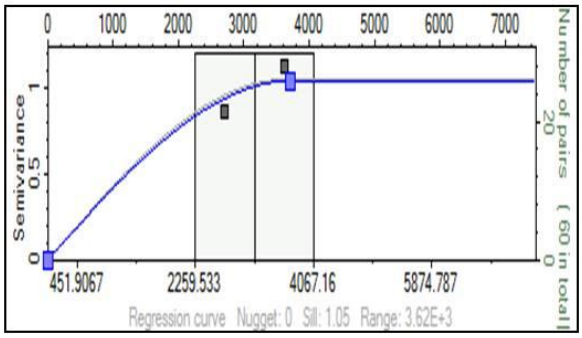

Figure 4-12: Variogram analysis of well data for the different fracture sets

Set2_2 Intensity Variogram
- Major Direction 270 degree
- Minor Direction 180 degree
- Major Range 4917.7
- Minor Range 2813.7
- Nugget 0
- Sill 0.837
- Spherical

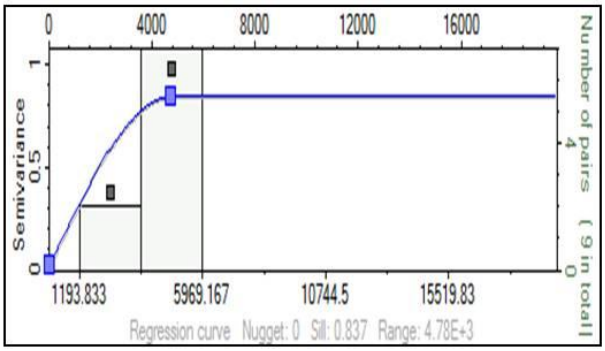

Set 3 Intensity Variogram
- Major Direction 0 degree
- Minor Direction 270 degree
- Major Range 6021
- Minor Range 3622.7
- Nugget 0
- Sill 1.24
- Spherical

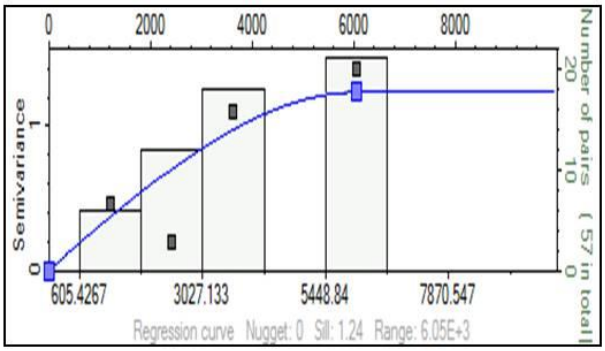

Set4_1 Intensity Variogram
- Major Direction 45 degree
- Minor Direction 315 degree
- Major Range 5242.8
- Minor Range 4685.9
- Nugget 0
- Sill 1.04
- Spherical

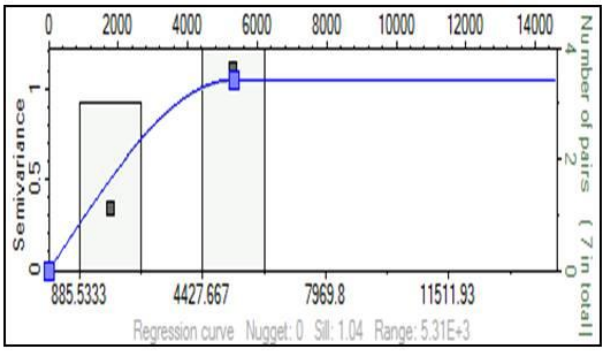

Set4_2 Intensity Variogram
- Major Direction 45 degree
- Minor Direction 270 degree
- Major Range 6774.3
- Minor Range 5541.2
- Nugget 0
- Sill 1.11
- Spherical

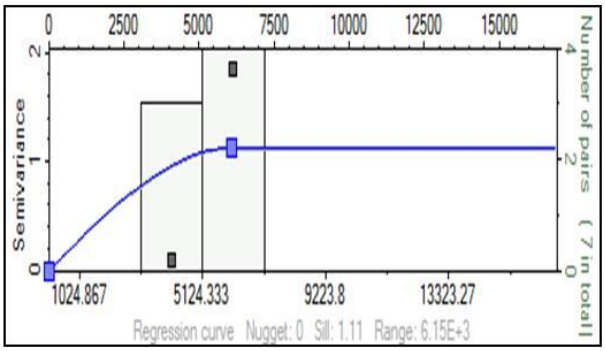

Figure 4-13: Variogram analysis of well data for the different fracture sets

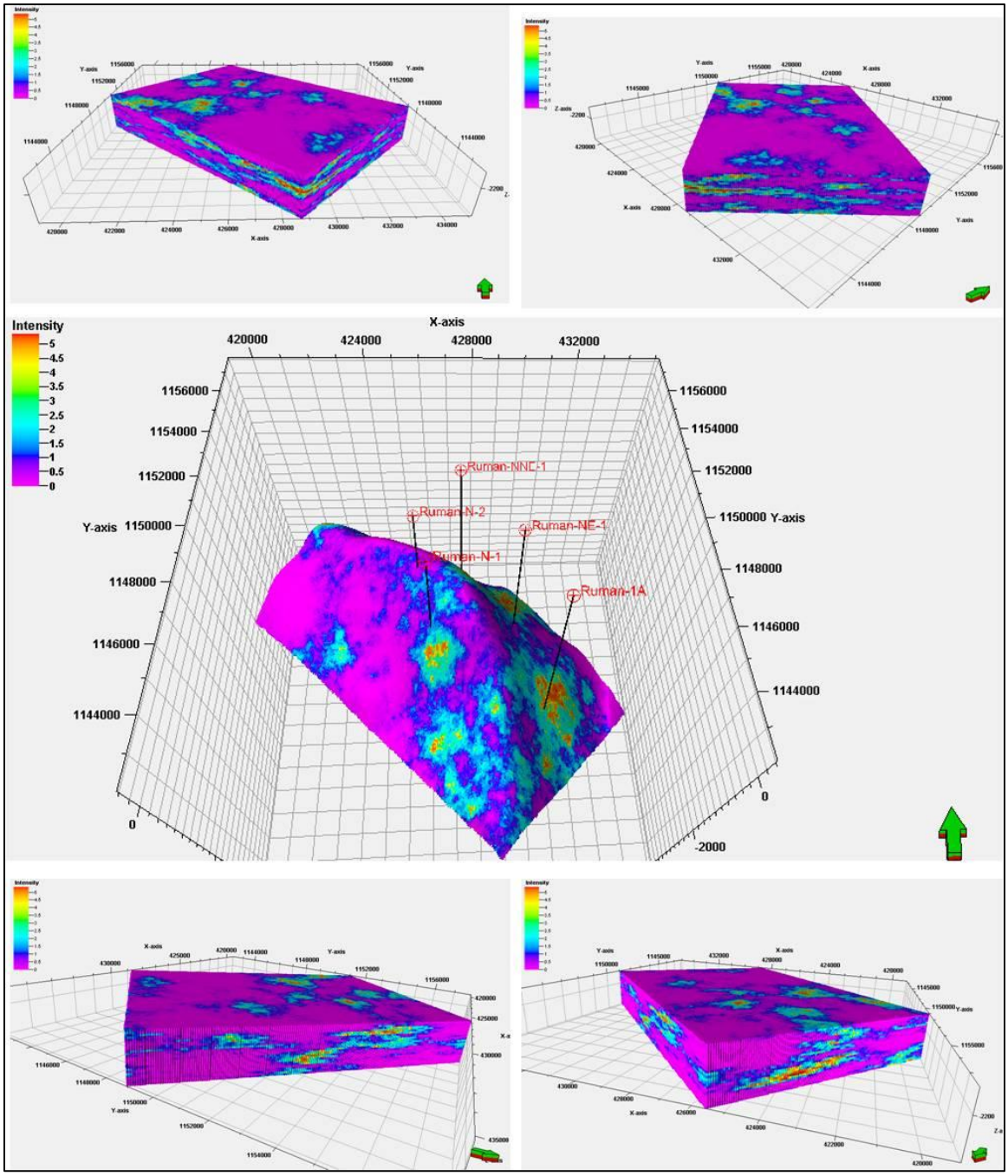

Figure 4-14: The interpolated total intensity in Ruman area

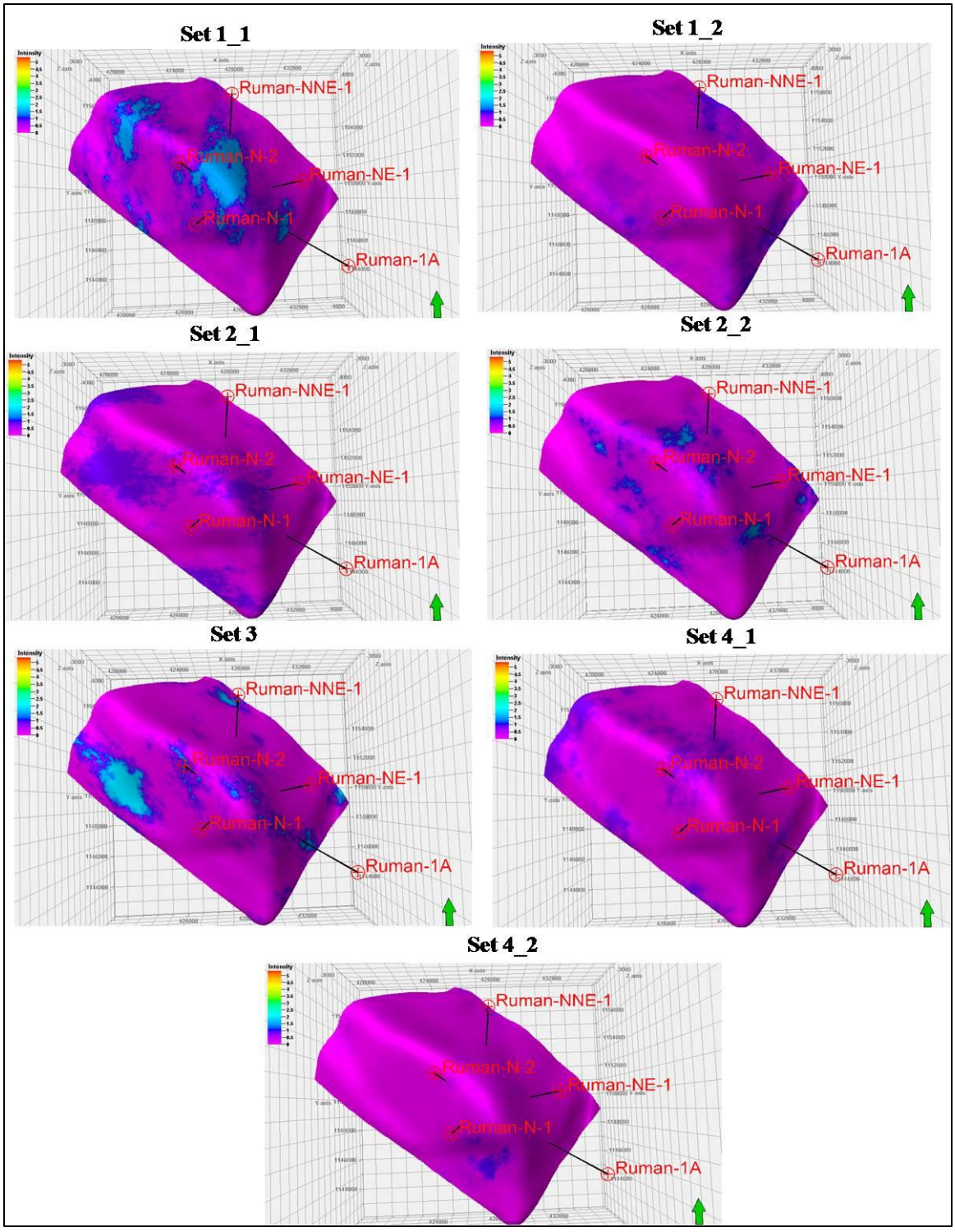

Figure 4-15: The interpolated intensities for the each fracture set in Ruman area

4.5.1.1 Fracture Distribution

Distribution of fractures consists of deciding which fracture intensity input and definition should be used. For defining the fracture distribution, the number of fractures perunit line length was converted to fracture area per unit volume. This upscaling process gives the fracture area per volume, orthe P32 value (total area of fractures per unit volume of rock). In this work, fracture intensity values were first calculated directly from fracture dataat wellbores for each fracture set as we shows in the previous step. Intensity models of the field are thendeveloped using deferent fracture sets (Figure 4-15). It is important to mention that, simulation offracture intensity plays a significant part in developing DFN model for fractures distribution.

4.5.1.2 Fracture Geometry

Geometry of fractures decides the shape and length of the fractures.Forfracture geometry, the shape of the fractures must be defined, as wellas the number of sides, and an elongation ratio. In this study, thefractures were represented as squares.Generally, length can be described using exponential, power law, log-normal, normal or constant distributions with minimum and maximum cut offs. Cut offs are required for exponential and power law distributions and will define how much of the defined fracture intensity will be modeled explicitly in the fracture network.

Power law distributions are constrained by a min and max cutoff number and defined by scale and shape parameters. The scale and shape defines the Probability Distribution Function (PDF) of the power law. Power law is a polynomial relationship of scale invariance. The power law distribution useful for describing the distribution of

fracture size, which can exhibit scale independent behavior. It is normally described by two parameters, a minimum value and exponent. Generally the probability density function (PDF) is defined as:

P(x) = a - 1/xmin (x/xmin) pow - a

Where - a is the scaling factor ensuring correct normalization.

It is a fact that, fracture length cannot be determined from well data because the wells describe only small part from the fracture. To solve this problem, fracture interpreted from different sets of data (Seismic, Gravity and satellite) were analyzed based on length.

Satellite image for the basement rock around the study area were used as analogue for two reasons: The first reason because the subsurface and surface basements have same rock types and the second reason because orientation analysis shows same orientation in the surface and subsurface. In this study, fracture lengthdistribution was defined using power law model. And use wide range of length from 100 m to 1000 m based on the outcrop lineaments length analysis.

4.5.1.3 Fracture Orientation

Orientation of well scale fractures decides the mean dip angle and dip azimuth and concentration are used as input in fisher model.The fisher model method describes a distribution of angles where the directions are not the fracture planes themselves, but the normal to the planes. These poles are scattered around a mean dip and azimuth based on a concentration.For thefracture orientation, Fisher models were used and constant

parameters generated from the well data wereconsidered for the seven fracture sets.The constant parameters are presented in Table 2.

More than 900 fractures were generated stochastically in the DFN model; these were distributed among the 4 sets (Set 1: 312 fractures, Set 2: 224 fractures, Set 3: 126 fractures and Set 4: 306 fractures).Thefracture networks corresponding to the different fracture sets and all fracture sets arepresented in Figure 4-16 and Figure 4-17 respectively. For the purposes of Quality Control (QC), Schmidt stereonet for the DFN model for the seven fracture sets was extracted (Figure 4-18) and correlated with the input parameters (Figure 4-6). It shows very good correlation for all fracture sets.

4.5.2 Deterministic Model

Faults were interpreted manually from the seismic data and then modeled deterministically in the DFN and create separate fracture set. This set is representing the major faults at the study area (more than 1 km length) (Figure 4-16 and Figure 4-17).

Fracture Set	Mean Dip Azimuth (o)	Mean Dip Angle (o)
Set1_1	250	60
Set1_2	50	40
Set2_1	10	70
Set2_2	180	30
Set3	80	80
Set4_1	150	45
Set4_2	315	45

Table 2: The constant parameters for the Fisher model used for each fracture set to define the fracture orientation for the DFN model

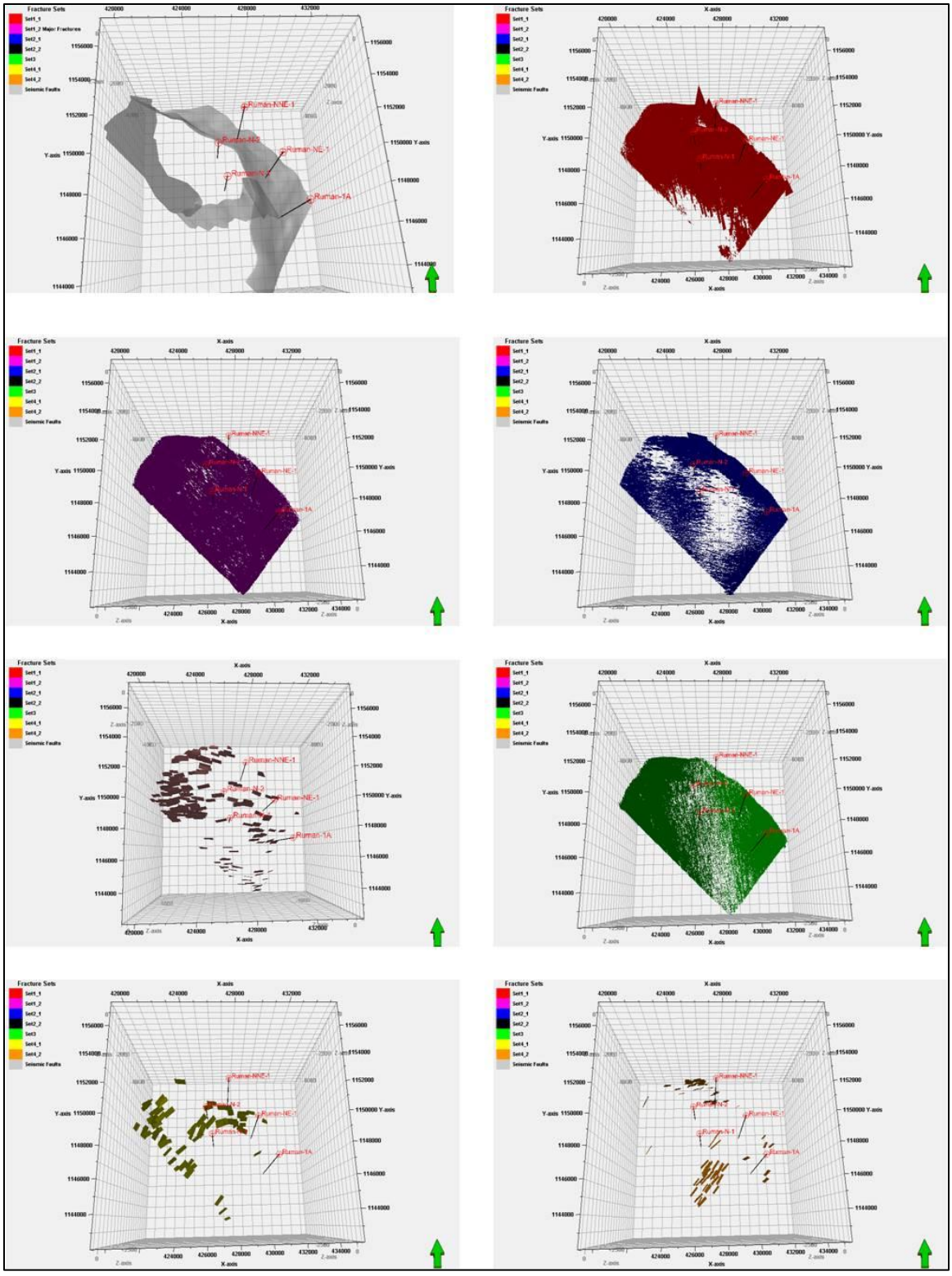

Figure 4-16: Three Dimensional Discrete Fracture Network (DFN) Model corresponding to each fracture set, which were generated deterministically and stochastically

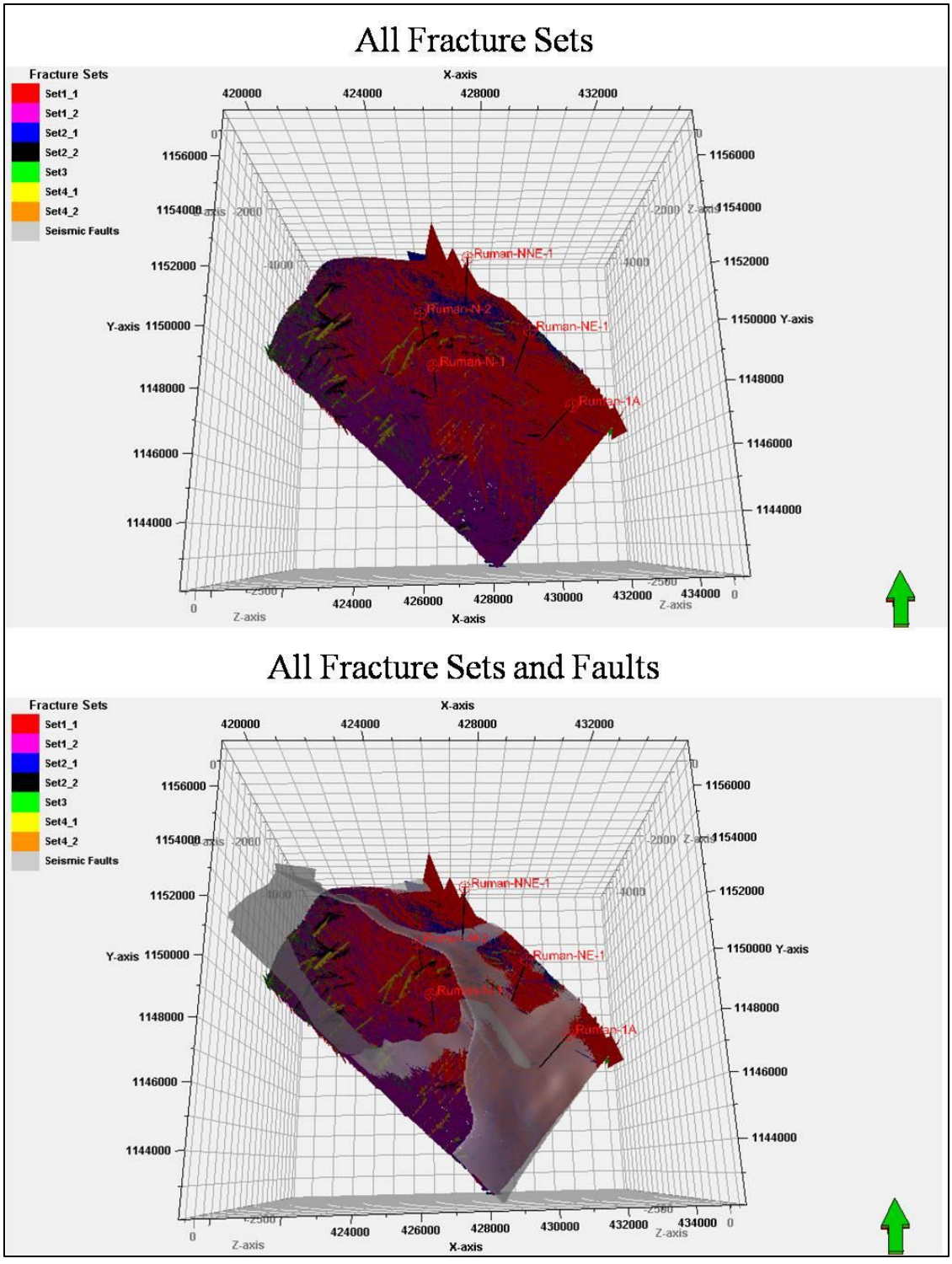

Figure 4-17: Three Dimensional Discrete Fracture Network (DFN) Model corresponding to all fracture sets

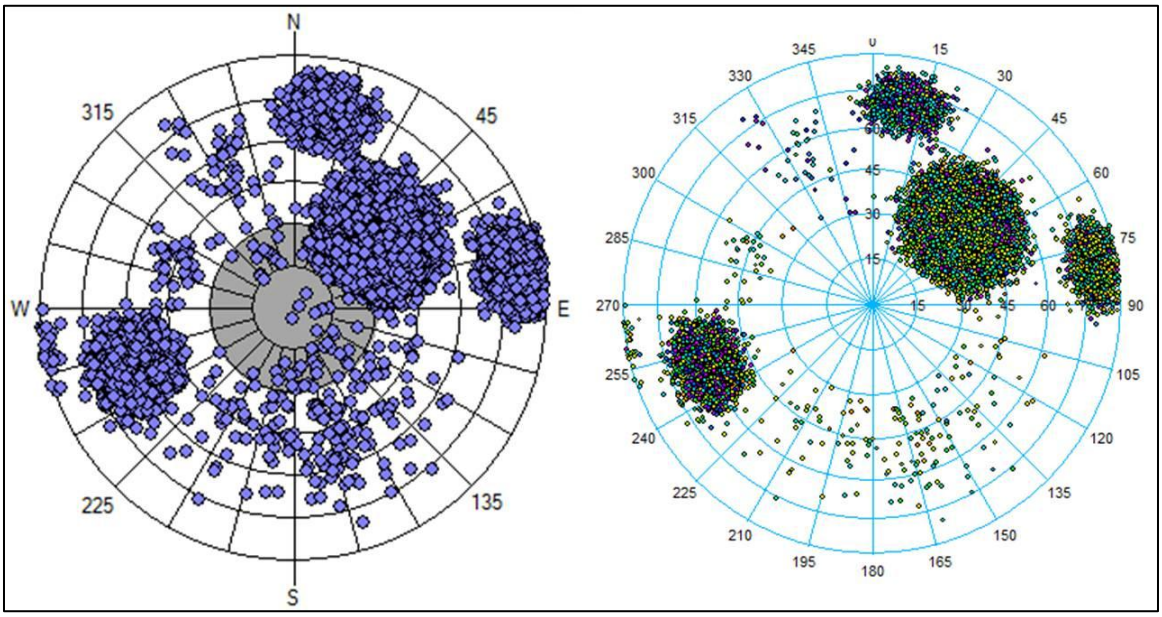

Figure 4-18: Schmidt stereonet extracted from the DFN model for the seven fracture setsfor the purposes of QC

CHAPTER FIVE

CONCLUSIONS AND RECOMMENDATIONS

4.6 Conclusions

The occurrence of potential oil reserves in naturally fractured basement reservoirs has been reported innorth Melut Basin after the drilling of Ruman-N-2 well.

In this study,fractures and faults associated with basement in the area wereinterpreted and characterized using different sets of data. Data sets included well data, gravity, seismic and lineaments from satellite image, and the characterization factors are based on orientation, length and intensity. In all data sets trends determined by rose diagram are comparable and similar, which may indicate the same origin and causes. The surface linear features in the outcrops around Melut basin (NubaMountains to the west and IngessanaHills to the east) show four preferred orientations (NW-SE, NNW-SSE to N-S, WNW-ESE to E-W and NE-SW. A majority of the surface linear features in the area are oriented in NW-SE and NNW-SSE. On the contrary, those surface linear features oriented in NE-SW are less prevalent.The gravity lineaments appear primarily in four sets of directions: two major sets oriented in NW-SE and NNW-SSE to N-S, and the

minor sets oriented along NE-SW and WNW-ESE to E-W. Well data shows that they have four preferred orientations, majority of the fractures and liner features oriented in three directions (NW-SE, NNW-SSE to N-S , WNW- ESE to E-W) and minor directions toward NE-SW. Major and minor faults and fractures within the basement were interpreted from seismic data. There are three orientations NW-SE, NNW-SSE to N-S, and WNW-ESE to E-W. The majority of the fractures and liner features toward NW-SE.

Those fracture and lineaments trends may be related to different origin. Three stages model were proposed for the origin of the fractured basement; fractures formed during the basement emplacement and cooling, fractures that are inherited from earlier (Proterozoic) tectonic events and fractures formed during faulting and related to major normal faults developed during the Melut rift.This study suggests that the fractures associated with basement and hosting the hydrocarbon resources in Melut basin are mostly of the indicted origin. However, the earlier formed fracture systems related to the basement emplacement and Pretorozioc tectonic event may have affected and reactivated later by the latest tectonic event associated with the rifting of Melut basin that took place during the Cretaceous- Tertiary time.

This study is also emphasizing the importance of considering all events; basement emplacement and cooling, Pretorozic tectonic events and faulting related to rifting in studying and characterization of fractures hosting hydrocarbon in basement. Fault related to rifting acted also as the conduit for hydrocarbon migration.

Seven fracture sets for different orientations were built based on well data and tectonic history and then modeled stochastically. During this study, a model that integrateddifferent fractures scales that interpreted from different source of data

wereconstructed. Moreover, a comprehensive Discrete Fracture Network (DFN) model for the basement in Ruman area was carried out.

Fractures usually form most of the storage and permeability of the reservoir. Cross-cut relationship is very important for permeability. The DFN model resulted in this study described this relationship carefully.

Fractured basements are commonly believed to be charged through the flanks or through thetop of the basement structure. Ruman traplinked with the source rock by major fault, this provides very good charging mechanism. From the in-situ stress analysis, it is believed that the NW-SE and NNW-SSE faults and fractures trends may be the most susceptible to dilation (open) at present day.

4.7 Recommendations

As a result of this study the following recommendations might be considered for future follow up and further studies in this area or other areas with similar settings:

- Lineaments delineation and trends obtained from satellite images need to be ground trusted through filed works. Filed studies need to be conducted on the basement outcrops present in and around Melut basin for better defining and understanding of fractures pattern and trends, geometrical parameters like shape, length and fracture connectivity.
- Re-process the seismic data through advanced techniques might be of importance to delineate determined information about the subsurface fractures.

- As the wells data used in this study is limited (only five wells),more wells need to be drilled based on this model in the fault foot wall close to Ruman N-2 well where extracted fractures are anticipated .Information of current and proposed wells will provide more precise model and will enhance the Discrete Fracture Network Model (DFN) suggested by this study.

- The obtained data from well and seismic data will also help to conduct geomechanical study (Stress and strain mapping) to predict the fractures openness and closeness. This will help to target the area where strain concentrated during deformation, leading to potentially higher fracture densities.

References

Abdel Rahman, E.M., Matheis, G., Schandelmeier, H., Karfis, M.A., Abdel Gadir, I., and El Khedir, M., 1993, Evolution of the Keraf back-arc basin; constraints on the Nubian Shield margin, A.A. Balkema, Rotterdam, Netherlands, p. 93-98.

Abdelsalam, M.G., Abdel-Rahman, E.-S.M., El-Faki, E.-F.M., Al-Hur, B., El-Bashier, F.-R.M., Stern, R.J., and Thurmond, A.K., 2003, Neoproterozoic deformation in the northeastern part of the Saharan Metacraton, northern Sudan: Precambrian Research, v. 123, p. 203-221.

Abdelsalam, M.G., and Dawoud, A.S., 1991, The Kabusophioliticmelange, Sudan, and its bearing on the western boundary of the Nubian Shield: Journal of the Geological Society of London, v. 148, Part 1, p. 83-92.

Abdelsalam, M.G., LiAgeois, J.-P., and Stern, R.J., 2002, The Saharan Metacraton: Journal of African Earth Sciences, v. 34, p. 119-136.

Ahmed, F., Hagaz, Y.A., and Andrawis, A.S., 1984, Landsat model for groundwater exploration in Nuba Mountains, Sudan: Advances in Space Research, v. 4, p. 123-131.

Binks, R.M., and Fairhead, J.D., 1992, A plate tectonic setting for Mesozoic rifts of West and Central Africa: Tectonophysics, v. 213, p. 141-151.

Bosworth, W., 1992, Mesozoic and early Tertiary rift tectonics in East Africa: Tectonophysics, v. 209, p. 115-137.

Browne, S.E., and Fairhead, J.D., 1985, Gravity study of the Central African Rift system; a model of continental disruption; 1, The Ngaoundere and Abu Gabra rifts: Tectonophysics, v. 94, p. 187-203.

Cressie, 1991, Statistics for spatial data, John Wiley and amp; Sons, New York, NY, United States, 900 p.

Deutsch, C.V., and Journel, A.G., 1999, Book review: GSLIB: Geostatistical Software Library and User's Guide, Second Edition: Computers & Geosciences, v. 25, p. 309-312.

Dou, L., Xiao, K., Cheng, D., Shi, B., and Li, Z., 2007, Petroleum geology of the Melut Basin and the Great Palogue Field, Sudan: Marine and Petroleum Geology, v. 24, p. 129-144.

Eisawi, A., and Schrank, E., 2008, Upper Cretaceous to Neogene palynology of the Melut Basin, southeast Sudan: Palynology, v. 32, p. 101-129.

El Ageed and El Rabaa. , 1981, The geology and structural evolution of the northeastern Nuba Mountains, southern Kordofan Province, Sudan, University of Khartoum, Khartoum, Sudan, 50 p.

Fairhead, J.D., 1986, Geophysical controls on sedimentation within the African rift systems: Geological Society Special Publications, v. 25, p. 19-27.

Fairhead, J.D., 1988, Mesozoic plate tectonic reconstructions of the central South Atlantic Ocean: The role of the West and Central African rift system: Tectonophysics, v. 155, p. 181-191.

Friedman, M., Logan, J.M., Handin, J.W., and Stearns, D.W., 1972, Experimental "drape-folding" of rocks under confining pressure: Abstracts with Programs - Geological Society of America, v. 4, p. 512-513.

Gass, I.G., and Neary, C., 1975, The granitic association of the Northeast Sudan: Travaux des Laboratoires des Sciences de la Terre, Serie B, p. 81-83.

Genik, G.J., 1993, Petroleum geology of Cretaceous-Tertiary rift basins in Niger, Chad, and Central African Republic: American Association of Petroleum Geologists Bulletin, v. 77, p. 1405-1434.

Geological Research Authority of the Sudan "GRAS" (1988): Geological map of Sudan (unpublished report).

Geological Research Authority of the Sudan"GRAS" (2005): Geological map of Sudan, scale 1:2000, 000 (unpublished report).

Guiraud, R., and Bosworth, W., 1997, Senonian basin inversion and rejuvenation of rifting in Africa and Arabia: synthesis and implications to plate-scale tectonics: Tectonophysics, v. 282, p. 39-39.

Guiraud, R., and Maurin, J.-C., 1992, Early Cretaceous rifts of Western and Central Africa; an overview: Tectonophysics, v. 213, p. 153-168.

Hansen, S., 2008, Borehole stress orientation: Schlumberger. Unpublished report

Hariri, M.M., 1995, Lineament studies and fracture control on the Tertiary gold-silver deposits, northern Black Hills, South Dakota, USA, : [Ph.D. thesis]: South Dakota School of Mines and Technology, , p. 159.

Hariri, M.M., and Abdullatif, O.A., 2004, Characterization of fractures within Dammam Dome, eastern Saudi Arabia: GeoArabia (Manama), v. 9, p. 76.

Klitzsch, E., and Lejal-Nicol, A., 1984, Flora and fauna from strata in southern Egypt and northern Sudan (Nubia and surrounding areas): Berliner GeowissenschaftlicheAbhandlungen, Reihe A: Geologie und Palaeontologie, p. 47-79.

Koning, T., 2000, Oil production from basement reservoirs; examples from Indonesia, USA and Venezuela: Proceedings - World Petroleum Congress - CongresMondial du Petrole, v. 16, Vol. 2, p. 250-251.

Kroner, A., 1975, The Namaqua mobile belt within the framework of Precambrian crustal evolution in southern Africa: Opsommings van Referate - GeologieseVereniging van Suid-Afrika, Abstracts of Papers - Geological Society of South Africa, p. 73.

Landes, K.K., Amoruso, J.J., Charlesworth, L.J., Jr., Heany, F., and Lesperance, P.-J., 1960, Petroleum resources in basement rocks: Bulletin of the American Association of Petroleum Geologists, v. 44, p. 1682-1691.

Lawn, B., and Wilshaw, R., 1975, REVIEW INDENTATION FRACTURE: PRINCIPLES AND APPLICATIONS: Journal of Materials Science, v. 10, p. 1049-1081.

Lillesand, T.M.a.K., R.W., 1979, Remote sensing and image interpretation, John Wiley and Sons, New York, N.Y., United States, 612 p.

Mann, C.D., 1989, Thick-skin and thin-skin detachment faults in continental Sudanese rift basins: Journal of African Earth Sciences, v. 8, p. 307-322.

McHargue, T.R., Heidrick, T.L., and Livingston, J.E., 1992, Tectonostratigraphic development of the Interior Sudan rifts, Central Africa: Tectonophysics, v. 213, p. 187-202.

Moores, T.a., 1992, Structural geology, W.H. Freeman and Company, New York, NY, United States, 532 p.

Nelson, R.A., 2003, Exploration for fault-related fractured reservoirs: The Bulletin of the Houston Geological Society, v. 46, p. 27.

Norris, D.K., 1966, Structural analysis of the Queensway folds, Ottawa, Canada: Transactions - American Geophysical Union, v. 47, p. 191.

Petford, N., and McCaffrey, K., 2003, Hydrocarbons in crystalline rocks; an introduction: Geological Society Special Publications, v. 214, p. 1-5.

Pollard, D.D., and Aydin, A., 1988, Progress in understanding jointing over the past century: Geological Society of America Bulletin, v. 100, p. 1181-1204.

Price and Cosgrove, 1990, Analysis of geological structures, Cambridge Univ. Press, Cambridge, United Kingdom, 502 p.

Qureshi, I.R., and Sadig, A.A., 1967, Earthquakes and associated faulting in central Sudan: Nature (London), v. 215, p. 263-265.

Rowell, A., 2010, Sudan's Oil Figures Don't Add up, Undermining Peace Deal: Internet, v. unpublished reports.

Schandelmeier, H., Huth, A., Harms, U., Franz, G., and Bernau, R., 1987a, The East Sahara Craton in southern Egypt and northern Sudan; lithology, metamorphism, magmatism, geochronology and structural development: Berliner GeowissenschaftlicheAbhandlungen, Reihe A: Geologie und Palaeontologie, v. 75, p. 25-48.

Schandelmeier, H., Richter, A., and Franz, G., 1983, Outline of the geology of magmatic and metamorphic units between Gebel Uweinat and BirSafsaf (SW Egypt/NW Sudan): Journal of African Earth Sciences (1983), v. 1, p. 275-283.

Schandelmeier, H., Richter, A., and Harms, U., 1987b, Proterozoic deformation of the East Saharan Craton in Southeast Libya, South Egypt and North Sudan: Tectonophysics, v. 140, p. 233-246.

Schlumberger, 2009, PETREL 2009 User's Guide, Fracture Modeling.

Schull, T.J., 1988, Rift basins of interior Sudan; petroleum exploration and discovery: AAPG Bulletin, v. 72, p. 1128-1142.

Stearns, D.W., 1971, Mechanisms of drape folding in the Wyoming Province: Guidebook - Wyoming Geological Association, v. 23, p. 125-143.

Tchalenko, J.S., and Ambraseys, N.N., 1970, Structural analysis of the Dasht-e Bayaz (Iran) earthquake fractures: Geological Society of America Bulletin, v. 81, p. 41-59.

Vail, J.R., 1972, Pre-Nubian tectonic trends in northeastern Sudan: Journal of the Geological Society of London, v. 128, p. 21-31.

Vail, J.R., 1978, Outline of the geology and mineralization of the nubian shield east of the Nile Valley, Sudan: Precambrian Research, v. 6, p. A39-A40.

Vail, J.R., 1982, Geology of the central Sudan, A.A. Balkema, Rotterdam, Netherlands, p. 51-63.

Vail, J.R., 1988, Lexicon of geological terms for the Sudan, A. A. Balkema, Rotterdam, Netherlands, 199 p.

Vail, J.R., Hohendorf, A., and Meinhold, D., 1990, Petrological and isotopic studies of selected anorogenic alkaline complexes from the Sudan: Publication Occasionnelle-Centre International Pour la Formation et les EchangesGeologiques Occasional Publication - International Center for Training and Exchanges in the Geosciences, v. 20, p. 411.

Vail, J.R., and Hughes, D.J., 1987, The contact between the continental Sudan Shield and the orogenic Nubian Shield in Blue Nile Province, Sudan: Extended Abstracts - Colloquium on African Geology, v. 14, p. 105-108.

Vail, J.R., and Sadig, A.A., 1987, Gravity patterns across the Sudan and their tectonic implications: Extended Abstracts - Colloquium on African Geology, v. 14, p. 307-309.

Van Golf-Racht, T.D., 1982, Fundamentals of fractured reservoir engineering, Elsevier Sci. Publ. Co., Amsterdam, Netherlands, 710 p.

Whiteman, 1971, The geology of the Sudan Republic, Oxford Univ. Press, 290 p.

Vita

Name

Mohamed Abdelgader Ahmed Yassin

Date of Birth

22/10/1977

Nationality

Sudanese

Academic Qualifications

M.Sc. in Geology (GPA 3.813/4.0), (2.4 Years) Earth Sciences Department, King Fahd University of Petroleum & Minerals (KFUPM), Saudi Arabia (From Feb, 2010 to June, 2012)

MBA, (2 Years) School of Management Studies, University of Khartoum-Sudan (From Jan, 2003 to Jan, 2005)

B.Sc. Honors (5 years) in Geology (Second Class Division One), Department of Geology, Faculty of Science, University of Khartoum- Sudan (From Sep, 1997 to Sep, 2002)

Work Experience

(Sept, 2004 up to date) Geoscientist at Sudapet Company.

(Feb, 2003 up to Sep, 2004) Teaching Assistant at Sudan University of Science and Technology

Temporary Address

KFUPM, P.O Box: 8646, Dhahran 31261 Saudi Arabia

Email: mohamedgadir@kfupm.edu.sa

Mobile: 00966 502928667

Permanent Address

Sudapet Company Ltd.Africa Street, Block 9/10 Resident No. 22/1 Khartoum- Sudan

P.O. Box 331 Khartoum North, Sudan

E-mail: mohamedgadir@sudapet.com.sd or mohamedgadir@gmail.com

Mobile: 00249 9 12205757